REPUBLIC OF TURKEY
YILDIZ TECHNICAL UNIVERSITY
GRADUATE SCHOOL OF NATURAL AND APPLIED SCIENCES

FATE OF PESTICIDE IN SOIL AND PHOTOCATALYTIC DEGRADATION BY PERLITE SUPPORTED TITANIUM DIOXIDE

EMMANUEL NGAHA

PHD THESIS
DEPARTMENT OF CHEMICAL ENGINEERING
CHEMICAL ENGINEERING PROGRAM

ADVISER
ASSOC. PROF. DR. DİLEK DURANOĞLU

İSTANBUL, 2019

REPUBLIC OF TURKEY
YILDIZ TECHNICAL UNIVERSITY
GRADUATE SCHOOL OF NATURAL AND APPLIED SCIENCES

FATE OF PESTICIDE IN SOIL AND PHOTOCATALYTIC DEGRADATION BY PERLITE SUPPORTED TITANIUM DIOXIDE

A thesis submitted by Emmanuel NGAHA in partial fulfillment of the requirements for the **Philosophy of Doctorate** degree is approved by the committee on 18.07.2019 in Department of Chemical Engineering, Chemical Engineering Program.

Thesis Adviser
Assoc. Prof. Dr. Dilek DURANOĞLU
Yildiz Technical University

Co- Adviser
Prof. Dr. Emmanuel GUILLON
University of Reims Champagne Ardenne

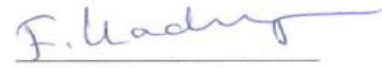**Approved By the Examining Committee**
Assoc. Prof. Dr. Dilek DURANOĞLU
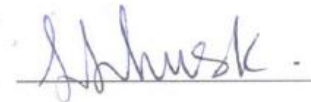Yildiz Technical University

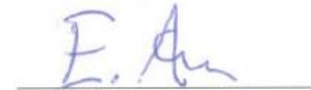Prof. Dr. M. A. Neşet KADIRGAN, Member
Marmara University

Prof. Dr. Figen KADIRGAN, Member
Istanbul Technical University

Assist. Prof. Dr. İlknur KÜÇÜK, Member
Yildiz Technical University

Assoc. Prof. Dr. Emel AKYOL, Member
Yildiz Technical University

ii

ACKNOWLEDGEMENT

TABLE OF CONTENTS

LIST OF SYMBOLS

H_O Null Hypothesis
K_d Distribution Coefficient
K_H Henry's constant
K_{oc} Distribution coefficient based on Organic Content
K_{OW} n-octanol/water partition coefficient
LD_{50} Lethal Dose
$ProbF_2$ Probability of finding a ratio equal to 1

LIST OF ABBREVIATIONS

AF	Air Flow
AFNOR	French Association for Standardization
AOPS	Advanced Oxidation Processes
BBD	Box Benkhen Design
BCF	Bioconcentration Factor
BET	Brunauer Emmett and Teller
CCD	Colony Collapse Disorder
CEC	Cation Exchange Capacity
DF	Degree of Freedom
DEG270	Degradation Percentage after 270min of irradiation
DFSAS	Degree of Sum of Average Squares
DO	Dissolved Oxygen
DOC	Dissolved organic carbon
DOE	Design of Experiment
EE/O	Electric Energy per Order
ESI	Electrospray Interface
EU	European Union
GTHB	Turkey Ministry of Food, Agriculture and Livestock
GUS	Grounwater Ubiquity Score
HPLC	High Performance Liquid Chromatography
JMP	Statistical Software Pronounced "Jump"
LC-MS	Liquid Chromatography Mass Spectroscopy
LEACH	Leaching index
LFE1	Lock of Fit of Model (bios of the lack of fit)
LIN	Leachability Index
LOD	Limit of Detection
LOQ	Limit of Quantification
LW	Longwave light
SW	Shortwave light
MLEACH	Modified LEACH
MSAS	Model Sum of the Average Squares
OFAT	One Factor At a Time
OM	Organic Matter
PE	Pure or Natural Error
PST	Perlite Supported Titanium Dioxide

RSM	Response Surface Methodology
RSS	Residual Sum of Squares
SEM	Scanning Electron Microscope
THX	Thiamethoxam
THX-E	Thiamethoxam in Eforia 247 zc
TOC	Total Organic Carbon
USC	United State Code
UVA	Ultraviolet A
UVB	Ultraviolet B
XRD	X-ray Diffractometer
λ-CHT	Lambda Cyhalothrin
λ-CHT-E	Lambda Cyhalothrin in Eforia 247 zc

LIST OF FIGURES

LIST OF TABLES

xv

ABSTRACT

FATE OF PESTICIDE IN SOIL AND PHOTOCATALYTIC DEGRADATION BY PERLITE SUPPORTED TITANIUM DIOXIDE

Emmanuel NGAHA

Department of Chemical Engineering

PhD. Thesis

Adviser: Assoc. Prof. Dr. Dilek DURANOĞLU

Co-adviser: Prof. Dr. Emmanuel GUILLON

The pesticides have been detected in many countries in water, soil and air. Moreover, some recent studies reported that the presence of Thiamethoxam (THX), one of the most used insecticides, in the drinking water. How does THX, which is harmful for living life, interact in the environment after being used both in its pure form and in its commercial formulation? How can it photocatalytically degraded? In this study, the answers of these questions were sought.

The fate of THX in the environment is the main subject of the first part of this study. THX contamination risk of groundwater was investigated in the pure form and also in the commercial formulation (THX-E) by the adsorption/desorption studies on three different soils (S_1, S_2, S_3) taken from Tekirdağ/Turkey. Adsorption kinetic constants, adsorption isotherm parameters (Langmuir, Freundlich models), distribution coefficients K_d, were determined in batch processes. As a result, for 1.46 mg.L^{-1} initial THX concentration, the highest adsorption did not exceed 20% for S_1, S_2 and S_3. The K_d and K_{oc} for all the three soils varied from 2.1 to 6.4 L.kg^{-1} and from 200.7 to 500.4 L.Kg^{-1}, respectively. The leaching potential was evaluated by using the Groundwater Ubiquity Score (GUS) and a multivariate approach: the Global Leachability Index (GLI) which combines different environmental partition indexes (the GUS, the Modified LEACH (M.LEACH) Index and the Leaching Index (LIN)) into a single ranking. THX in the pure form (THX) or in the commercial formulation (THX-E) exhibited similar behavior in terms of leaching potential. The risk was "INTERMEDIATE" for almost all soils except S3-THX and "HIGH" for all soils with GUS and GLI index assessment, respectively. It was concluded that THX has high potential for groundwater contamination.

The second part of this study concerned photocatalytic degradation of THX by using perlite supported TiO_2 composite material (PST). Box Behnken Experimental Design method was employed in order to evaluate the effect of process parameters and also optimize them. Accordingly, effects of three process parameters (pH, load of PST (PT (g/L)), and air flow rate (AF (L/h))) were investigated on two responses: (i) the THX degradation percentage after 270 min (DEG270 (%)) and (ii) the electric energy per order (EE/O (kWh/m^3)). THX degradation was improved by decreasing pH value and increasing the air flow rate. Increasing load of PST increased the degradation percentage until a critical value of about 8 g/L, then caused a decrease. Statistically significant second order polynomial models were developed by regression analysis of experimental data. Optimum conditions were obtained as follows: pH 4, PT 8.30 g/L and AF 18 L/h. These conditions led to a response of 87±5% for DEG270 and 120±21 kWh/m^3 for EE/O. Control experiments confirmed a good optimized process and reusability of PST without any regeneration step. Mineralization and possible intermediate products were also investigated by using Total Organic Carbon content, Chemical Oxygen Demand, and LC-MS studies, respectively, then a degradation pathway was proposed accordingly.

Keywords: Pesticide, Leaching Potential, Adsorption, Photocatalytic Degradation, Design of Experiment.

YILDIZ TECHNICAL UNIVERSITY

GRADUATE SCHOOL OF NATURAL AND APPLIED SCIENCES

ÖZET

PESTİSİTİN TOPRAKTA DAĞILIMI VE PERLİT DESTEKLİ TİTANYUM DİOKSİT İLE FOTOKATALİTİK BOZUNMASI

Emmanuel NGAHA

Kimya Mühendisliği Bölümü

Doktora tezi

Tez Danışmanı: Doç. Dr. Dilek DURANOĞLU
Eş Danışman: Prof. Dr. Emmanuel GUILLON

Bir çok ülkede tarım ilaçları doğada (su, toprak ve havada) tespit edilmiş, ayrıca son zamanlarda yapılan bazı çalışmalarda bir böcek ilacı olan Tiyametoksamın (THX) içme suyundaki varlığı bildirilmiştir. Canlı yaşam için son derece zararlı olan THX gerek saf halde gerekse ticari formülasyonu içinde kullanıldıktan sonra doğada nasıl bir yol izler ve fotokatalitik olarak nasıl bozunur? Bu çalışmada bu soruların cevabı aranmıştır.

THX'ın çevreye dağılımının izlenmesi bu çalışmanın ilk kısmını oluşturmaktadır. Yeraltı sularına THX kontaminasyonu riski Tekirdağ'dan toplanan üç farklı toprak örnekleri (S_1, S_2, S_3) ile yapılan adsorpsiyon / desorpsiyon çalışmalarıyla incelenmiştir. THX'ın saf çözeltisi ve ticari formulasyonu (THX-E) ile ayrı ayrı çalışılmıştır. Adsorpsiyon kinetik sabitleri, adsorpsiyon izotermler parametreleri (Langmuir, Freundlich modelleri) ve dağılım katsayısı (K_d) kesikli proseste gerçekleştirilen deneylerle belirlenmiştir. 1,46 mg.L^{-1} THX konsantrasyonu için en yüksek adsorpsiyon S_1, S_2 ve S_3 için % 20'yi geçmemiştir. Her üç toprak için K_d ve K_{oc} sırasıyla 2,1 ila 6,4 L.kg^{-1} ve 200,7 ila 500,4 L.kg^{-1} arasında değişmiştir. THX'ın yeraltına sızma potansiyeli, Yeraltı Suyunda Bulunabilme Skoru (Groundwater Ubiquity Score, GUS) ve çok değişkenli bir yaklaşım olan Küresel Sızdırmazlık İndeksi (Global Leachability Index, GLI) ile değerlendirilmiştir. Küresel Sızdırmazlık İndeksi, Yeraltı Suyunda Bulunabilme Skoru (GUS), Sızdırmazlık İndexi (Leaching Index, LIN) ve Modifiye Sızdırmazlık İndeksi (M.LEACH) gibi farklı çevresel paylaşım endekslerinden gelen bilgileri birleştirerek tek bir sıralama yapmaktadır. THX'in gerek saf halinde gerekse ticari formulasyonu içinde benzer sızdırmazlık potansiyelleri elde edilmiştir. GUS değerlendirmesinde S_3-THX hariç tüm toprak örneklerinde çevresel risk faktörü "ORTA", GLI indeksinde ise tüm

toprak örnekleri için risk faktörü "YÜKSEK" bulunmuştur. Sonuç olarak THX'ın yeraltı sularının kirlenmesinde yüksek risk teşkil ettiği tespit edilmiştir.

Çalışmanın ikinci kısmı perlit destekli Titanium dioxide (TiO_2) kompozit malzemesi (PST) ile THX'ın fotokatalitik bozunması ile ilgilidir. Proses parametrelerinn etkisini incelemek ve proses şartlarını optimize etmek için Box Behnken Deneysel Tasarım Metodu uygulanmıştır. Seçilen üç proses parametresinin (pH, PST miktarı (PT, g/L) ve hava akış hızı (AF, L/sa)) etkileri iki ayrı cevapla incelenmiştir: (i) 270 dakika sonra THX'ın bozunma yüzdesi (DEG270, %) ve (ii) sarf edilen elektrik enerjisi (EE/O, kWh/m^3). Düşük pH değerlerinde ve yüksek hava akış hızlarında THX bazunma yüzdesinin arttığı gözlenmiştir. Artan PST miktarı ile bozunma yüzdesinin yaklaşık 8g/L'lik kritik bir değere kadar arttığı, daha sonra azaldığı belirlenmiştir. Deneysel verilerin regresyon analizi ile her iki cevap için istatistiksel olarak anlamlı model denklemler geliştirilmiştir. Yapılan optimizasyon çalışması sonucu optimum koşullar: pH 4, PT 8,30 g/L ve AF 18 L/sa olarak belirlenmiştir. Optimum koşullarda yapılan deneyler sonucu degredasyon yüzdesi %87±5 ve sarf edilen elektrik enerjisi 120±21kWh/m^3 olarak bulunmuştur. Kontrol deneyleri ile herhangi bir rejenerasyona ihtiyaç olmadan PST'nin yeniden kullanılabilirliği gösterilmiştir. Ayrıca mineralizasyon ve fotokatalitik degredasyon sırasında oluşabilecek olası ara ürünlerin varlığı Toplam Organik Karbon, Kimyasal Oksijen İhiyacı ve LC-MS analizleri ile araştırılmış ve olası bozunma reaksiyonu basamakları için öneride bulunulmuştur.

Anahtar kelimeler: Pestisit, Sızdırmazlık Potansiyeli, Adsorpsiyon, Fotokatalitik Bozunma, Deneysel Tasarım.

1.1   Literature review

Pollutants have multiple adverse effects on the environment by direct or indirect exposure. Pesticides are pollutants, which can reach water (drinking, surface and groundwater) [1, 2] by running off from treated plants and soils [1, 3]. Although they greatly contribute to the nutrition of a growing world population (projected to reach 9.8 billion in 2050, and 11.2 billion in 2100 [4], there is a concern about their presence in natural water resources. Thiamethoxam (THX), a neonicotinoid insecticide [5, 6], is used at application rates of 10-200 $g.ha^{-1}$ [7]. Despite interesting properties like flexible applications, favourable safety profiles, a broad spectrum and many others, THX is toxic, bio-accumulative and difficult to mineralize. It is therefore necessary to understand not only its fate in the environment, but also efficient disposal methods. The fate of THX in post-application is not well understood, and this can be assessed by its chemical properties and physicochemical properties of soil [5, 6]. Its half-life varies from 46.3 to 301 days depending on the conditions [8]. Klarich and coworkers (2017) recently reported for the first time the presence of neonicotinoids pesticides in finished drinking water at the concentration ranging from 0.24 to 57.3 ng/L and demonstrated their persistence during conventional water treatment [2]. This also proves that THX is not naturally eliminated in the environment.

Among the various available experiments in the literature for understanding the fate of pesticides in the nature, adsorption/desorption onto soil is still one of the most used method. Pesticides can be found in dynamic equilibrium partitioned between solid soil, solution and pores of soils once they enter into the soil. Thus, the sorption behaviour of

the soil governs the fraction of the residues present in soil solution phase available for leaching and water contamination [9]. There are just a few studies related to the fate of THX in the environment. These studies were reviewed and summarized below.

Banerjee and coworkers investigated the sorption of THX in three Indian soils by using Lindstrom model, the obtained K_d was between 0.17 and 6.40 and the K_{oc} was between 111 and 601 mL/g. They concluded that THX was in medium leaching potential category [10].

Adsorption of THX on Hawaiian soils was studied by Campbell et al. (2005). They found K_{oc} values of 0.23 and 0.53 mL/g for two different soils and 80% of THX adsorption [11].

Carbo et al. (2007) found K_{oc} values from 104 to 2877 mL.g^{-1}. By observing this almost 30 times variation of K_{oc}, they pointed out the doubts about the applicability of this coefficient to evaluate the potential of groundwater contamination. It was also concluded that the interaction of THX and mineral constituents of soil played an important role in the sorption process [12]. Traisup (2012) also reported that sorption of THX could not be explained just by the organic carbon content of soil [6].

The leaching potential of 71 pesticides was investigated by Papa and coworkers [13]. A multivariate approach was proposed using information from different environmental partition indexes: the Groundwater Ubiquity Score (GUS), the Modified LEACH (M.LEACH) Index and the Leaching Index (LIN) into a single ranking; the Global Leachability Index (GLI). This tool provided the prioritization of chemicals for an analytical survey [13].

Pesticide use in Turkey has been rapid growth since 1993 [14]. Unfortunately, there are very few studies on the fate of pesticides in Turkey's soils. Recently, Akay and coworkers (2017) performed a preliminary pesticide groundwater leaching potential assessment and ranked 157 organic pesticides commonly employed in Turkey [15]. By applying index-based approaches, 15 different indices were used. THX was ranked in the 12th position while the highest leachability was found for the "clopyralid" and the lowest for the "diafenthiuron". However, these kinds of theoretical works have to be verified by the laboratories and/or field experiments like the present study. It was not possible to find a study focusing on the fate of THX in Turkey's field. As several pesticides used throughout Turkey are not currently monitored, it may be useful to investigate the fate and the

transport mechanism in laboratory and field scale to predict possible environmental concentrations.

Conventional treatment methods tend to partially remove pesticides, which persist in the water. Several alternative water treatment methods are currently being investigated, including Advanced Oxidation Processes (AOPs), which introduce hydroxyl radicals into the medium. These radicals unselectively attack organic molecules, mineralizing them eventually into water and carbon dioxide [16, 17]. AOPs have been shown to be particularly effective at detoxifying low concentrations of micro-organic pollutants like pharmaceuticals and pesticides [18, 19, 20]. Heterogeneous photocatalysis with TiO_2 is an especially powerful AOPs [19] that has shown great potential as a low-cost, environmental friendly and sustainable treatment technology providing "zero" waste in water/wastewater treatments. The main technical barrier that impacts its commercialization is the drawback of the catalyst nanoparticles recovery after water treatment. Immobilization of TiO_2 nanoparticles onto the surface of a support material could facilitate the filtration at the end of the water treatment process.

In addition to being done on transparent materials like glass, immobilization is also carried out on opaque materials such as activated charcoal and metals [21]. In the case of opaque material, photons cannot reach TiO_2 particles deposited inside the pores, hence, photocatalytic activity decreases. Using light transparent glass-like supports suffers from the limited lifetime of the supported photocatalyst. This short lifetime is due to the instability of TiO_2 that can separate from the smooth surface of the support material. This situation will lead to a decrease in the photocatalytic efficiency just after a few cycles. In addition, an adsorptive affinity of the smooth surface for the contaminants would be low.

Several researchers have tried the use different support materials in order to improve the separation of photocatalyst after treatment without decreasing the photocatalytic efficiency of TiO_2. Ideally, a good support material for immobilization of photocatalyst should i) be chemically inert, ii) be enough transparent to provide passage of photons, iii) have porous structure, iv) have high adsorption potential for pollutants, v) not reduce photocatalytic efficiency, vi) strongly keep the photocatalyst physically and/or chemically, vii) allow the use throughout many cycles without a significant decrease of degradation efficiency [22]. Activated carbons [23], natural clays [24], glass plates, steel

fibers [25] glass slide [26] and perlite granules [27, 28, 25] have been used as support material in order to immobilize TiO_2 nanoparticles.

Lower density and higher light transparency compared to alternative porous materials such as zeolite, activated carbon and clays make perlite an ideal support material for photocatalysts. TiO_2 can be attached to the perlite surface with Ti-O-Si bonds. The bond formed will then be strong enough to make possible the development of a stable and reusable photocatalyst. The structure of TiO_2 do not change during immobilization process and TiO_2 / Perlite composite material has showed a fairly good performance [29]. In addition, the high porosity of perlite granules allows them to stay afloat on the water surface, making them unique among the support materials for photocatalytic degradation [25].

Mir et al. (2013) studied the photocatalytic degradation of thiamethoxam in an aqueous suspension of TiO_2. The degradation kinetics was investigated by using spectrophotometric method under numerous conditions like substrate concentration, catalyst type, catalyst dose, pH, and within the presence of electron acceptors (hydrogen peroxide, potassium bromate, and ammonium persulphate). All these parameters strongly influenced the process. The authors also demonstrated that with 265 nm UV wavelength, 125W Power, 1g/L of TiO_2 (Degussa P25) and 26.3 mg/L of THX, photocatalysis followed pseudo-first-order kinetics and could generate several intermediate products including clothianidin [30]. After testing three different commercially available TiO_2 photocatalysts (Degussa P25, UV100, PC500) on the degradation kinetics of model pollutant, Degussa P25 was found to be the more active photocatalyst for THX [30], the similar results have been reported earlier by other researchers [31].

Zabar et al. (2012) focused on photocatalytic degradation of imidacloprid, thiamethoxam and clothianidin by using a tailored photoreactor with six polychromatic fluorescent UVA (broad maximum at 355 nm) lamps and immobilised TiO_2 on glass slides. The disappearance was followed by high pressure liquid chromatography (HPLC) analyses, where the efficiency of mineralization was monitored by the measurements of total organic carbon (TOC). All molecules were degraded within two hours of photocatalysis, following first-order kinetics and several other transformation products were formed instead. The formation of clothianidin, as thiamethoxam transformation product, was additionally reported [26].

Urzedo et al. (2007) investigated the photodegradation of thiamethoxam in an aqueous medium, which was incessantly exposed to a UV radiation. The total organic carbon (TOC) content remained constant during the experiment, then, they concluded that THX was not mineralized but continuously converted into other compounds which were identified as part of their study by using LCMS [32].

The research papers dealing with the study of photocatalytic degradation of THX are usually considering high THX initial concentrations: Zabar et al. (2012) carried their study at 100 ppm [26], Mir et al. (2013) used 26.3 ppm [30], and 5 ppm was investigated by Pena et al. (2011) in the study of THX persistence in water [33]. Considering initial concentrations ranging from 50 to 300 ppm, Zhao et al. (2016) observed a decrease of removal percentage from 88.8 to 68.9% although the total amount of removed contaminants increased from 44.4 to 206.7 ppm [20]. Despite the fact that the comparison of these works is not possible because of different used AOPs, reactor types, UV wavelengths and radiation sources, we can say that the pollutant concentration is a very important parameter in water and wastewater treatment [20]. To our knowledge, THX concentrations under 5 ppm were not examined in the existing studies, whereas it is known that the TiO_2 photocatalytic reaction rate is dependent on the contaminant concentration [24, 34]. In some works, the degradation rate of pollutants increased with increasing the substrate concentration until a critical value and then declined [35, 36]. However, in other studies, the degradation percentage decreased with an increase of the initial concentration of the pollutant [37, 36]. Under similar operating conditions, a change in the initial THX concentration could give different results. It is thus important to investigate the photocatalytic degradation process of THX at low concentrations (< 5 ppm), especially as this pesticide was detected at a maximal concentration of 57.3 ng.L^{-1} in drinking water [2].

Optimization of process conditions in order to achieve high photodegradation rate is another concern to be solved. Researchers have tried to solve it by using a classical approach like initial factors and experimental approach [38]. There is now increasing recognition that traditional one factor at a time (OFAT) approach ought to be replaced by chemometric methods such as response surface methodology (RSM) based on the statistical design of experiments (DOE) [38]. OFAT approach examines the effect of each process parameter individually although RSM considers interaction effects between process variables by fewer experiments. Yang et al. (2014), optimized the photocatalytic

degradation kinetics of THX by using OFAT and central composite design based on the surface methodology. They also evidenced that, surface reactions with photon holes and $\cdot$OH on TiO_2 surface were responsible for THX photocatalytic degradation and that the thiophene ring was the most active site reacting with reactive oxidative species [34].

After reviewing the literature following findings can be concluded: (i) pesticides such as THX can reach water sources, hence investigating their fate in environment is essential for the prevention and remediation. (ii) photocatalytic degradation could be a useful alternative to the conventional treatment methods, (iii) depositing TiO_2 onto a support material would facilitate filtration after treatment, (iv) DOE methods can be effectively used for optimization photocatalytic degradation.

1.2 Objective of the Thesis

Firstly, it was aimed to understand the retention of THX pesticide in soil and its potential transfer to the aquifers with the study of sorption phenomena. Secondly, the process optimization for photocatalytic degradation of thiamethoxam (in presence of perlite supported TiO_2) by using response surface methodology was aimed.

For these purposes, following steps were carried out:

- Selection of one of the most used pesticide in the selected agricultural region. Then, Thiamethoxam (THX) was selected.

- Investigation of the fate of THX compared with THX in the commercial formulation, Eforia 247 ZC (THX-E), in soil by using batch adsorption/desorption studies. By this way, we will be able to estimate the potential environmental risk of THX.

- Preparation and characterization of perlite supported titanium dioxide (PST).

- Investigation the photocatalytic degradation of low concentration of THX at 365nm wavelength by PST.

- Determination the optimum conditions of photocatalytic degradation of THX by using Box-Behnken experimental design (BBD) method.

- Evaluation the reusability of PST without regeneration, degradation of THX at optimum conditions.

- Comparison the photocatalytic degradation of THX and THX in commercial formulation (THX-E)

- Investigation the possible intermediate product by using LC-MS and proposing a degradation pathway.

1.3 Hypothesis

A proportion of THX used in the agricultural land cannot be retained by soil and could therefore contaminate to the surface and/or groundwater. Fate of a pesticide in the environment can be followed by using adsorption/desorption studies on soil. Determining distribution coefficient between soil and water can provide to predict leachability index, which is used to specify possible environmental risk of the pesticide.

The use of TiO_2, the most effective photocatalyst, requires expensive nanofiltration step. Immobilizing TiO_2 by using perlite could be a good solution in order to overcome this problem due to the fact that perlite supported TiO_2 can be easily separated from the solution using flotation method. Photocatalytic degradation of THX with TiO_2/Perlite composite material could significantly reduce the amount of THX contamination in polluted water. The retention of THX by soil as well as its photocatalytic degradation could depend on whether it is in the commercial formulation or in pure form.

Box Behnken experimental design could be effective for optimizing the degradation process conditions in order to maximize degradation and to minimize electrical energy consumed during the degradation process.

GENERAL INFORMATION

Contaminants have been found in water from $ng.L^{-1}$ to $\mu g.L^{-1}$ levels, therefore, environmental pollution is a problem that is gaining more and more importance [35]. In order to better understand of this study, it is essential to provide brief information on pesticides in the environment, on treatment methods, and on modelling and optimization of treatment processes using Design Of Experiment (DOE).

2.1   Pesticides

Farmers have for several years been using synthetic products produced by the industry to protect their crops: the pesticides. That word is coming from English and has been gradually imposed in certain languages such as French, where the term phytosanitary product is often preferred [39]. According to United State Code (USC)(2012), a pesticide is a substance intended for preventing, destroying, repelling, or mitigating any pest (insects, mites, nematodes, weeds, rats, etc.) [40, 41]. The pesticide consumption has increased every day since the first use of synthetic pesticides in 1940 [38, 39]. The worldwide deaths and chronic diseases due to pesticides poisoning are about 1 million per year [1]. About 90% of the deaths caused by pesticides are registered in developing countries whereas they consume only 25% of world production [38, 39]. Today, we can find over 20,000 different pesticides with approximatively 900 different active ingredients [40]. They are generally used as insecticides (against insects), herbicides (against weeds), fungicides (against moulds and fungi), rodenticides (against rats, mice and moles) and fumigants (these are gas at room temperature and may kill all living organism). The formulation could include liquid, gel, paste, chalk, powder, granules,

pellets, and baits [40]. In Table 2.1, we can see the classification of pesticides according to their chemical composition [42]. The five main categories of active ingredients used in pesticides production are carbamates, organophosphates, organochlorides, pyrethroids, and neonicotinoids [41]. Neonicotinoids are derived from nicotine. They are effective on selected insects including aphids, whiteflies, thrips, leaf miners, beetles, and some lepidopteran species [41, 42]. The first neonicotinoids were available in 1991, and they have been used in many different applications, from seed treatment to field applications [23]. In this study, we focused on one of neonicotinoids, namely thiamethoxam.

Table 2.1 Pesticides classification according to the chemical composition

Group	Main composition
Organochlorine	Carbon chlorine, hydrogen and oxygen. Nonpolar and lipophilic
Organophosphate	Phosphorus atom, high stability and less toxicity. Aliphatic, cyclic or heterocyclic.
Carbamates	The base of the chemical structure is a plant alkaloid physostigma venenosum.
Pyrethroids	Similar to synthetic pyrethrins: an alkaloid
Biologicals	Viruses, microorganisms or their metabolic products.
Thiocarbamates	Their molecular structure contains an S group (thio) that also make the difference with carbamates.
Organosulfurs	The central atom is sulfur and they are very toxic to insects or mites,
Dinitrophenols	In their molecule, two nitro groups (NO_2) are bonded to a phenol ring.
Urea derivatives	Compounds which include the urea bound to aromatic compounds.
Neonicotinoids	Possess either a nitromethylene, nitroimine, or cyanoimine group.

2.1.1 Thiamethoxam (THX)

Thiamethoxam (THX) is the first commercial neonicotinoid insecticide belonging to thianicotinyl subclass and manufactured by Syngenta Ltd. [5, 6]. It is slightly cream fine crystalline powder at room temperature [39], it can be synthesized in only a few steps

from easily accessible starting materials with high yield. It has been developed both for foliar/soil application and seed treatment use in most agricultural crops all over the world. It is used for controlling of aphids, whiteflies, thrips, rice hoppers, rice bugs, mealybugs, leaf miners, white grubs, flea beetles, Colorado potato beetle, ground beetles, wireworms and some lepidopterous species [7]. Its low use dosages , flexible application methods, excellent efficacy, long-lasting residual activity and favourable safety profile make this insecticide well-suited for modern integrated pest management programmes in many cropping systems [43, 26]. THX interferes with a specific receptor site in the insect's nervous system. Insect feeding is irreversibly stopped after contact, and insect damage halts [41]. The molecule is widely preferred and frequently employed in the management of insect pests of various agriculture crops. [44]. The Neonicotinoids including thiamethoxam have received a lot of attention concerning their possible involvement with honeybee (Apis mellifera) die-off or Colony Collapse Disorder (CCD) in the United States and Europe [45]. That is why European Union (EU) member states have voted in favour of a total outdoor ban on three neonicotinoids pesticides (Clothianidin, imidacloprid and thiamethoxam) on April 2018, after being restricted to use on non-flowering crops since 2013 [46].

2.1.2   Lambda-cyhalothrin (λ-CHT)

Lambda-cyhalothrin is a pyrethroid insecticide used in agriculture, public health, construction and households. With a half-life more than three weeks, it is a colourless solid at room temperature but may appear yellowish in solution, the fate of lambda-cyhalothrin in aquatic ecosystem depends on the nature of system components such as suspended solids (mineral and organic particulates) and aquatic organisms (algae, macrophytes, or aquatic animals) [47].

2.1.3   Pesticide Formulation

The need for manufacturing a product, which has optimum biological efficiency, and convenient to use with lower toxicity, lead researchers to develop different pesticide formulations. Active ingredients are mixed with solvents, adjuvants, and fillers at required ratio in order to obtain the desired product called pesticide formulation. Physical forms or formulation are variable; water dispersible granules, dusts, aerosols, emulsifiable concentrates, flowable concentrates, solutions, solid baits, or liquid baits.

10

Using a pesticide molecule in a formulation has an impact on the pesticide release (on the soil or on the surface of the plant), the adsorption by the plant, its movement in the soil, and finally, the formulation influences leaching or runoff of pesticides in rain or irrigation water [46]. In our study, we selected Eforia 247 ZC (EFR) from Syngenta that contains a mixture of thiamethoxam and lambda-cyhalothrin. These molecules have large consumption and there is only limited number of studies about their fate in soils and waters.

2.1.4   Pesticides in Turkey

Pesticide use in Turkey has been rapid growth since 1993 [47]. However, farmers are not always well informed about application techniques, and this leads to excessive and unnecessary use [47]. There are very few studies on the fate of pesticides in general and THX in particular in the agricultural lands of Turkey. In 2014, the Turkish Ministry of Food, Agriculture and Livestock (GTHB) noted the use of 18 million 114 thousand kg of powder and 21 million 608 thousand liters of liquid pesticides in Turkey [48]. Figure 2.1 [48] shows the pesticide usage in Turkey in 2014 by class, it can be noticed that fungicides occupy the first place followed by herbicides, insecticides and the others.
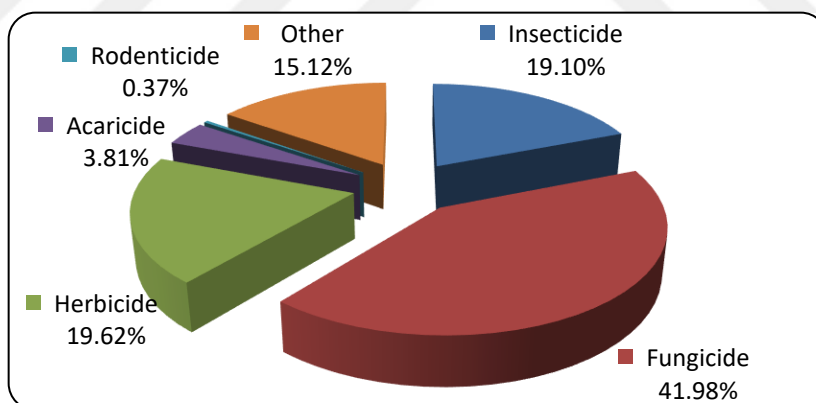
Figure 2.1 Turkey pesticide usage in 2014

Recently, Akay and coworkers (2017) has ranked THX in 12th position of leachability among the other 157 pesticides by applying index-based approaches using 15 different indices, while the highest leachability was found for the clopyralid and the lowest one was diafenthiuron [15]. The most used pesticides throughout Turkey has not been monitored, then, it would be useful to investigate the fate of them in the environment, and the transport mechanism in order to predict possible concentrations in the environment.

2.1.5 Environmental fate of pesticides

After releasing of pesticide into the environment, not all molecules reaches the target site [49], thus they may enter into the atmosphere, aquatic system and soil through drift, surface runoff, drainage and leaching [6]. The main parameters governing their fate in the environment are pesticide characteristics (water solubility, tendency to adsorb to the soil and the pesticide persistence), soil characteristics (clay, sand and organic matter content) and environmental conditions [6, 49]. Considering the point of fall of the pesticides in the environment after application, problems can be underlined on three levels, economic loss to farmers, inefficient control of pests, and environmental contamination [49]. Some progresses have been made on understanding the fate of pesticides in soil, however, there is still much to do.

The engineers responsible for the monitoring the quality of water resources, probably contaminated by pesticides, must answer the following questions [50]:

- What is the quality and quantity of pesticides used in the studied watershed?

- What is the frequency of the use and the application type?

- What is the risk level for groundwater?

- Which molecules should be searched first in the laboratory?

- What are the characteristics of the soil and the possibilities of exchanges between groundwater and river?

- How to select and implement measurement points?

In any case, the answer to these questions necessarily involves understanding phenomena such as volatilization, photodegradation, adsorption/desorption to/from soil and sediments, leaching, hydrolysis and biodegradation by which the pesticide will likely pass before ending up in the atmosphere, soils, surface water and groundwater. That ending point can vary according to the natural affinity for soil's solid matter (mineral matter and particulate organic carbon), liquid (solubility in water, surface and soil water), gaseous form (volatilization) and biota [42]. Figure 2.2 shows the different transformations that pesticides can undergo in the environment, we can notice that leaching, dilution, photolysis, hydrolysis and degradation occupies a preponderant place within these processes [42].
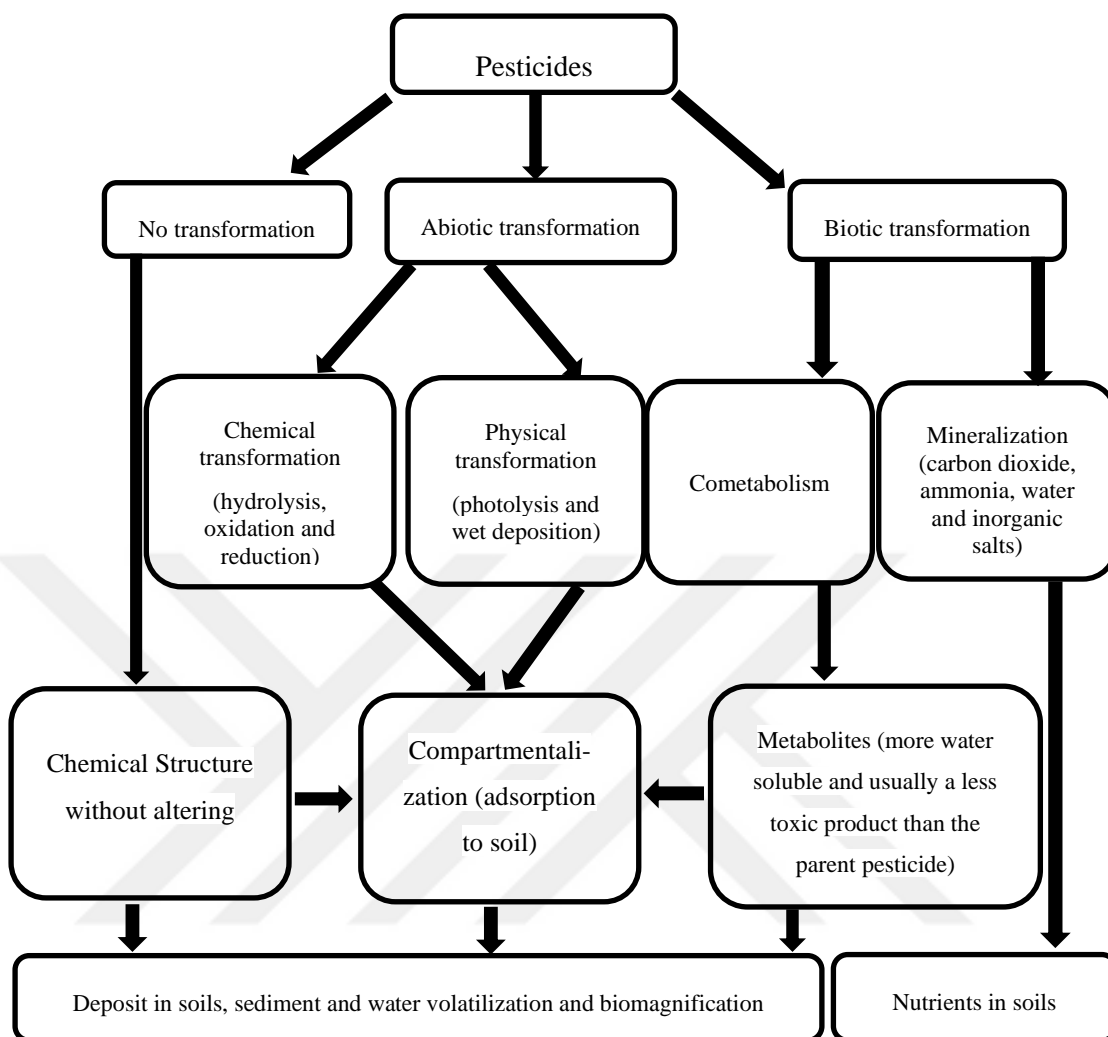
Figure 2.2 Fate of pesticides in the environment

2.1.5.1   Fate of pesticides in the atmosphere

Pesticides enter the atmosphere through volatilization either by application drift, post-application vapour losses or wind erosion of pesticide-treated soil. Volatilization that is the process whereby a pesticide changes in form from the solid and/or liquid phase into the gas phase [6], highly depend on the vapour pressure of the molecules (and its Henry's Law constant), soil sorption capacity, pesticide temperature and soil moisture [6, 50]. The atmospheric concentration of pesticide increases with temperature, according to Yeo et al. (2004), the re-volatilization of the pesticide from plant and soil surfaces could explain this situation [51]. THX volatilization is not expected to significantly contribute to its dissipation in the atmosphere because of its low vapour pressure and Henry's Law Constant [52]. Pesticides frequently detected in the atmosphere are organochlorine

insecticides, organophosphate insecticides, triazine herbicides and acetanilide herbicides [49]. It was found that an average individual organochlorine concentration ranged from 574 pg.m^{-3} to 3917306 pg.m^{-3} in Izmir/Turkey in 2003 [49].

2.1.5.2 Fate of pesticides in aquatic system

Many pesticides are present in water at low concentrations. They are often detected in surface waters in US and European countries [53, 2]. For example, metazachlor (herbicide) has been found at high concentrations in tap water in Etais-la Sauvin / France. This has led to the ban of consumption of these water since October 2016 by the prefecture and the Regional Agency of Health [54]. According to a report by the ''UFC-Que Choisir'' association, pesticides could be the leading cause of non-compliant tap water in France [55]. The factors, such as soil quality, pesticides properties and crop management practices, govern the potential for surface and groundwater contamination by pesticides [49]. The ecological impacts of pesticides in the aquatic system can be determined by toxicity, persistency, degradability and fate of them. Toxicity is usually expressed as LD$_{50}$ ("Lethal Dose": concentration of the pesticide which will kill half the test organisms over a specified test period). Persistency is measured as half-life (time required for the ambient concentration to decrease by 50%). Persistency is determined by biotic and abiotic degradational processes. Biotic processes are biodegradation and metabolism; abiotic processes are mainly hydrolysis, photolysis, and oxidation [56].

Pesticides enter surface waters (streams, rivers, lakes, reservoirs and oceans) through run-off, wastewater discharges, atmospheric deposition and spills [49]. Surface runoff streams and reservoirs supply approximately 50% of the drinking water in the World [49]. The pesticides susceptible to surface runoff are those within the runoff-soil interaction zone or the top from 0.5 to 1 cm of soil. Pesticides solubility also govern the pollution of the aquatic system by them [49]. The main factors affecting pesticide inputs into surface waters via drainage are soil texture, site, drainage system, pesticide molecule properties, weather, application rate and season. The total losses of most commercial pesticides are greater than 0.5% of the amounts applied. Pesticides with solubilities of 10 ppm or higher like THX are lost mainly in the water phase of runoff.

The solubility of the pesticide, the sandy soil, raining event shortly after spraying and the low pesticide adsorption can increase leaching. Renaud et al. (2004) suggested five factors that impact leached loads: presence of macropores, sorption capacity of soils,

degradation of pesticides in soil, sorption kinetics of pesticides and diffusion of pesticides into soil-aggregates [57]. A lysimeter experiment conducted by Beulke and his coworkers (2004) showed that an increase in the sorption of pesticide at higher temperature can result in less availability for leaching [6, 58]. This could increase the potential for groundwater contamination in hot regions and during the summer.

To understand how a chemical will accumulate in biota, bioconcentration factor (BCF) is used as an indicator. It is the accumulation of a chemical in living organisms compared to the concentration in water. Chemicals with high BCF generally have high toxicity in living organisms, low water solubility, large K_{ow} (octanol/water partition coefficient) and a large soil adsorption coefficient [59]. Since living organisms do not always have specific mechanisms for eliminating pesticides, they will accumulate in the species at the end of the food chain, including humans and reach concentrations up to 1000 times higher than the initial concentrations in water [59]. Biomagnification or bioaccumulation is the increase in the concentration of a chemical as it moves through a food chain [60].

2.1.5.3 Fate of pesticides in soil

The soil is a natural body of mineral and organic constitution differentiates in horizons of varying thickness, which differs from the underlying material in its morphology, physical and chemical properties, composition and biological characteristics. It is a porous medium that can contain a liquid phase (the soil solution) and a gaseous phase (the soil atmosphere) that can move. The soil has several functions namely: the biological environment function, the environmental function because of the important role it plays in the determinism of the quality of the water, the air and the food chain, the technological function gathering the function mechanical support and source of materials and finally the socio-economic function [9]. The main factors that theoretically influence the Pesticide Residues in the soil are presented in Table 2.2 below [61].

Table 2.2 Factors affecting pesticide residue in soil

Pesticide factors	Water solubility, vapor pressure, pK_a, pK_b, stability, polarity, ionizability
Soil factors	Soil texture and structure, the content of organic matter, salinity, moisture content, porosity, temperature, pH, cation exchange capacity (CEC), permeability, kind and content of heavy metals ions, kind and population of microorganism, hydraulic conductivity
Agricultural factors	Cropping pattern, cropping practices, crop type, pesticide formulation, application method, time and rate, frequency and times, irrigation time and volume.
Environmental factors	Rainfall, air temperature, evapotranspiration, illumination intensity and duration, wind

Adsorption/desorption onto soil is one of the most widely used method among the available techniques in the literature dealing with the behaviour of pesticides in the environment [62], it is the key for process controlling contaminant migration where chemical equilibrium exists [63]. Once the pesticide molecules enter into the soil system, they are dispersed between solid soil, solution phase and soil pores maintaining dynamic equilibrium. Therefore, the sorption behaviour governs the fraction of residues present in soil solution phase, in which it is available for leaching and groundwater contamination [62]. The soil sorption coefficient, K_d, (the amount of the pesticide in the solution divided by the amount of adsorbed to the soil) and the soil organic carbon sorption coefficients, K_{oc} of pesticides are used by environmentalist and regulatory agencies worldwide for describing the environmental fate and behavior of pesticides. K_{oc} is regarded as a 'universal' parameter related to the hydrophobicity of the pesticide molecule, which applies to a given pesticide in all soils [64]. Although this assumption is known to be inexact, it is used for modeling and estimating the risk of pesticide leaching and runoff. In addition, for soils, it is common knowledge that contaminant adsorption can deviate from the linear relationship required by the K_d [64]. Table 2.3 shows the mobility of the pesticide in the soil as a function of K_{oc} and K_d distribution coefficient [65]. We can see that the lower K_{oc} and K_d, the more likely the pesticide will move in the soil and therefore pollute the groundwater. Low adsorption in the soils leads to a great leaching amount [66, 67].

Table 2.3 Mobility classification based on soil distribution coefficients of pesticide

$K_{oc}(mL.g^{-1})$	$K_d(mL.g^{-1})$	Mobility	Class (typical)
0-50	0-0.5	Very high	Aliphatic acids
50-150	0.5-1.5	High	Carbamates
150-500	1.5-5.0	Medium	Benzoic acids
500-2000	5.0-20	Low	Triazine
2000-5000	20-50	Slight	Organophosphates
>5000	>50	Immobile	Organochlorines

2.2   Adsorption of pesticides onto soil

The study of pesticide adsorption on soil can help us to understand the kinetics of pesticide retention by soil and also to determine the different models for describing adsorption, hence, drawing scientifically sound conclusions. In all cases, the kinetic and equilibrium studies are the different steps taken during adsorption studies.

2.2.1   Adsorption kinetics

Adsorption process can be followed by taking into account the number of particles adsorbed per unit time. The prediction of the adsorption rate, which is generally used in the design and modeling of adsorption process, can be made by using kinetic parameters [68]. The Lagergren's pseudo-first order kinetic model (Eq. 2.1) and pseudo-second order model (Eq. 2.2) can be used in order to determine these kinetic parameters [69, 70].

The Lagergren's pseudo-first order kinetic model can be expressed as follow:

$$\ln(q_e - q_t) = \ln q_e - k_1 t \qquad (2.1)$$

k_1 (min^{-1}) is the pseudo first-order rate constant, q_e and q_t are the amount of solute adsorbed (mg.g^{-1}) at equilibrium and time t (min), respectively.

k_1 and q_e can be determined from the slope and the intercept of the plot of $\ln(q_e$-$q_t)$ versus t, respectively.

The pseudo-second order adsorption kinetic model is expressed as follow [69, 70]:

$$\frac{t}{q_t} = \frac{1}{k_2 q_e^2} + \frac{1}{q_e} t \qquad (2.2)$$

k_2(mg.g^{-1}.min^{-1}) is the pseudo-second-order rate constant.

k_2 and qe can be determined from the intercept and slope of the plot of t/q_t versus t, respectively.

2.2.2 Adsorption Isotherm Models

Langmuir and Freundlich models are frequently used in the literature to describe the adsorption of molecules at the solid-solution interface.

2.2.2.1 Langmuir model

Langmuir isotherm model defines the monolayer adsorption onto the homogeneous adsorbent surface. The linear form of the Langmuir isotherm is [71]:

$$\frac{1}{q_e} = \frac{1}{q_m K_L C_e} + \frac{1}{q_m} \qquad (2.3)$$

where K_L is the Langmuir equilibrium constant (mg.L^{-1}) and q_m the maximum monolayer pollutant concentration in the solid phase (mg.g^{-1}).

In practice, $1 / q_e = f (1 / C_e)$ is plotted with the experimental data, then, q_m and K_L parameters are derived from the intercept and slope of the line, respectively.

2.2.2.2 Freundlich model

Freundlich isotherm model defines the adsorption onto the adsorbent with the heterogeneous surface. The linear form of Freundlich adsorption isotherm model is as follow [72]:

$$\log q_e = \log K_F + n \log C_e \qquad\qquad (2.4)$$

where q_e is the equilibrium concentration in the solid phase (mg.L^{-1}), C_e is the equilibrium concentration in the aqueous phase (mg.L^{-1}), K_F (L.g^{-1}) and n are Freundlich constants.

The parameters K_F and n are determined by plotting the function $\log q_e = f (\log C_e)$ from the experimental q_e and C_e data. The straight line obtained has a slope equal to n and a y-intercept equal to $\log K_F$.

2.2.2.3   Distribution coefficient, K_d

Distribution coefficient (or partition coefficient), between the solid and the liquid phases, K_d, is determined by plotting q_e as a function of C_e (Eq.2.5).

$$K_d = \frac{q_e}{C_e} \qquad\qquad (2.5)$$

This model corresponds to Freundlich model when n is equal to 1. THX adsorption isotherm data are fitted by Ordinary Least Square (OLS) Regression. The K_d values correspond to the slope of the linear fit through zero. Normalization of the K_d based on organic carbon content (% OC) (Eq. 2.6) is frequently used due to the fact that organic carbon is widely identified as the primary adsorbent of hydrophobic organic compounds,

$$K_{oc} = \frac{K_d.100}{\%OC} \qquad\qquad (2.6)$$

Distribution coefficient on the base of organic carbon content (K_{OC}), the solubility, Henry's Law Constant (K_H) and the n-octanol/water partition coefficient (K_{OW}) are generally used in order to predict environmental fate of the pesticide.

2.3   Natural degradation of pesticides in the environment

Natural processes such as photodegradation, hydrolysis and biodegradation may lead to the removal of pesticides from different compartments of the environment.

2.3.1   Photodegradation

Photodegradation is the most important abiotic transformations for pesticides in the aquatic environment. By this process, the high energy of sunlight causes bond scission, cyclization, and rearrangement [73]. Photodegradation includes processes of photolysis and phototransformation. Photolysis occurs when compounds receive enough energy

from either visible and/or ultraviolet light to cause the breakdown of the molecule. Light can degrade the pesticides in the aqueous phase, in soil (first millimeters from surface) or on the surface of plants. The intensity of the light and the proportion of ultraviolet radiation with a wavelength between 10 and 400 nanometers strongly influence the rate of degradation [6, 65].

2.3.2 Hydrolysis

Hydrolysis is an important reaction which takes place in water for pesticide degradation. Hydrolysis of a pesticide is a reaction with a water molecule catalysed by proton, hydroxide, or sometimes by inorganic ions present in the aquatic environment [74]. Organophosphorus pesticides are primarily susceptible to alkaline hydrolysis with less acidic catalysis, but some of phosphorodithioates are found to be acid labile. In the case of carbamates, the pKa value of a leaving group is known to control its hydrolysis mechanism [74]. The pH of the water affects the hydrolysis rate of some pesticides [75]. Huil et al. (2010) showed that in the case of chlorpyrifos, by increasing pH or temperature of the solution, degradation increased [76].

2.3.3 Biodegradation

Biodegradation is the degradation process of substances by the action of aerobic or anaerobic microorganisms such as plants, algae, bacteria or fungi. It is often applied for the degradation of pollutants. Material can be said to be biodegradable if it is capable of undergoing under the action of microorganisms a decomposition process to form the simple molecules like carbon dioxide, methane water, nitrates, nitrites or sulphates. The biodegradation can be completed or not; however, incomplete biodegradation may have a negative impact on the environment. For example, a safe substance can be converted into a toxic substance. The natural environment is suitable for biodegradation but some modifications can be brought to encourage the organisms to degrade the pollutant at a faster rate in a limited time frame, for example by adding air as it is done during the biological treatment of wastewater [77]. The mechanisms and factors affecting the biodegradation are very important in order to choose the best bioremediation strategy. The main factors which limit the overall biodegradation rate are contaminant characteristics, bioavailability, microorganism's number, catabolism evolution, the

availability of essential nutrients (carbon, nitrogen and phosphorus and also oxygen), soil type, humidity, temperature and pH [78].

2.4 Treatment methods for pesticides pollution

Once it enters the water, a pesticide may be naturally degraded or adsorbed by suspended solids; in case of persistency, water quality will be affected, and additional or special treatment will be necessary before using water. The prioritization of pollutants may be used as a first step. After defining the strategy in the year of 2000 to spot the priority of substances regarding aquatic ecosystems, the environmental quality standards (EQS) was defined in 2008 and in 2013, it had been launched the Directive 2013/39/EU, which highlight the necessity to develop new water treatment technologies to handle such issues [79].

Thermal, chemical, physical and biological treatment methods can be used for the removal of pesticides from wastewater. In recent years, advanced oxidation processes have become more attractive for water treatment as compared to conventional treatment. Given the techniques used in our study, we only provided here the background and principle of adsorption, and photocatalysis (one of the advanced oxidation processes, AOPs).

2.4.1 Advanced oxidation processes (AOPs)

AOPs are treatment processes, which involve the formation of hydroxyl radicals ($^{\bullet}OH$) for water and wastewater at room temperature and pressure [80]. Hydroxyl radicals can destroy recalcitrant compounds or, at least, can transform them into biodegradable species [79]. These methods are environmentally friendly and they do not transfer pollutants from one phase to another like adsorption; they do not produce massive amounts of sludge like biological treatment. In addition, AOPs used to oxidize complex organic constituents found in wastewater are made in ambient temperature and pressure [81]. A powerful oxidant, hydroxyl radicals ($^{\bullet}OH$) can degrade all types of organic pollutants into harmless products up to their mineralization. This can be explained by the fact that $^{\bullet}OH$ radical has the highest oxidation potential (2.80 ev) after fluoride (3.03 ev).

Advanced oxidation comprises a range of similar but different chemical processes aimed at tackling pollution in water, air and soil [82]. This method can be divided into four categories: AOP based on photolysis (UV, UV/H_2O_2), AOP based on ozonation (O_3,

O_3/UV, O_3/H_2O_2, $O_3/H_2O_2/UV$), AOP based on the Fenton reactions (Fe^{2+}/H_2O_2, $Fe^{2+}/H_2O_2/UV$, $Fe^{3+}/H_2O_2/UV$, Electro-Fenton), and AOP based on semiconductors (TiO_2/UV): photocatalysis.

2.4.2   Photocatalysis

Heterogeneous photocatalysis is the second most used treatment method to destroy pollutants defined in the Directive 2013/39/EU of European Union [79]. Photocatalysis uses semiconductor metal oxides such as TiO_2, which is chemically inert, non-toxic, easy to obtain, inexpensive, and have high photoactivity. As the most promising photocatalyst, TiO_2 is expected to play an important role in helping solve many serious environmental and pollution challenges [83].

Although TiO_2 is very effective photocatalyst used in photocatalytic degradation processes, it requires very expensive nanofiltration step after usage in water treatment. In order to allow the photocatalytic treatment of water and wastewater to take its real place among the other treatment methods, immobilization of TiO_2 nanoparticles seems to be one of the first steps that will lead to increase of the industrialization of the process [25].

2.4.2.1   Principle of photocatalysis

The photocatalyst materials employed are, semiconductors, often oxides or sulfites (TiO_2, ZnO, CeO_2, ZrO_2, SnO_2, CdS, ZnS, etc.). The electronic structure of the semiconductors is characterized by a valence band (fully filled) and a conduction band (completely empty). Light action on its surface causes a jump of electrons from the valence band to the conduction band [84]. This phenomenon leads to the formation of a positive hole with the consequence of the presence of an oxidizing and a reducing site on the surface of the semiconductor [84]. The energy of the photons must be greater than or equal to the energy difference between the valence and conduction bands. In the case of TiO_2 the difference in energy between the valence and conduction bands is 3.02 eV, this imposes radiation such that $\lambda < 400$ nm. The recombination of electrons and holes is the main factor limiting the oxidation rates of organic substances. For effective photocatalysis, this fast recombination must be avoided. This is made possible by the transferring and trapping of free charges to intermediate energy levels (structural irregularities or adsorbed molecules).

The reactions on the surface of the UV-induced TiO_2 particle are listed below:

1. Formation of electron-hole pair:

$$TiO_2 + hv \rightarrow e^- + h^+ \tag{2.7}$$

2. Reaction with adsorbed water molecule on surface and h⁺ migration to catalyst surface:

$$TiO_2(h^+) + H_2O_{ads} \rightarrow TiO_2 + HO^\cdot + H^+ \tag{2.8}$$

3. In the electron transfer, molecular oxygen acts as an acceptor and e^- migrates to the catalyst surface: Denklemi buraya yazın.

$$TiO_2(e^-) + O_2 \rightarrow TiO_2 + O_2^- \tag{2.9}$$

$$O_2^- + H^+ \rightarrow HO_2^\cdot \tag{2.10}$$

$$O_2^- + 3HO_2^\cdot \rightarrow HO^\cdot + 3 O_2 + H_2O + e^- \tag{2.11}$$

$$2HO_2^\cdot \rightarrow H_2O_2 + O_2 \tag{2.12}$$

$$H_2O_2 + TiO_2(e^-) \rightarrow TiO_2 + HO^- + HO^\cdot \tag{2.13}$$

4. Disintegration of organic substances adsorbed by hydroxyl radicals formed on the semiconductor surface

$$HO_2^\cdot + \text{Organic substance} \rightarrow \text{by products} \rightarrow CO_2 + H_2O + \text{mineral acids} \tag{2.14}$$
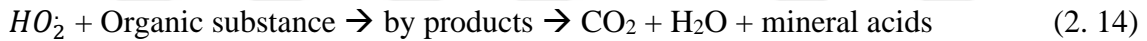
5. Finally, recombination of electron and hole occurs and reaction is terminated:

$$TiO_2(e^-) + TiO_2(h^+) \rightarrow \text{heat} \tag{2.15}$$

$$TiO_2(e^-) + \cdot OH_{ads} \rightarrow TiO_2 + OH \tag{2.16}$$

In Figure 2.3, the schematic diagram of the generation of oxidative species during the photocatalytic degradation of pesticide is shown.
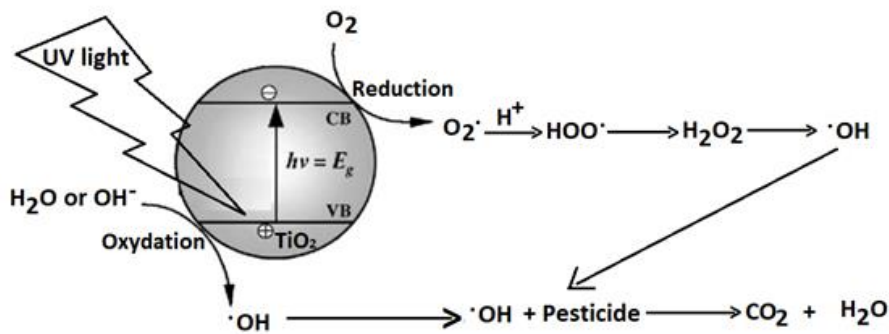
Figure 2.3 Representative diagram of the principle of photocatalysis

Several factors can determine the outcome of the photocatalysis reaction like: UV dose, pollutant concentration, initial pH of the solution, degradation time, oxygen, hydroxyl radical production rate, etc.

2.4.2.2 Photocatalytic degradation kinetics

Numerous researchers showed that the degradation rates of photocatalytic oxidation of various organic contaminants fitted the Langmuir–Hinshelwood (L– H) kinetic model over illuminated TiO_2.

$$r = \frac{dC}{dt} = \frac{kKC}{1+KC} \tag{2. 17}$$

where r is the reaction rate ($mg.L^{-1}.min^{-1}$), C is the concentration of the reactant ($mg.L^{-1}$), t is the illumination time in minutes, k is the reaction rate constant (min^{-1}), and K is the adsorption coefficient of the reactant ($L.mg^{-1}$).

For the solution with low initial concentration the equation can be simplified to a pseudo-first-order equation.

$$r = kKC = k_{app}C \tag{2. 18}$$

Integration of 2.18 gives:

$$ln\frac{C_0}{C} = k_{app}t \tag{2. 19}$$

A plot of ln C_0/C versus time represents a straight line, the slope of which upon linear regression equals the apparent first-order rate constant k_{app} (or just k). Generally, first-order kinetics is appropriate for the entire concentration range of ppb or a few ppm [85].

2.4.2.3 Photocatalyst loading

The degradation rate of pollutant may increase with increasing catalyst concentration and sometimes becomes constant above a certain level and then decreased after an optimum dose. One reason for this is a clustering of catalyst particles at higher concentrations and thus leading to a decrease in the number of active sites on its free surface. The decrease in degradation is thus due to the decrease in surface area of the catalyst due to aggregation of TiO_2 [16, 24]. The excess catalyst particles can create a light screening effect that reduces the surface area of TiO_2 being exposed to light illumination and the photocatalytic efficiency so that the reaction rate would indeed be lower with increased catalyst dosage. Increasing the amount of photocatalyst beyond the saturation level results in an increase

in turbidity, which results in a decrease in the rate of adsorption of light. Then, the rate of the catalyst and light scattering effect must be considered with more attention [24].

2.4.2.4   Initial pH of the solution

An organic molecule exists as a neutral state at pH below its pKa value, and above this pKa value it attains a negative charge. Some molecules can be positive, neutral or negatively charged in aqueous solution depending of pH. This variation impact significantly their adsorptive behaviour, hence, photocatalytic degradation of them. Therefore, the pH of the solution can play a key role in the adsorption and photocatalytic oxidation of pollutants. The ionization state of the surface of the photocatalyst can also be protonated and deprotonated under acidic and alkaline conditions, respectively. Moreover, the pH of the solution affects the formation of hydroxyl radicals by the reaction between hydroxide ions and photo-induced holes on the TiO_2 surface [24]. The positive holes are considered as the major oxidation steps at low pH, whereas hydroxyl radicals are considered as the predominant species at neutral or high pH levels. It would be expected that the generation of $^{\bullet}OH$ is higher due to the presence of more available hydroxyl ions on the TiO_2 surface. Thus, the degradation efficiency of the process will be enhanced at high pH [86].

2.4.2.5   Oxygen

Dissolved Oxygen (DO) has electron scavenger role in TiO_2 photocatalysis reaction. Depending on the degradation reaction mechanism, oxygen might hinder or improve the photodegradation rate. Pure oxygen has shown more effective relative to air for the enhancement of decontamination. Adsorption of oxygen on the titanium dioxide surface was proved by several researchers [24]. An excessive amount of oxygen can decrease the degradation rate.

2.5   Design of Experiment (DOE)

Statistical methods are used in the analysis of data brought together to obtain pieces of information from observations and to give a sense to representative numbers. The purpose of statistical analysis is to find or reveal a relationship between data. [87]. Experiments are often conducted in a serie of trials or tests that produce quantifiable outcomes. For continuous improvement in product/process quality, it is fundamental to understand the process behaviour, the amount of variability, and its impact on processes. One of the

common approaches employed by many engineers for experimentation in companies is one-variable-at-a-time (OVAT) where engineers vary one variable at a time keeping all other variables fixed. One variable-at-a-time experiment is often unreliable, inefficient, time-consuming, and may yield false to the optimal condition for the process [88]. DOE allows finding a suitable approximation of the true relationship between a response and independent variables [89, 90]. DOE also helps to understand the interrelationships between factors that are called factor interactions.

When examined from the point of view of laboratory and time, it is stated that statistically designed experiments provide about tenfold earnings. Today, almost every branch finds a wide range of design of experiment applications, especially in biology, physics, chemistry, engineering, economics, astronomy, psychology, sociology, agriculture and transportation [91].

Scientists or engineers in charge of DOE deal with Factorial Designs, 2^k Factorial Design, 2-level Fractional Factorial Designs, 3-level and Mixed-level Factorials and Fractional Factorials, Response Surface Designs and Robust Parameter Designs. We will mark a breakpoint just on Response Surface Methodology.

2.5.1 Response Surface Methodology (RSM)

RSM is a collection of mathematical and statistical techniques useful for the modelling and analysis of problems, in which a response of interest is influenced by several variables. Central Composite Designs (CCD) and Box-Behnken Designs (BBD) are two of the major RSM. BBD will be investigated here in detail.

2.5.2 Box Behnken Design (BBD)

The Box-Behnken design (BBD) is a useful statistical tool for the optimization of different processes and provide estimation of quadratic models [92]. In this method, the leading objective is to optimize the response surface that is influenced by different parameters [93, 94].

A geometrical view of BBD for three factors is illustrated in Figure 2.4, 12 edges of the cube correspond to 12 experimental runs. The center of the cube can be considered as the center of the field of study. 3-factors BBD plan with three central experiments has 12 + 3 = 15 experimental runs as it can be seen in Table 2.4 [95, 96].

26

Table 2.4 Experimental Matrix used for BBD

Run	Pattern X₁	X₂	X₃	Run	Pattern X₁	X₂	X₃	Run	Pattern X₁	X₂	X₃
	X_1	X_2	X_3		X_1	X_2	X_3		X_1	X_2	X_3
1	-	0	-	6	0	-	-	11	0	0	0
2	0	+	-	7	+	-	0	12	0	-	+
3	+	+	0	8	0	0	0	13	-	-	0
4	0	0	0	9	+	0	-	14	0	+	+
5	+	0	+	10	-	0	+	15	-	+	0

Centre point
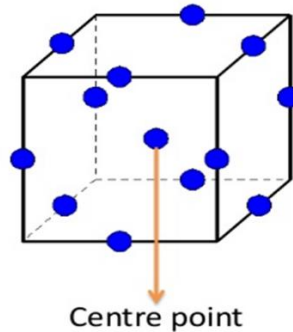
Figure 2.4 A geometrical view of BBD for three factors

One advantage of BBD is that it does not contain a combination for which all factors are simultaneously at their highest or lowest levels. So, these designs are useful in avoiding experiments performed under extreme conditions, for which unsatisfactory results might occur. Conversely, they are not indicated the situations that we would like to know the responses at the extremes, that is, at the cube vertices [89, 90].

2.5.3   Statistical analysis of the DOE results

Statistical tools must be used in order to check all the assumptions made upstream of experimental design. These tests allow evaluation of the quality of the model (descriptive and predictive), and its validation (analysis of the variance).

2.5.3.1   Analysis of the Variance (ANOVA)

ANOVA allows comparing the variances of the values calculated by the model and the residues. It is a statistical test (Fisher-Snedecor test) that provides the answers to the two following questions:

- Does the model bring us something? Is the regression significant? Does it explain to a large extent the observed variations of the response? This is the test of the global significance of the regression that we will call the validation test A.

- Does the model represent the phenomenon? If yes, the model introduces an acceptable bias otherwise, it is necessary to look for another one. The first validation, therefore, concerns the analysis of model residues. We will call this step, the validation test B.

Validation test A

The Ficher-Snedecor (F_1) test provide if the model brings something, if the equation establishes a relation between the variation of the factors and the answer, or if it is due to a change, a fluctuation random response in the experimental domain. Table 2.5 summarizes the different calculations and ratings of test A. The details are as follow. MSAS (model sum of the average squares) is calculated with the following equation:

$$MSAS = \sum_{i=1}^{N}(y_i - \bar{y})^2 \qquad (2.20)$$

with $df_{SAS} = P-1$ $\qquad (2.21)$

(df_{SAS} = degree of freedom of Sum of Average Squares)

RSS (Residus Sum of Squares)

$$RSS = \sum_{i=1}^{N} \varepsilon_i^2 \qquad (2.22)$$

with $df_{SAS} = P-1$ $\qquad (2.23)$

TSS (Total Sum of Squares)

TSS=MSAS+RSS $\qquad (2.23)$

The correlation coefficient can also be calculated using these ratings

$$R^2 = \frac{SAS}{RSS} \qquad (2.24)$$

and we get

$$R^2_{adjusted} = 1 - \frac{RSS/(N-p)}{TSS/(n-1)} \qquad (2.25)$$

with

$$F_1 = \frac{MSAS/(p-1)}{RSS/(N-p)} \qquad (2.26)$$

Table 2.5 Summarizes of the different calculations and ratings of test A

Source	Sum of squares	df		F test	Probability
Model	MSAS	p-1	SAS/ p-1	F_1	ProbF$_1$
Residus	RSS	N-p	RSS/ N-p		
Total	TSS	N-1			

The larger the ratio, the fewer residue is, in this case, we can say that the model provides suitable information. In practice, we use computer software to do this.

The F_1 report expresses the ratio of two variances. For the ith treatment of the experimental design, the observed value y_i of the test result represents a particular value of the random variable characterizing the response for this treatment. Therefore, the F_1 statistic itself is a random variable whose values follow a theoretical distribution function, called the law of F or the law of Snedecor.

Here the hypothesis H_0 of the Ficher-Snedecor test is as follows:

the model does not make it possible to describe the variation of the test results. We use this law to know from what particular value, called critical value, the numerator of the quantity F_1 is significantly higher than the denominator. F_1 tells us about the ProbF$_1$ probability of rejecting the null hypothesis. The lower this probability is, the better for model conservation and below 5% we are not right to reject the model.

Validation test B

Although the difference between the observed values and the values calculated by the model have been minimized by the choice of the least squares method, it is necessary to ensure that the residues are not abnormally large locally. Table 2.6 summarizes the different calculations and ratings of test B. First, we calculate from the equation of the model the different y_i, we obtain the value of the residues:

$$\varepsilon_i = y_i - \hat{y}_i \tag{2.27}$$

We then calculate the residues sum of squares noted RSS:

$$RSS = \sum_{i=1}^{N} \varepsilon_i^2 \tag{2.28}$$

RSS=LFE1 + PE (2. 29)

With LFE1 the error due to the lack of fit of the model also called the bias or the Lack of Fit.

PE the pure or natural error also called Pure Error.

To estimate whether what one obtains is acceptable, one carries out a test of Fischer-Snedecor or law of F. Or, the law of F depends on the number of degrees of freedom (ddl) of each of the two populations.

with

$$F_2 = \frac{LFE1/df_{LFE1}}{PE/df_{PE}}$$ (2. 30)

Reminder on the degree of freedom: the number of degrees of freedom of the model is the sum of the actions which it comprises. The degree of freedom of action represents the number of coefficients that the regression will make it possible to estimate.

Then we have:

$df_{RSS} = df_{LFE} + df_{PE} = N-p$ (2. 31)

The test F (F_2) will be made by setting a null hypothesis (Ho: null hypothesis that the ratio is equal to 1, that is to say, if the residues linked to the model are the same order of magnitude as the natural error we test if the model is fair and faithful). We will obtain the probability (ProbF2) of finding a ratio equal to 1. We will say that above 5%, we have no reason to reject the model.

$ProbF_2 > 5\%$ => No reason to reject the model.

This test is feasible only in the presence of repetitions which makes it possible to know PE.

Table 2.6 Summarizes the different calculations and ratings of test B

Source	Sum of squares	df		F test	Probability
Lack of Fit	LFE	df_{LFE}	$SCE1/ddl_{SCE1}$	F_2	$ProbF_2$
Pure Error	PE	df_{PE}	$SCE1/ddl_{SCE2}$		
Residues	RSS	df_{RSS}			

The non-significant lack of fit relative to the pure error (ProbF2>0.05) indicates good predictability of the model. The low coefficient of variation indicates high precision and good reliability of the experimental values [97, 98].

The hasty conclusions are not welcome here because:

- If we have a very low "error" and a bad "validity", we can also have a good regression,

- If we have a very low "error" and a good "validity", we can also have a bad regression.

In summary:

Best is the fit of the model if:

R^2 is close to 1

ProbF1 <5% F_1 as small as possible

Prob F2> 5% F_2 as large as possible [99, 100].

MATERIALS AND METHODS

3.1   Materials and Methods for the study of Pesticide Fate

3.1.1   Selected agricultural area

Tekirdağ, with an area of 6.313 km², is surrounded by Istanbul, Kırklareli, Edirne, Çanakkale and Marmara Sea [101]. Climate of Tekirdağ is defined as mildly semi-moist. Tekirdağ is usually rainy and its climate allows intensive agriculture. The overground water potential is 713.00 hm³/year, and due to the pollution coming from industries, agricultural areas and municipal wastewater discharge, the surface waters are highly polluted [101]. According to the report from Tekirdağ Water and Sewerage Administration [102], 92% of water distributed to drinking water network originates from groundwater, 5% from the pond and the rest from the other sources. The groundwater quality has decreased gradually due to the intensive agricultural activities in Tekirdağ. Therefore, it is very important to understand the behavior of pesticides in contact with the soil [101, 102].

3.1.2   Soil

The three soil samples used in this work were extracted from Muratlı, Hayrabolu and Malkara region in Tekirdağ. Sampling points were selected based on the geography of the region, farmers' habits as well as the exposure to pesticides. The codes given to the soil samples points for simplification purposes in this work are as follows: Muratlı (S_1), Hayrabolu (S_2) and Malkara (S_3). Procedure reported by Boudescocque and coworkers (2006) was followed for sampling soil [103]. In practice, five samples of each soil were taken from the upper 20 cm layer, and then they were blended together in order to obtain

a homogeneous soil sample. Each blend was then manually ground to keep their structure [9], sieved under 2 mm, then open air dried before characterization and sorption experiments.

3.1.2.1 Characterization of the soil samples

After preparation of soil samples, their physical and chemical properties were determined. Soil textural analysis was carried out by the size distribution of soils in the Departmental Laboratory of Analysis and Research (LDAR) in University of Champagne Ardenne (France). Other characteristics such as the organic carbon content (OC) and limestone, pH and the Cation Exchange Capacity (CEC) were also determined. All these analyses were conducted according to the standards of the French Association for Standardization (AFNOR) [104, 105, 106, 107, 108] as it can be seen in Table 3.1.

Table 3.1 Soil analysis and corresponding AFNOR standards

Soil analysis	AFNOR
Size without decarbonization	NF X 31-107 [104]
pH$_{Water}$	NF ISO 10390 [105]
organic carbon	NF ISO 14235 [106]
cation exchange capacity	NF X 31-130 [107]
total limestone	NF ISO 10 693 [108]

Particle size analysis shows the distribution of mineral soil particles by size (clays, silts, sands) and determines the soil texture. Prior to this analysis, soils were oxidized with hydrogen peroxide in order to degrade the Organic Matter (OM), which acts as a cement between the aggregates. The particle size was determined without decarbonization of soils.

Organic carbon (OC) content was determined after treatment of soil by a powerful oxidant, the potassium dichromate in sulfuric acid medium. Dichromate ions (Cr^{6+}), which are originally orange, become green blue (Cr^{3+}) due to the oxidation of the organic fraction. The intensity of this color that is proportional to the amount of oxidized carbon was measured spectrophotometrically at 585 nm wavelength. OM content is then calculated from the OC using the formula:

$$OM = 1.72\%OC \qquad (3.1)$$

The total limestone amount was determined by the soil digestion with hydrochloric acid. The reaction released carbon dioxide (CO_2) coming from the dissolution of calcium carbonate ($CaCO_3$). A known amount of pure calcium carbonate was treated in the same manner. Soil limestone rate was calculated by comparing the amounts of CO_2 generated by the pure calcium carbonate and the soil sample [109]. Regarding cation exchange capacity (CEC), the measurement principle is to move all the cations adsorbed on the exchange sites and saturate these sites by a single cation, ammonium (NH_4^+) [109]. Ammonium was then removed, and the rate was determined by Spectrophotocolorimetry. The number of exchange site (CEC) was the number of ammonium ions and was generally measured in the number of loads for 100g of soil (mEq/100g).

3.1.2.2 Hydration time

Hydration time of soil corresponds to the time necessary to achieve the balance between the solid and the solution. It depends on the nature of the solid, its particle size, and the porosity. Hydration time was determined by potentiometric titrations made as follows [109]: soil suspensions (1g soil in 25 mL of 0.1 mol.L^{-1} KNO_3) were stirred at 20°C for varying periods ranging from hours to several days, prior to titration with potassium hydroxide 0.1 mol.L^{-1}. The moisture balance was achieved when two titrations performed after different agitation periods giving superimposed curves. Hydration time is an important factor that must be respected in each sorption experiment. According to work from Achouak et al., (2010), for any type of soil, hydration time is generally less than 24 hours [109], accordingly, it was decided to choose 24 hours as hydration time in this study.

3.1.2.3 Soil/solution ratio

The best soil/solution ratio adapted to this study should allow to see and compare the retention capacities of different soils. Three soil/solution ratios are generally used for adsorption studies; each of them was tested: i) the ratio 1/5 (200 g.L^{-1}): 5 g of soil in 25 mL of solution. According to the recommendation of the Organization for Economic Co-operation and Development Economics for the study of the adsorption of organic pollutants [110]. The use of this ratio would facilitate the comparison with the literature and European databases since it is often used. ii) ratio 1/25 (40 g.L^{-1}): 1 g of soil in 25 mL of solution. iii) ratio 1/200 (5 g.L^{-1}): 0.125 g of soil in 25 mL of solution. The three

soil samples were used for preliminary studies and finally, the ratio 1/25, which corresponds 5.10^{-6} mol. L^{-1} pesticide concentration was selected.

3.1.3 Studied pesticides and commercial formulation
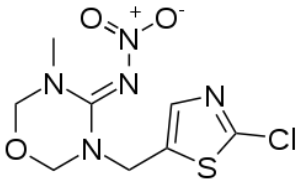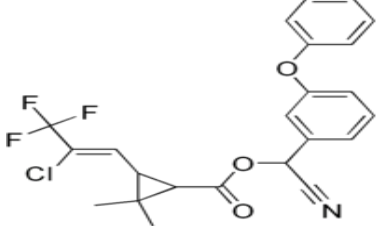
3.1.3.1 Thiamethoxam (THX)

The IUPAC name of THX is (EZ)-3-(2-chloro-1,3-thiazol-5-ylmethyl)-5-methyl-1,3,5-oxadiazinan-4-ylidene(nitro)amine [111], the molecular formula is $C_8H_{10}ClN_5O_3S$ and the CAS number is 153719-23-4 [111]. THX was purchased from Sigma-Aldrich (purity > 99%). It was dissolved in distilled water in order to prepare a stock solution at 291.71 ppm (10^{-3} mol.L^{-1}). For photocatalytic degradation experiments, 1.46 ppm THX solution (5×10^{-6} mol.L^{-1}) was prepared by diluting the stock solution in distilled water. 0.20µm nylon membranes from Sigma-Aldrich were used for filtration processes since there was no THX adsorption on nylon membranes during filtration.

3.1.3.2 Lambda-cyhalothrin (λ-CHT)

The IUPAC name of the molecule is [cyano - (3-phenoxyphenyl) methyl] (1*R*,3*R*)-3[(*Z*)-2 - chloro-3,3,3-trifluoroprop - 1-enyl] -2 , 2 – dimethylcyclopropane - 1 - carboxylate, the molecular formula is $C_{23}H_{19}ClF_3NO_3$, and the CAS number is 91465-08-6 [112]. λ-CHT was purchased from Sigma-Aldrich (purity > 99%). It was dissolved in distilled water in order to prepare a stock solution at 449.9 ppm (10^{-3} mol.L^{-1}). For each experiment, a needed solution was then prepared by diluting the stock solution in distilled water. 0.20 µm nylon membranes from Sigma-Aldrich were used for filtration since there was no λ-CHT adsorption on nylon membranes during filtration. Some properties of THX and λ-CHT can be seen in Table 3.2.

Table 3.2 Properties of Thiamethoxam and Lambda-cyhalothrin

Characteristics	Thiamethoxam (THX)	Lambda-cyhalothrin (λ-CHT)
Developed Formula		
Type	Insecticide	Insecticide
MW (g.mol^{-1})	291.7	449.9
Family	Neonicotinoids	Pyrethroids
Usage	Maize, colza, fruit, etc.	Potatoes, tomatoes, melons, squash, etc.
	Large Spectrum	
Solubility in water (mg.L^{-1})	4100	5×10^{-3}
log K_{ow}	- 0.13	7.0

3.1.3.3   EFORIA 247 ZC

According to information taken from agricultural engineers working in Tekirdağ, on behalf of the Ministry of Agriculture of Turkey, several pesticides formulations were used in Tekirdağ during 2014 (Roundup®, Shangdong 240EC, Axial 45EC, Eforia 247 ZC, etc.). Eforia 247 ZC was selected for this study due to the fact that it is a mixture of two pesticides (THX and λ-CHT) with very different solubilities that can be exploited in order to understand the interactions between the two molecules during soil adsorption and photocatalytic degradation. As an active ingredient, we can find glyphosate, pinaxaden, acetamiprid, thiamethoxam, imazamox, lambda-cyhalothrin and many others in this formulation. As indicated in the Material Safety data sheet [113], Eforia 247 ZC is composed by: 12.7%(w/w) of thiamethoxam, 9.5%(w/w) of lambda-cyhalothrin, 5 - 10 % w/w of highly aromatics solvent naphtha (petroleum), 1 - 5 %(w/w) of titanium dioxide, and 0.05 - 1 % (w/w) of 1,2-benzisothiazol- 3(2H)-one and water. The main active pesticide molecules in the EFORIA are THX and λ-CHT.

3.1.4   Adsorption/Desorption of THX onto soil

Adsorption studies were conducted in duplicate at room temperature (20 °C) in dark condition by using the batch technique in 60 mL polypropylene (PP) tubes covered with aluminium foil in order to keep the solution in the dark. All sorption experiments were carried out at natural pH and 40 g.L^{-1} soil. Control experiments were also carried out with the solutions containing THX at the desired concentration without soil. 24 h hydration time was used for each experiment. The amount of pesticide adsorbed and desorbed by the soil in each flask was calculated using Eq. (3.2) and (3.3), respectively, while their corresponding percentage (%) was calculated using Eq. (3.4) and (3.5), respectively.

$$q_e = \frac{(C_0 - C_e)V}{w} \tag{3.2}$$

$$q_{desorp} = \frac{(q_e - C_e)V}{w} \tag{3.3}$$

$$\% \ adsorbed = \frac{(C_0 - C_e)}{C_0} x100 \tag{3.4}$$

$$\% \ desorbed = \frac{(q_e - C_e)}{q_e} x100 \tag{3.5}$$

Where; q_e is the amount of pesticide adsorbed by soil (mg.g^{-1}), C_0 and C_e are the initial and final pesticide concentrations (mg.L^{-1}), respectively, V is the volume of solution (L), and w is the soil mass (g).

3.1.4.1   Adsorption kinetics

The prediction of the adsorption rate, which is generally used in the design and modeling of the adsorption process, can be made by using kinetic parameters [68]. Applied experimental protocol was as follow: in a first step, 20 mL of distilled water was added to 1g dry soil in a 60 mL polypropylene (PP) bottle. The suspension obtained was then stirred for 24 hours (hydration time). The pesticide was then added and the total volume adjusted to 25 mL by addition of distilled water so as to obtain a final concentration of THX equal to 1.46 mg.L^{-1} and a solid load in the water of 40 g.L^{-1}. Several flasks were prepared, and the suspensions were shaken vigorously at 20°C at the natural pH of the soil for variable periods ranging from 10 minutes to 72 hours (contact time per batch). After stirring, the suspension is filtered using cellulose acetate membranes (pore size = 0.22 μm).

The filtrates were then analyzed by High Performance Liquid Chromatography (HPLC) to determine the residual amount of pesticide in the solution. The pesticide concentration adsorbed by the soil was obtained by the difference between the initial concentrations and the residual concentration. Two repetitions were performed for each sample of soil, insecticide and duration of stirring. Witnesses to the same pesticide concentration (1.46 mg.L^{-1}) but without soil were also conducted to check for retention on the walls of the bath, vials or filters. Then adsorption kinetics was tested by using the Lagergren's pseudo-first order kinetic model (Eq. 2.1) and pseudo-second order kinetic model (Eq. 2.2).

3.1.4.2   Desorption kinetics

Batch experiments were conducted in PP box to determine the desorption percentage of THX. In practice, 1 g of THX-contaminated soil was put into each PP box with 25mL of distilled water. The samples were then shaken vigorously on the same shaker used for adsorption experiments. Samples were collected periodically in order to determine the desorption rate of THX.

3.1.4.3   Adsorption isotherms

Different volumes (from 25 to 2500µL) of stock THX (291.71 mg.L^{-1}) solution were added to 1g of the soil samples, which were previously hydrated in 20 mL of distilled water for 24 hours. The total volume was then adjusted to 25mL by addition of distilled water so as to obtain pesticide concentrations between 0.29 and 29.17 mg.L^{-1}. The suspensions obtained were stirred at 20°C in natural pH for a fixed period of time, which was equal to the previously determined equilibrium time for each soil. After shaking, soil suspensions were filtered through membranes of cellulose acetate (0.22 microns) and the filtrates were analyzed by HPLC to determine the residual amount of pesticide in the solution. At least two repetitions were performed for each soil's sample, insecticide and initial concentration introduced. The pesticide adsorption capacity of the soil (q_e) was calculated by the difference between the initial concentration and the concentration in solution at equilibrium (C_e). Sorption isotherms represent the change of q_e as a function of C_e.

Langmuir and Freundlich adsorption isotherm models are frequently used in the literature to describe the adsorption of molecules at the solid-solution interface. Linear models that permit to determine K_d are widely used for adsorption onto soils. Therefore, the

experimental data of adsorption isotherms were described using these models in order to deeply understand the process and also compare our results with the literature.

3.1.4.4 Determination of K_d Values

Five methods can be used to determine K_d (distribution coefficient) values, (i) laboratory batch method, (ii) in-situ batch method, (iii) laboratory flow-through (or column) method, (iv) field modelling method, and (v) K_{oc} method [114]. Each method is quite different and may be led to different values. In this study, we used laboratory batch method. It is the most common laboratory method for determining K_d values. The method used in this study was illustrated in Figure 3.1. As can be seen, the soils are hydrated with distilled water for 24 h before adding the soil and then stirred for a time necessary for adsorption and then centrifuged and filtered. Soils previously polluted are hydrated to promote desorption, and then sieved and filtered. In both cases, the analysis of the filtrate was made by the HPLC and the results noted for exploitation. Plot of q_e as a function of C_e was used in order to determine the distribution coefficient, K_d, between the solid and the liquid phases.
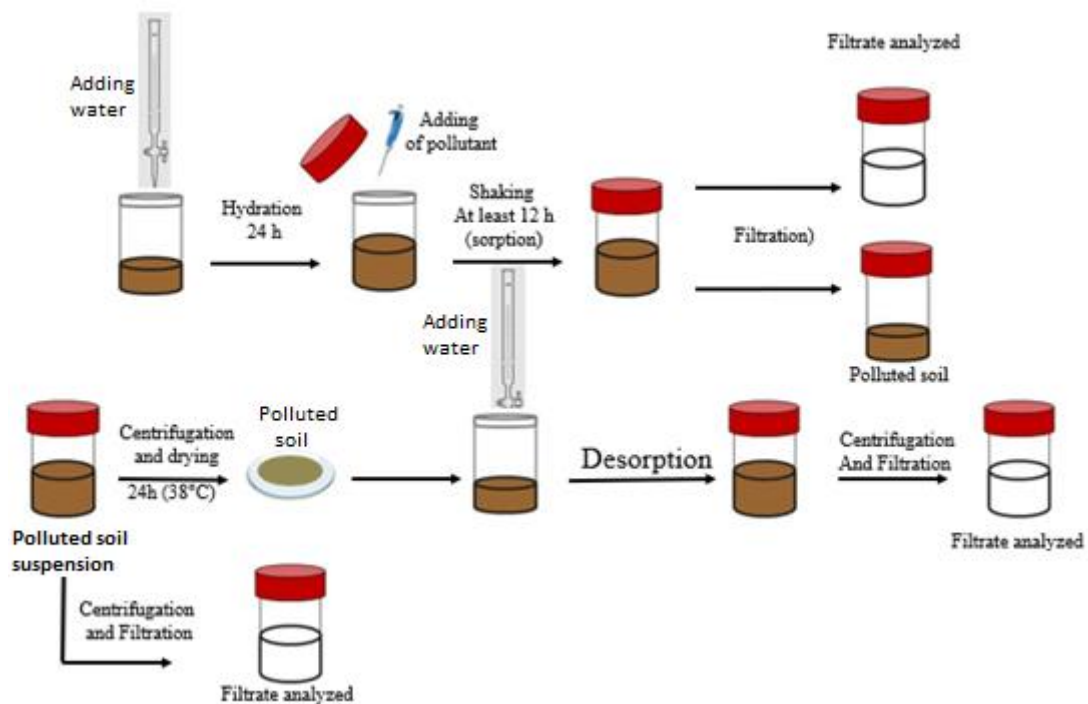
Figure 3.1 Batch procedure for adsorption-desorption

3.2 Materials and methods for the photocatalytic degradation study

3.2.1 Perlite

Perlite granules have a porosity of more than 95%, that property provides them to stay afloat on the water surface. Supporting photocatalyst TiO_2 with perlite allowed TiO_2 to get used with the polluted solution without requiring any nanofiltration. Expanded perlite, as photocatalyst support, was obtained from TAŞPER Perlit Company, Turkey.

3.2.2 Titanium dioxide (Degussa P25)

Titanium dioxide (TiO_2) is a semiconductor that has been widely used as a pigment and in sunscreens, paints, ointments, toothpaste, etc. Titanium dioxide (Degussa P-25®), was supplied from Evonik Degussa Specialty Chemicals Co. Ltd. The properties of perlite and TiO_2 were given in Table 3.3 [115, 116, 117].

Table 3.3 Properties of perlite and TiO_2 [115, 116, 117]

Properties	Perlite	TiO₂ (Degussa P25)
Composition	SiO_2 (74%), Al_2O_3 (12.8%), Fe_2O_3, MgO, CaO, Na_2O, K_2O, TiO_2	80% anatase and 20% rutile
Density	$0.1 g/cm^3$	$4.23 g.cm^{-3}$
Conductivity	Insulator	Semi-conductor
Color	White	White

3.2.3 Perlite supported TiO₂ (PST)

Perlite supported TiO_2 (PST) was prepared as follow: first, expanded perlite was sieved to the particle size of 1-2 mm, then rinsed with distilled water with the aid of air bubbling (5 mL air/min) till no powder was detected in the filtrate, and dried in an oven at 105 °C overnight. Then, 2.4 g TiO_2 (Degussa P-25®) was added to 50 mL of absolute ethanol. After adding 5 mL of diluted nitric acid (at pH 3.3), the suspension was placed in an ultrasonic bath for 15 minutes in order to provide homogeneity. Then, 6 g of prepared perlite were added to the mixture while stirring for 10 minutes at 130 rpm. Next, the mixture was kept in an ultrasonic bath for 15 minutes to disperse the possible flocculated TiO_2 powder. After drying in an oven at 120 °C for 12 hours, the mixture was calcined at

450 °C for 1 hour to provide a stronger adherence between perlite and titanium dioxide powder. After being cooled in a desiccator, PST was washed in distilled water under air bubbling for few minutes in order to remove titanium dioxide powder which had not been precipitated on perlite surface. After filtration and drying in an oven at 120 °C for 4 h, PST was ready to use in photocatalytic degradation experiments. Zeiss EVO LS 10 Scanning Electron Microscope (SEM) was used to characterize the surface morphology. The crystalline structures were investigated with a Philips PANalytical X'Pert Pro X-ray diffractometer (XRD) using Cu Kα radiation. The surface area of perlite and PST sample was measured using a Quantachrome Quadrasorb SI surface analyzer. Specific surface area was calculated using Brunauer, Emmett and Teller (BET) equation for N_2 adsorption data between 0-0.3 relative pressure ranges.

3.2.4 Adsorption and photocatalytic degradation experiments

Adsorption kinetic studies were carried out by using the photoreactor (Figure 3.2) as a batch reactor in the dark condition in order to determine adsorption capacities of photocatalyst and also in order to differentiate both effects; adsorption and photocatalytic degradation process. The photoreactor temperature was kept at 20 °C using a cooling water circuit. The photoreactor was covered with aluminium foil to block transition of light. In order to compare THX removal by TiO_2, perlite and PST; TiO_2 (1.15 g), perlite (2.85 g) and PST (4.00 g) was added to 500 mL of 1.46 ppm THX solution at natural pH (6.5). The mass of materials was chosen according to our previous study [14], which indicates that 4.00 g of PST contains about 2.85 g and 1.15 g of perlite and pure TiO_2, respectively. The obtained suspension was stirred at 400 rpm at 20 °C for 300 minutes. Aliquots of 1 mL of the suspension were periodically collected from the reactor, filtrated using a 0.20 μm nylon membrane in order to remove particles, and the filtered solution was further analyzed by monitoring the absorbance at 252 nm by UV spectrophotometry (Analytic Jena Specord 200 Plus).

THX photocatalytic degradation experiments were carried out in stirred aqueous solutions (500 mL 1.46 ppm THX) in the photoreactor. The radiation source was 2x6W UV lamp (365 nm mercury lamps, Philips). Before UV irradiation, the suspensions were kept in the dark for 30 min (predetermined equilibrium time) under stirring to reach the THX adsorption equilibrium onto PST. In order to optimize the photocatalytic degradation process, a series of photocatalytic degradation experiments corresponded to the 15 runs

given in BBD matrix (Table 2.4) were performed. The initial solution pH was adjusted by using 0.1 - 1 M of HCl or NaOH in each case.

The schematic experimental details of photoreactor are shown in Figure 3.2. It consisted of a 500 mL cylindrical pyrex glass reactor equipped with 2x6W UV lamp. The UV lamp was located vertically in the center of the reactor.
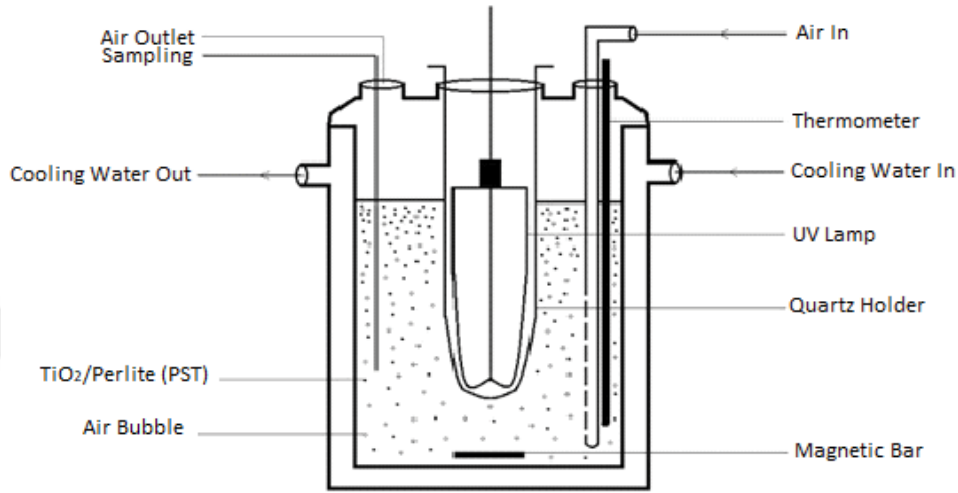
Figure 3.2 Experimental set-up of the photocatalytic degradation process

In order to evaluate the effect of photoreactor design, in another experiment, another UV lamp (6W, 365nm, Analytic Jena) was located horizontally at the top of the reactor. UV light was given as vertical direction through the reaction solution. Furthermore, effect of short-wave radiation was also investigated by using short wavelength UV lamp (2x6 W, 254 nm, mercury lamp, Philips).

3.2.5 Design of Experiment (DOE)

Relationship between a response and independent variables can be predicted by using DOE [89, 90]. Box-Behnken Experimental Design (BBD) method was employed for modeling and optimization of photocatalytic degradation of THX by using perlite supported TiO_2. BBD was chosen since it is well suited for fitting a quadratic surface and usually works well for process optimization [89, 90]. A general second-order model is defined as:

$$y = a_0 + \sum_{i=1}^{n} a_i x_i + \sum_{i=1}^{n} a_{ii} x_i^2 + \sum_{i=1}^{n} \sum_{j=1}^{n} a_{ij} x_i x_j \Big|_{i<j} \qquad (3.6)$$

where y is the theoretical response function, x_i and x_j are the design variables (independent variables or parameters or factors), a_i and a_{ij} represent the regression coefficients corresponding to the main factor effects and interactions, respectively, and n the number of parameters [118, 119]. JMP® 13 software was used in order to evaluate DOE findings. Three factors, pH of THX solution (pH), amount of PST (PT) and air flow rate (AF) were chosen as independent factors. The selected factors and levels can be seen in Table 3.4 and the experimental matrix of BBD can be seen in Table 3.5

Table 3.4 Process variables and their levels for BBD

Factors	Low (-1)	Middle (0)	High (+1)
pH	4	6.5	9
PT (g/L)	6	8	10
AF (L/h)	6	12	18

Two responses were selected for this study: THX degradation percentage after 270 min (DEG270 (%)) and Electric Energy per Order (EE/O (kWh/m^3)). EE/O is defined as the number of kWh of electrical energy required to reduce the concentration of a pollutant by 1 order of magnitude (90%) in 1 m^3 of contaminated water [120, 121, 122]. The EE/O values can be calculated from Eq. 3.7:

$$EE/O\,(kWh/m^3) = \frac{(P x t x 10^3)}{V x 60 \log(C_0/C)} \qquad (3.7)$$

where EE/O is the electric energy per order, P is the rated power of the UV lamp (kW), V is the volume of treated water (Liters), t is the irradiation time (min), C_0 and C are THX concentrations before and after the treatment, respectively. The experimental matrix of BBD can be seen in Table 3.5.

Table 3.5 Experimental matrix used for BBD

Run	Coded Values			Actual values		
	pH	PT	AF	pH	PT (g/L)	AF (g/L)
1	−	0	−	4	8	6
2	0	+	−	6.5	10	6
3	+	+	0	9	10	12
4	0	0	0	6.5	8	12
5	+	0	+	9	8	18
6	0	−	−	6.5	6	6
7	+	−	0	9	6	12
8	0	0	0	6.5	8	12
9	+	0	−	9	8	6
10	−	0	+	4	8	18
11	0	0	0	6.5	8	12
12	0	−	+	6.5	6	18
13	−	−	0	4	6	12
14	0	+	+	6.5	10	18
15	−	+	0	4	10	12

3.2.6 JMP software

JMP is a data analysis tool of choice of scientists, engineers and other data explorers worldwide. It was used for the evaluation of data obtained by experimental design study and process optimization.

3.3 Analytical Methods

3.3.1 High Performance Liquid Chromatography (HPLC) Analysis

The chromatographic chain (VARIAN ProStar) used for the analysis of THX is equipped with a UV-visible detector with a diode array and a non-polar C18 Kromasil® column based on silica (length = 100 mm, particle size = 5 μm). The detection wavelength of THX was 252 nm, and it was 265 nm for λ-CHT.

3.3.2   UV Spectrophotometer

Pesticides concentrations were determined at 252 nm for THX and 265 nm for λ-CHT by using Analytic Jena Specord 200 Plus UV Spectrophotometer.

3.3.3   TOC analysis

TOC is an essential environmental parameter used to measure water/wastewater quality from municipal and industrial sources. Torch combustion TOC/TN analyser was used for TOC analysis.

3.3.4   COD Analysis

The method used for COD analysis was based on the dichromate-reflux colorimetric method. The sample was added to the reagent vial and digested under closed reflux conditions and allowed to cool before measurement. Reference standards was made using potassium hydrogen phthalate (KHP), 1 mg of KHP is equal to 1.175 mg COD. Hanna COD Analyzer, which offers an absorbance measuring mode allowing for CAL Check standards to be used to validate the performance of the system, was used for COD analysis.

3.3.5   Analysis of degradation products by LC-MS-MS

Degradation products were investigated by liquid chromatography-tandem mass spectrometry (Agilent 6200 Series TOF/6500 Series Q-TOF LC/MS System). An Electro Spray ionization (ESI) was used for the MS and MS-MS measurements in positive ionization mode, and full scan acquisition was performed between m/z 50 and 1000. A mixture of ultra-pure water (90%) and methanol (10%) was used as mobile phase at a flow rate of 0.4 mL/min in isocratic conditions using an Agilent HPLC Column Poroshell 3x50 mm x 2.7 µm Ec-c18 model. The limit of detection (LOD) (0.73 µg/L) was determined using the Sigma method by using Eq. 3.8, where σ is the standard deviation and S is the slope of the calibration curve. The limit of quantification (LOQ) was calculated with Eq. 3.9 as 2.19 µg/L.

$$LOD = \frac{3,3\sigma}{S} \tag{3.8}$$

$$LOQ = \frac{10\sigma}{S} \tag{3.9}$$

After having many measurements, conversely to the literature we could not find any degradation products, then, the samples were further analyzed by using LC-UV-PDA (photo-diode array) at 255 nm and LC-MS (Shimadzu 2010 EV) with using ESI just after degradation (without any awaiting period).

RESULTS AND DISCUSSION

4.1 Evaluation of the fate of THX

4.1.1 Soil characterization

The physico-chemical properties, which showed the clay loam texture of the three soil samples were given in Table 4.1. Carbonate ($CaCO_3$) content was very low for S_1 (0.1%) and S_2 (0.2%) while S_3 presented a highest value (5.8%). Organic content and CEC of the soil generally play a predominant role in adsorption. The poor organic matter content (under 2.5% for each soil) and the CEC values from 22.0 to 28.5 cmol kg^{-1} indicated the possible low adsorption capacity for pesticides, although the surface charge of the soils could enable electrostatic interaction [123].

Table 4.1 Physico-chemical properties of the soil samples

Soil property	S_1	S_2	S_3
pH (water)	8.0	7.3	8.4
Carbonate content (%)	0.1	0.2	5.8
Organic Content (OC) (%)	2.2	1.7	1.8
Sand content (%)	31.0	30.4	23.1
Clay content (%)	38.4	33.9	37.0
Silt content (%)	30.6	35.8	40.0
CEC (cmol.kg^{-1})	28.5	22.0	23.0

S_1 and S_3 revealed a basic pH, 8.0 and 8.4, respectively, whereas S_2 was close to neutrality (7.3). Silt percentage was 30.6%, 35.8% and 40.0% for S_1, S_2 and S_3 respectively. These results showed the low variability among soils although they were collected at significant distances. S_3 differs slightly with the highest silt content (40%) and also with a carbonate content 58 times higher than S_1 and 29 times higher than S_2 in term of percentage.

4.1.2 Adsorption kinetics

Adsorption kinetics of THX and THX-E (THX in Eforia formulation) onto the three soil samples can be seen in Figure 4.1 a, b and c. All these adsorption kinetics can be decomposed into two steps. The first step took place in less than 120 minutes for each system and corresponded to the adsorption of the pesticide on the most accessible sites, probably located on the external surface of the soil particles. Adsorption of THX (and THX-E) continued more slowly during the second step (between 120 minutes and the plateau). This limitation is often attributed to the molecular diffusion of the pesticide towards less accessible sites such as soil micropores, clay interfacial spaces, or inside organic matter [109]. At the end of these two steps, the amount of pesticide remained constant, the presence of a plateau indicating that the adsorption equilibrium has been reached. Equilibrium time was determined as 480 minutes (8 h) for S_1-THX, S_1-THX-E, S_2-THX-E, S_3-THX and S_3-THX-E and 1440 minutes (24 hours) of contact time for S_2-THX. At equilibrium, S_1 approximately adsorbed 15% (5.5 $\mu g.g^{-1}$) of THX and 17% (6.2 $\mu g.g^{-1}$) of THX-E, S_2 adsorbed about 20% of THX (7.3 $\mu g.g^{-1}$) and 14% (5.1 $\mu g.g^{-1}$) of THX-E, when S_3 adsorbed 10% (3.6 $\mu g.g^{-1}$) of THX and 11%(4.0 $\mu g.g^{-1}$) of THX-E (Figure 4.1d). The adsorption capacity (q_e) for the different systems which in ascending order can be classified as follows: S_2-THX > S_1-THX-E > S_1-THX > S_2-THX-E > S_3-THX-E> S_3-THX. Soils S_1 and S_2 exhibited similar behaviors while soil S_3 adsorbed only a few amount of pesticide. We also noticed that THX-E and THX adsorption was slightly different. It is difficult to interpret this difference because of the complexity of the soil and the formulation. This observation led us to conclude that although the active substance was supposed to leave from the formulation almost instantaneously after application [124], adsorption has remained slightly influenced by the formulation Eforia, which seemed to increase its retention rate by soils S_1 and S_3 and decreased it for S_2.
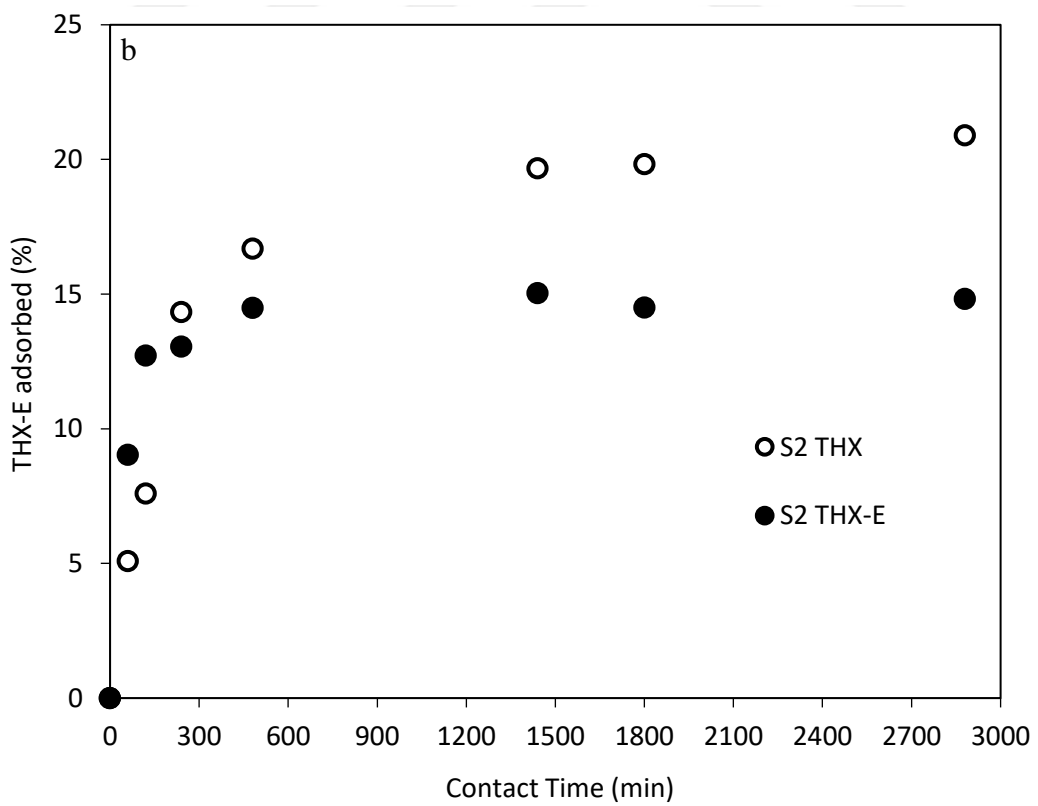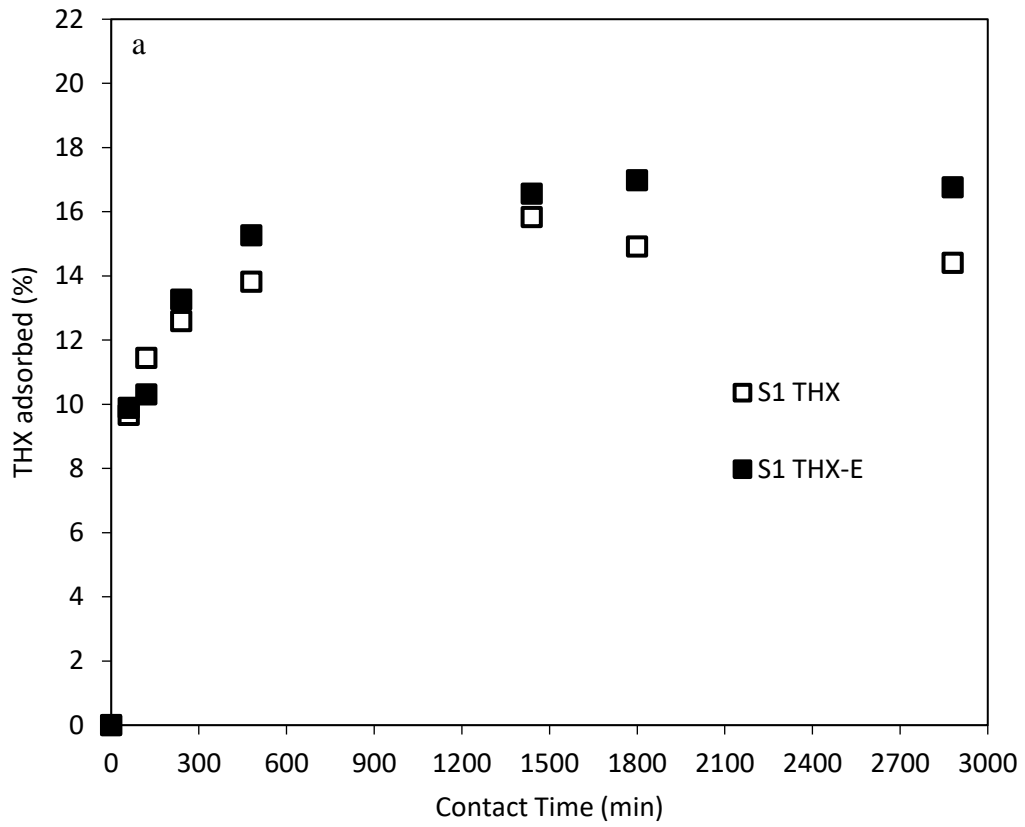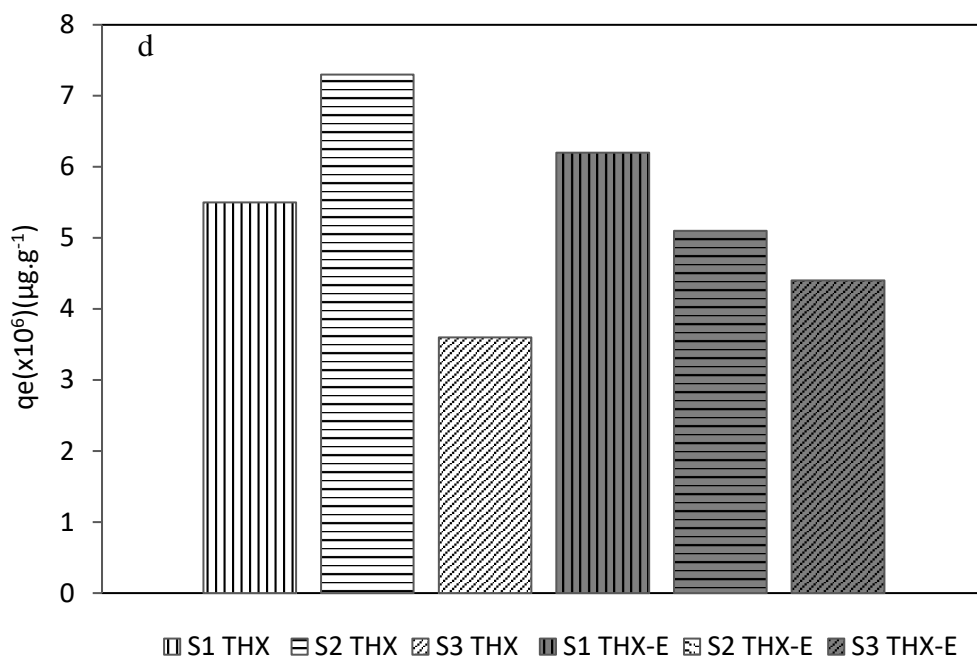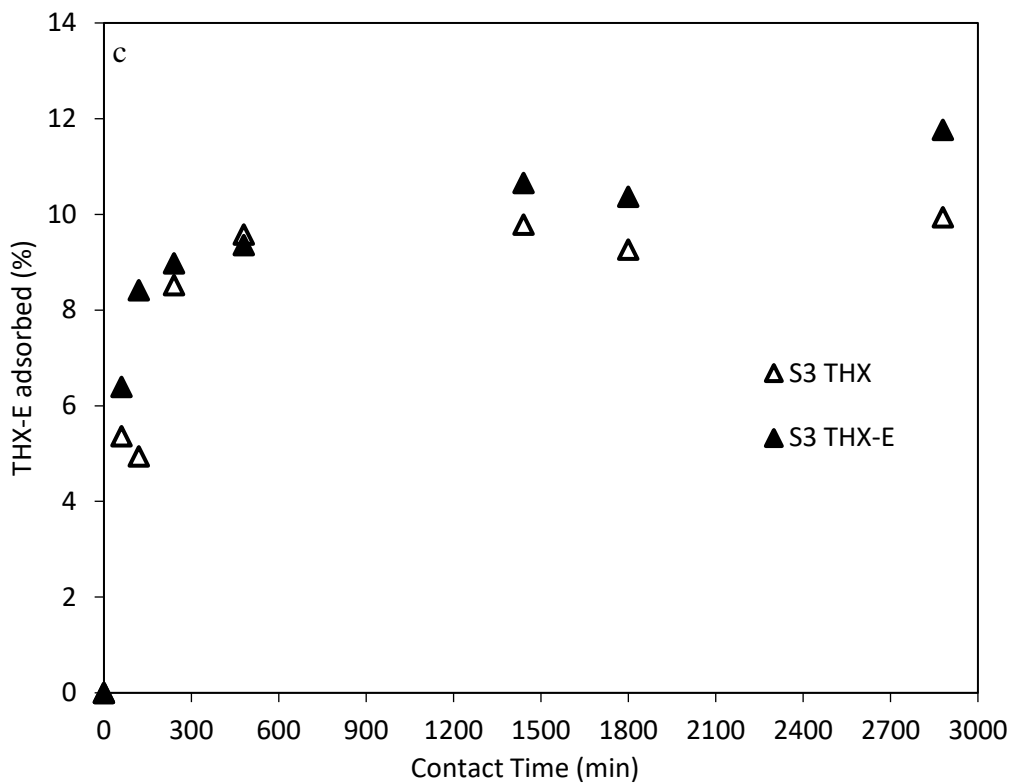
Figure 4.1 THX and THX-E adsorption kinetics onto S_1(a), S_2(b) and S_3(c) and the equilibrium adsorption capacities of each system in µg.g^{-1} (d), ([THX]$_0$ = [THX-E]$_0$ = 1.46 mg.L^{-1}, T = 20°C, soil concentration = 40 g.L^{-1}).

Adsorption kinetic data were fitted to the pseudo-first (fitting data not shown) and pseudo-second order model (Figure 4.2). The corresponding parameters were listed in Table 4.2. The determination coefficient and also the error between q_e^{exp} and q_e^{model} were used to evaluate the accuracy of the models. For all the tested systems, the best fit was obtained with the pseudo-second-order model, with higher R^2 values (very close to 1) and better agreement between q_e^{exp} and q_e^{model} as indicated by lower error (E_2) values (Table 4.2). It was suggested that the adsorption of THX followed pseudo-second kinetic order.

Figure 4.2 Pseudo-second order model kinetic fitting

Table 4.2 Kinetic model parameters

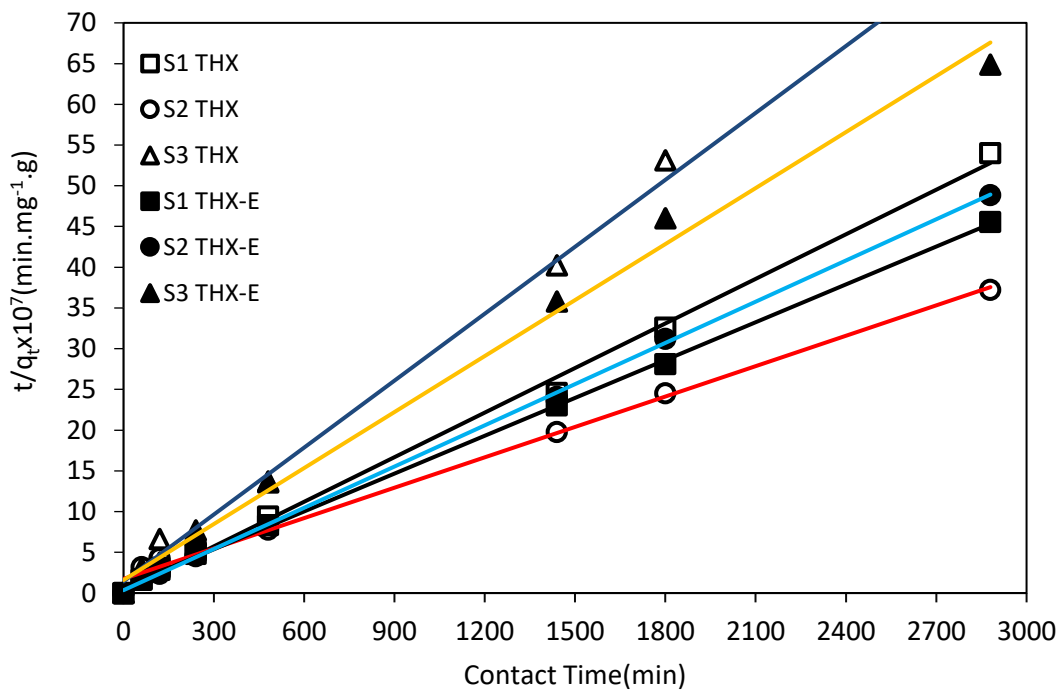| Soils		q_e^{exp} (µg.g^{-1})	k_2(x10^{11} mg.g^{-1}min^{-1})	q_e^{model2} (µg.g^{-1})	*E$_2$(%)	R^2	k_1	q_e^{model1} (µg.g^{-1})	*E$_1$(%)	R^2
			Pseudo Second Order Kinetic Model					Pseudo First Order Kinetic Model		
S$_1$	THX	5.50	1.27	5.49	0.18	0.99	0.36	3.16	42.55	0.91
	THX-E	6.20	0.33	6.45	4.03	1	0.17	3.39	45.32	0.94
S$_2$	THX	7.30	0.09	8.06	10.41	0.99	0.10	5.26	27.95	0.92
	THX-E	5.11	0.82	5.92	15.85	1	0.43	3.68	27.98	0.92
S$_3$	THX	3.60	0.53	3.65	1,39	0.99	0.09	1.33	63.06	0.56
	THX-E	4.38	0.33	4.37	0.23	0.99	0.05	1.94	55.71	0.68

$$*E = \left| (q_e^{exp} - q_e^{model})/ q_e^{exp} \right|$$

4.1.3 Desorption kinetics

Desorption studies are important in order to evaluate the risk of pesticide release. To study the desorption kinetics of THX, each soil was first spiked with the same amount of THX or THX-E (36.5 µ.g^{-1}). After the determination of the adsorbed amount for each system (Table 4.3), the desorption experiments were carried out in distilled water. As it can be seen in Figure 4.3, desorption equilibrium was achieved within 120 minutes (2 hours) for all systems and the desorption percentage compared to the initial amount of THX and THX-E at equilibrium varied from 3% (1.1 µg.g^{-1}) to 6% (2.0 µg.g^{-1}), which means, at least 18% of adsorbed THX and THX-E was released in a relatively short time in the presence of water. Consequently, it can be suggested that a high amount of desorbed THX or THX-E already been adsorbed onto soil's surface, mesopores and macropores while the rest was probably located in micropores. The corresponding desorbed amounts of THX were, 1.5 µg.g^{-1}, 1.3 µg.g^{-1} and 2.0 µg.g^{-1} for S$_1$, S$_2$, and S$_3$, respectively (Table 4.3). Although quantities are low, THX and THX-E can become hazardous to groundwater with repeated applications. Especially since it is used in an application rate of 10 to 200 g/ha. Similar results were obtained by Banerjee et al.(2008) [10] in their study about THX adsorption on three soils of India, 9.3µg.g^{-1} (45.8%) were adsorbed and 5.3 µg.g^{-1} (56.9%) was desorbed [10].

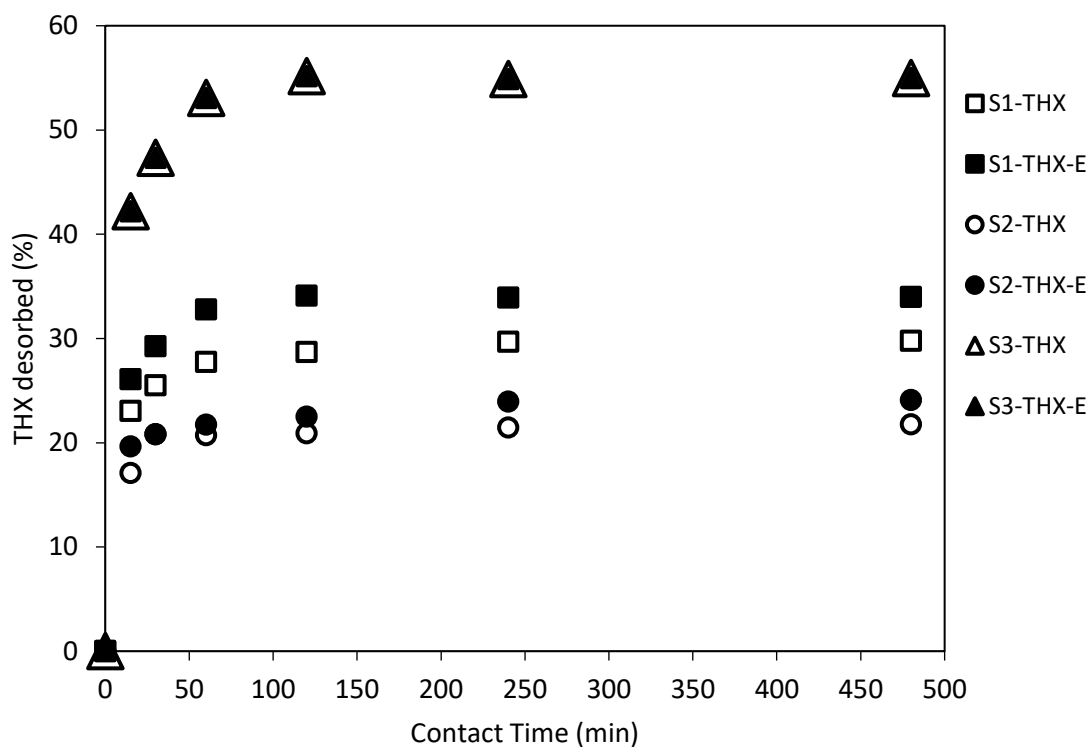Figure 4.3 THX and THX-E desorption kinetics

([THX]$_0$ = [THX-E]$_0$ = 1.46 mg.L^{-1}, T = 20°C, natural pH, soil concentration = 40 g.L^{-1})

Table 4.3 Adsorbed and desorbed amounts of THX and THX-E on each soil before performing desorption study

Soil		Adsorbed Amount ($\mu g.g^{-1}$)	Adsorption percentage (%)	Desorbed amount ($\mu g.g^{-1}$)	Desorption percentage (%)	Desorption percentage compared to the initial amount (%)
S_1	THX	5.50	14	1.50	27	4
	THX-E	6.20	16	1.90	31	5
S_2	THX	7.30	20	1.30	18	4
	THX-E	5.11	15	1.10	22	3
S_3	THX	3.60	10	2.00	56	6
	THX-E	4.38	12	2.00	46	6

4.1.4   Adsorption isotherms

The adsorption experiments as a function of THX introduced concentration allowed to plot the adsorption isotherms. The adsorption isotherms of THX and THX-E, plotted for the three soils, were presented in Figure 4.4. The Langmuir (K_L and q_m) and Freundlich (K_F and n) parameters obtained by linearization of the equations of the two models were

shown in Table 4.4. We can see with the Langmuir isotherm that, considering the three soils, the maximum adsorption capacity varied from 0.02 mg.g^{-1} to 1.02 mg.g^{-1}. These values seemed to be greater for THX compared to THX-E. Regression coefficients for THX and THX-E indicated that adsorption isotherms were better described by the Langmuir than by Freundlich model except for the S$_2$-THX system for which K_L is negative (-0.02 L.mg^{-1}) certainly due to the complex interaction between THX and S$_2$ soil. This makes it possible to envisage a monolayer adsorption at localized sites, without interactions between pesticide molecules. Banerjee et al. (2008) performed adsorption of THX on three Indian soils (sandy-loam, clay and silty-clay), the Langmuir model was not suitable for any of these soils [10].

In order to better understand the adsorption of THX onto the studied soils, the isotherms were considered only in their linear part (Figure 4.5) i.e. at low concentrations. The observation of a linear relation allowed us to determine the distribution coefficient K_d (Eq. (2.7)) given by the slope of the linear regression and valid in this concentration range. K_d reflects the partition of the THX between the solid phase (soil) and the liquid phase. The higher K_d value indicates the greater affinity of the pesticide to the soil. By considering Figure 4.5, the values of the K_d and K_{oc} (Eq. (2.8)) were determined and reported in Table 4.5 for the three studied soils. Considering all soils, the K_d of THX varies from 2.1 to 6.4 L.kg^{-1} and from 4 to 4.6 L.kg^{-1} for THX-E. These values reflected the weak affinity of soils to THX that led to a significant risk to the environment. In comparison, Banerjee et al. (2008) obtained K_d value between 0.62 and 1.66 L.kg^{-1}; and K_{oc} from 155.1 to 413.3 L.kg^{-1}, while Campbell et al. (2005) [11] obtained K_{oc} of 0.53 and 0.23 L.kg^{-1} for two different Hawaiian soils. Carbo et al. (2007) [12] for two Brazilian tropical soils obtained K_d from 1.27 to 13.81 L.kg^{-1} and K_{oc} from 104 to 2877. By considering our results and those obtained in the literature, this large variation of K_{oc} could put into question the fact of using this coefficient to evaluate groundwater contamination. For this reason, we choose a method for estimating the leaching potential including several other coefficients.
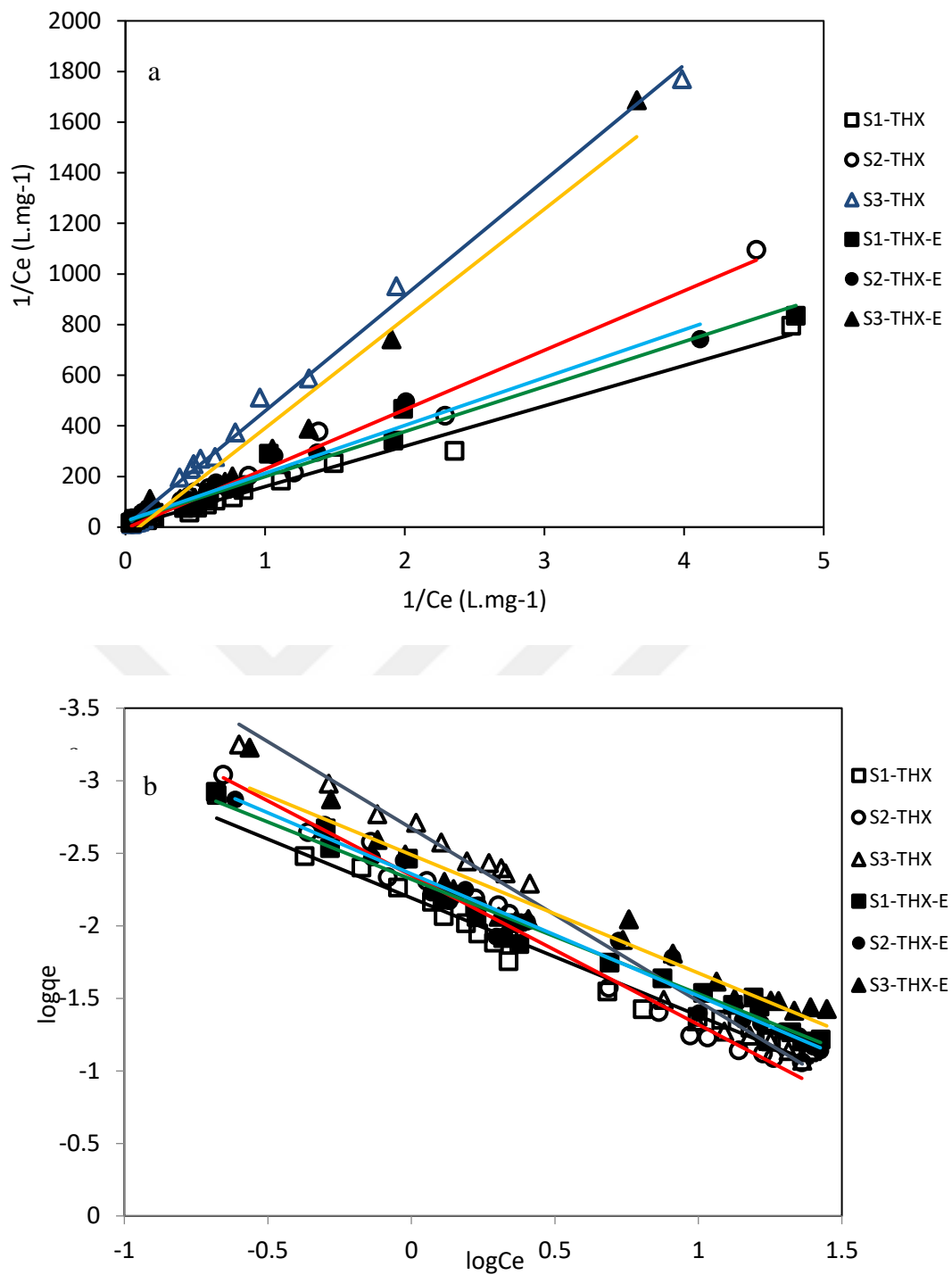
Figure 4.4 Langmuir (a) and Freundlich (b) isotherm at 20°C of THX and THX-E

(soil loading = 40 g.L^{-1}, 0.29mg.L^{-1} ≤ [THX]$_0$ (or [THX-E]$_0$) ≤ 29.17mg.L^{-1}, natural pH

of the soil)

Table 4.4 Langmuir and Freundlich model parameters

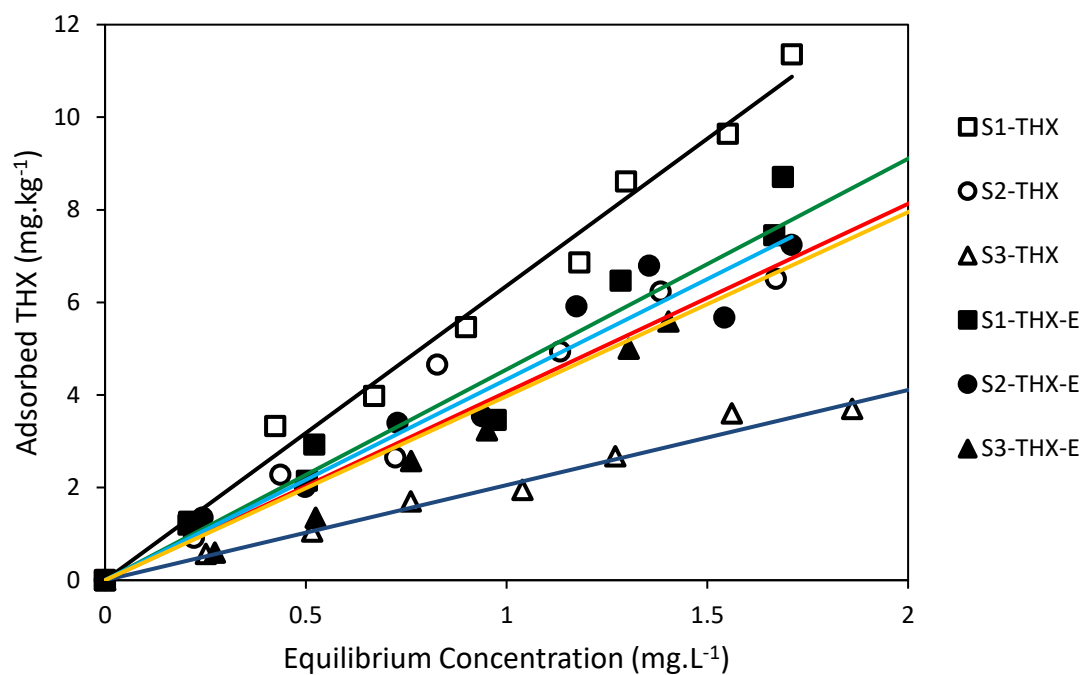|		Langmuir			Freundlich		
		$q_m(mg.g^{-1})$	K_L	R^2	K_F	n	R^2
S_1	THX	1.02	0.01	0.99	0.0065	0.80	0.98
	THX-E	0.05	0.12	0.98	0.0048	0.79	0.98
S_2	THX	0.18	-0.02	0.98	0.0046	0.83	0.96
	THX-E	0.05	0.11	0.96	0.0045	1.03	0.99
S_3	THX	0.41	0.01	0.99	0.0021	1.18	0.99
	THX-E	0.02	0.10	0.99	0.0032	0.95	0.75

Figure 4.5 Linear regressions corresponding to the adsorption isotherms at 20°C of THX and THX-E (solid loading = 40 g.L^{-1}, natural pH of the soil, 0 mg.L^{-1} ≤ [THX-E]$_0$ ≤ 2 mg.L^{-1})

Table 4.5 K_d and K_{oc} values

Soil	Pesticide	K_d (L.kg^{-1})	K_{oc} (L.kg^{-1})
S_1	THX	6.4	500.4
	THX-E	4.6	359.6
S_2	THX	4.3	435.0
	THX-E	4.5	455.3
S_3	THX	2.1	200.7
	THX-E	4	382.2

4.1.5 Leaching potential estimation

In order to differentiate the potential soil mobility of pesticides, many screening indexes have been developed by researchers. However, the most widely used is the GUS index proposed by Gustafson (1989) [125]. This index is calculated based on two pesticide properties, the half-life ($t_{1/2}$) (the time at which 50% of the applied mass was dissipated) and the K_{oc}. The literature and the results from this study exhibited the large variation of the K_{oc}. Several values of $t_{1/2}$ can be found in the literature for THX, 75.4 days as a geometric mean value [126], from 15.0 to 21.5 days [127], and from 7.1 to 92.3 days [128], from 46.3 to 301 days [8]. This large variation of the $t_{1/2}$, may be explained by the difference in soil moisture, temperature, available oxygen, microbial populations, soil pH, photodegradation and other factors [129]. This could result in a large variation of the GUS index depending on the $t_{1/2}$ values chosen or the K_{oc} values obtained. So, in addition to the GUS index, GLI index was used in this study. This method considers several other parameters such as octanol/water partition coefficient (K_{ow}), water solubility (S_w), vapor pressure (V_p), Henry's constant (K_H). The Global Leachability Index (GLI) combines into a single ranking the Leaching Index (LIN), the Groundwater Ubiquity Score (GUS), and the Modified LEACH (M.LEACH) index [13]. A $t_{1/2}$ value of 50 days from the study by Hilton et al. (2015) was used in this study in order to consider the medium situation [128]. The GLI reported in Table 4.7 were calculated using the equations reported in Table 4.6. As we can see, the GLI indicated a high environmental risk for all the systems while the GUS indicated the same result just for S_3-THX. The potential risk was intermediate for the other systems (S_1-THX, S_1-THX-E, S_2-THX, S_2-THX-E and S_3-THX-E). Those results obtained by GUS index were close to those obtained by Banerjee et al. (2008). THX was classified as a compound having an intermediate risk to groundwater in their

study [10]. It can also be concluded that whether the evaluation with the GUS index or with the GLI index, the Eforia formulation does not lead to a significant change that could affect the leaching potential of THX (Table 4.6).

Table 4.6 Leaching potential estimation index equation and evaluation criteria

Index Equation	Evaluation Criteria
$GLI = 0.579LIN + 0.558GUS + 0.595M.LEACH$ [a]	GLI >1: High GLI = -0.5 to 1: Medium GLI <-0.5: Low
LIN=-0.531 $logK_{ow}$ + 0.518 $logS_w$ - 0.495 $logK_{oc}$ - 0.23 $logV_p$ - 0.452 $logK_H$ [b]	Comparison
$GUS = [4 - \log(K_{oc})]x\log(t_{1/2})$ [b]	GUS > 2.8: High 1.8<GUS < 2.8: Intermediate GUS <1.8: No Risk
$M.LEACH = \dfrac{S_w * t_{1/2}}{K_{oc}}$ [a]	Comparison (Lower values; lower leaching potential)

[a] [13] [b] [125]
$t_{1/2}$: half-life (50 days) K_{ow}: octanol/water partition coefficient (-0.13)
S_w: water solubility (4100 g.mL^{-1}) K_{oc}: organic-carbon adsorption coefficient (mL.g^{-1})
V_p: vapor pressure (mmHg) K_H: Henry's constant

Table 4.7 Leaching potential of THX

Soil	Pesticide	GUS	GLI	GUS Evaluation	GLI Evaluation
S$_1$	THX	2.2	247.9	Intermediate	High
	THX-E	2.5	343.5	Intermediate	High
S$_2$	THX	2.3	284.6	Intermediate	High
	THX-E	2.3	272.1	Intermediate	High
S$_3$	THX	2.9	612.4	High	High
	THX-E	2.4	323.4	Intermediate	High

As a result, it was concluded that THX has high potential for groundwater contamination. Therefore, alternative treatment methods for removing this kind of pollutants should be developed. Photocatalytic degradation process, one of the advanced oxidation processes, can be considered as promising approach for this purpose.

4.2 Evaluation of Photocatalytic Degradation Studies

4.2.1 Characterization of the photocatalyst

The XRD pattern revealed that anatase was the main crystalline phase in TiO_2 and PST samples (Figure 4.6). No significant modification was observed after coating on perlite and calcination. Several researchers obtained the same results after coating and calcination for TiO_2/Perlite [130] and for TiO_2/zeolite [131]. The surface area of TiO_2 (Degussa P25) is 56 $m^2.g^{-1}$ [132]. The surface area of perlite and PST was found to be 9.11 $m^2.g^{-1}$ and 18.32 $m^2.g^{-1}$, respectively. The PST surface is almost twice as large as the perlite, this could be explained by the presence of TiO_2, of which fine particles occupied the pores of perlite. In Figure 4.7, are reported SEM images of TiO_2, perlite and PST, which evidenced a homogeneous coating of TiO_2 onto perlite.
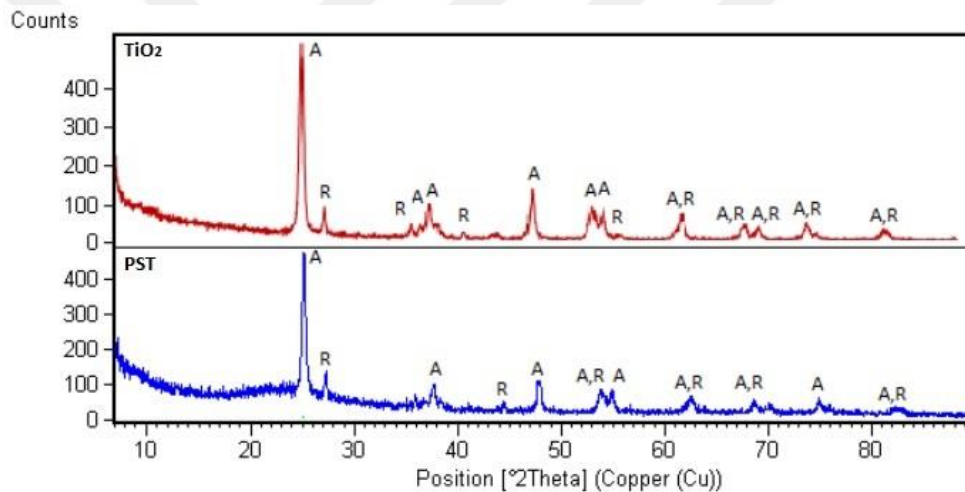

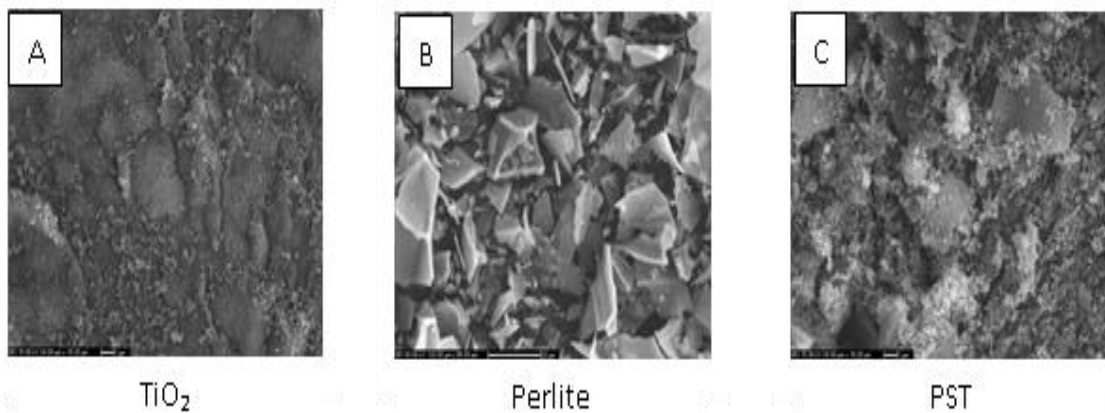Figure 4.6 XRD patterns of TiO_2 and PST

Figure 4.7 SEM images of TiO_2 (5000X), perlite (1000X) and PST (5000X) samples

4.2.2 Adsorption and photocatalytic degradation study

THX adsorption kinetics onto different solids (perlite, TiO_2, and PST) were studied in order to determine the corresponding adsorption equilibrium times. These preliminary experiments were also needed to distinguish between THX adsorption and photocatalytic degradation. Thus, experiments were performed with the three solids both in dark conditions (adsorption) and under UV light (photocatalytic degradation) after adsorption equilibrium time in dark conditions. Figure 4.8 reported the relative concentration (C/C_0) of THX in the solution as a function of time. Concerning experiments in dark condition, it can be deduced that THX was not adsorbed on perlite, whereas after about 30 minutes (equilibrium time), about 10% and 18% of THX were removed by adsorption onto TiO_2 and PST, respectively.

The results of the irradiation of THX (1.46 ppm, natural pH (6.5)) in the presence of PST and TiO_2 were also shown in Figure 4.26. Concerning TiO_2, approximately 95% of THX degradation was achieved within 180 minutes of irradiation, and 90% of THX was degraded by using PST.

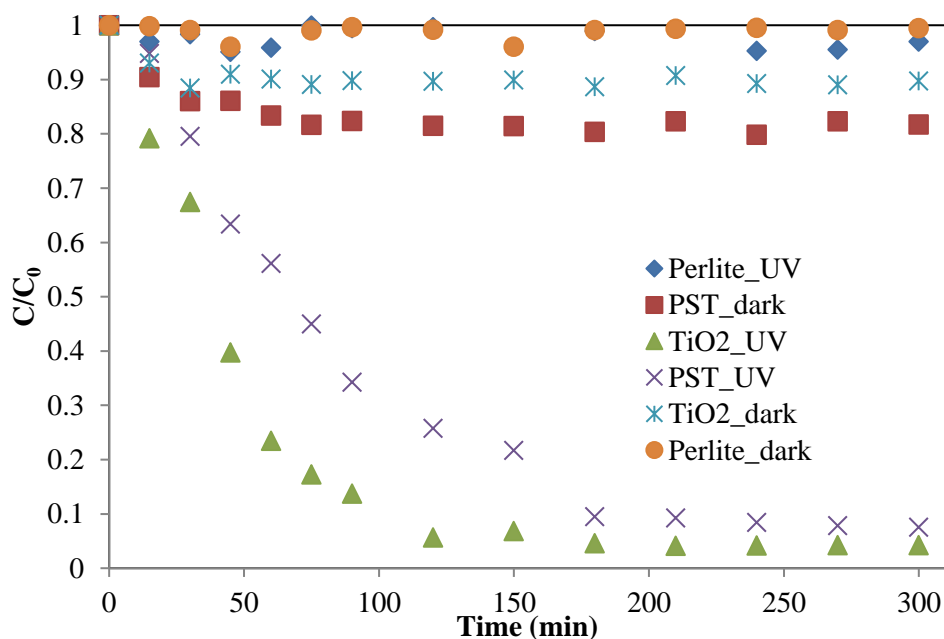Figure 4.8 Relative concentration of THX in solution in the presence of TiO_2, perlite or PST as a function of time, in dark conditions and under UV light

The degradation data fitted well with the Langmuir-Hinshelwood (L-H) model [19]. The simple term of the model is represented in Eq. 4.1, where k is the typical pseudo-first-order rate constant when the concentration of the organic molecule is low, C_0 is the initial

concentration and C is the concentration at time t. The k values were graphically determined and the THX half-lives ($t_{1/2}$) were calculated by using Eq.4.2 (Table 4.8):

$$\ln\left(\frac{C_0}{C}\right) = kt \tag{4.1}$$

$$t_{\frac{1}{2}} = \frac{\ln 2}{k} \tag{4.2}$$

In table 4.8 are reported the pseudo-first-order rate constants, k, and the half-lives, $t_{1/2}$, for the different tested conditions given in Table 4.8 (runs 1 to 15) and for the previous experiment with TiO_2 (1.15 g at natural pH (6.5)). As can be seen, $t_{1/2}$ values varied between 77 and 126 min (except TiO_2 data), and k values ranged from 41.21×10^{-4} min^{-1} to 90.00×10^{-4} min^{-1}. The fastest photodegradation kinetics (highest k and lowest $t_{1/2}$ values) was obtained with pure TiO_2 ($\approx$39 min) as expected, followed by PST in the conditions of run 6 (pH 6.5; PT 6 g/L and AF 6 L/h) ($\approx$77 min). $t_{1/2}$ are 77.02 min and 77.24 min for the runs 6 (0 - -) and 12 (0 - +), respectively. As can be seen, the only difference between these runs is air flow rate, which is 6 L/h for the run 6 and 18 L/h for the run 12. Therefore, it can be concluded that air flow rate has a weak effect on the half-lives.

Table 4.8 Rate constants k, half-lives $t_{1/2}$, and determination coefficients (R^2) for THX photodegradation

Run	1	2	3	4	5	6	7	8
k ($\times 10^{-4}$ min^{-1})	59.18	64.35	66.92	41.21	50.60	90.00	59.07	76.36
$t_{1/2}$ (min)	117.12	107.72	103.58	168.19	136.97	77.02	117.34	90.77
R^2	0.9862	0.9852	0.9906	0.9869	0.9850	0.9428	0.9796	0.9690
Run	9	10	11	12	13	14	15	TiO_2
k ($\times 10^{-4}$ min^{-1})	62.62	62.11	54.95	89.74	64.50	82.92	71.31	179.95
$t_{1/2}$ (min)	110.70	111.61	126.14	77.24	107.46	83.59	97.20	38.52
R^2	0.9933	0.9799	0.9702	0.9919	0.9766	0.9540	0.9897	0.9885

4.2.3 Response surface modelling

BBD was used for the analysis of the photocatalytic degradation of THX. The DEG270 and EE/O values obtained after carrying out the experimental runs given in Table 3.5 are reported in Table 4.9. DEG270 values were found between 71.41% and 88.49% and EE/O values were between 115.01 kWh/m^3 and 198.63 kWh/m^3 at the studied conditions.

Table 4.9 BBD matrix of three variables in coded and actual values with experimental (Exp) and predicted (Pred) responses

Run	Coded Values (pH; PT; AF)	Actual values			DEG270 (%)			EE/O (kWh/m^3)		
		pH	PT (g/L)	AF (g/L)	Exp	Pred	Error (%)	Exp	Pred	Error (%)
1	− 0 −	4	8	6	75.95	75.62	0.33	174.52	175.92	1.39
2	0 + −	6.5	10	6	79.02	76.81	2.21	159.25	169.84	10.59
3	+ + 0	9	10	12	71.41	72.08	0.67	198.63	194.71	3.92
4	0 0 0	6.5	8	12	83.82	84.26	0.44	136.52	137.83	1.31
5	+ 0 +	9	8	18	73.39	73.72	0.33	187.82	186.43	1.39
6	0 − −	6.5	6	6	80.81	82.05	1.24	150.63	144.25	6.38
7	+ − 0	9	6	12	85.40	83.09	2.31	129.24	140.16	10.92
8	0 0 0	6.5	8	12	85.62	84.26	1.36	138.23	137.83	0.40
9	+ 0 −	9	8	6	78.27	79.58	1.31	162.92	157.32	5.60
10	− 0 +	4	8	18	88.49	87.18	1.31	115.01	120.61	5.60
11	0 0 0	6.5	8	12	83.35	84.26	0.91	138.73	137.83	0.90
12	0 − +	6.5	6	18	83.16	84.90	1.74	139.60	131.15	8.45
13	− − 0	4	6	12	82.73	82.06	0.67	141.59	145.51	3.92
14	0 + +	6.5	10	18	80.42	79.66	0.76	152.49	156.74	4.25
15	− + 0	4	10	12	80.30	82.61	2.31	153.05	142.14	10.92

4.2.3.1 Development of regression model

The main objective of using BBD was to propose a regression model for the responses DEG270 and EE/O in this study. The quadratic models were used to find out the relationship between the responses and variables. The method of least squares was typically used to estimate the regression coefficients. P-value was used to identify process parameters, which had statistically significant effect on each response. P-values less than 0.05 indicated that parameters were significant in 95% confidence interval It was observed from Table 4.10 that the linear effects of pH, PT, and some interaction effects (with the asterisk in Table 4.10) were significant.

Table 4.10 Estimated coefficients of the developed model

Parameter	DEG270 (%)			EE/O (KWh)		
	Estimated	Std Error	P-Value	Estimated	Std Error	P-Value
Constant	84.2633	1.4167	<0.0001*	137.8267	6.5848	<0.0001*
pH	-2.8263	0.8676	0.0173*	13.8863	4.0324	0.0137*
PT(g/L)	-3.0700	0.8676	0.0122*	14.8763	4.0324	0.0102*
AF(L/h)	1.4263	0.8676	0.1513	-6.5500	4.0324	0.1554
pH*PT	-1.9875	1.2269	0.1564	10.3200	5.7026	0.1203
pH*AF	-4.3550	1.2269	0.0121*	21.1025	5.7026	0.0101*
pH*pH	-2.6142	1.2770	0.0866	11.6067	5.9354	0.0983
PT*PT	-0.7867	1.2770	0.5605	2.0317	5.9354	0.7438
AF*AF	-2.6242	1.2770	0.0857	10.6342	5.9354	0.1234

The final empirical models for DEG270 and EE/O were given in equation (4.3) and (4.4) obtained by using the regression coefficients given in Table 4.10. The terms pH, PT and AF represent the coded values of the factors.

$$DEG270 = 84.26 - 2.83 \times pH - 3.07 \times PT + 1.43 \times AF - 1.99 \times pH \times PT$$
$$- 4.36 \times pH \times AF - 2.61 \times pH^2 - 0.79 \times PT^2 - 2.62 \times AF^2$$

(4. 3)

$$EE/O = 137.83 + 13.89 \times pH + 14.88 \times PT - 6.55 \times AF + 10.32 \times pH \times PT$$
$$+ 21.10 \times pH \times AF - 11.61 \times pH^2 + 2.03 \times PT^2 + 10.63 \times AF^2$$

(4. 4)

4.2.3.2 Analysis of Variance (ANOVA)

The fitting of the model was investigated by the ANOVA using JMP software. According to the table given in Table 4.25, regression models were significant, and obtained F-value (7.4029 for DEG270 and 8.1540 for EE/O) and the P-value inferior to 0.0500 (0.0126 for DEG270 and 0.0098 for EE/O) indicated that the models were in agreement with the experimental results at 95% confidence level. In other words, there is only a 1.26% and 0.98% chance of error from the model of DEG270 and of EE/O, respectively (Table 4.11).

Table 4. 11 ANOVA for THX photocatalytic degradation.

Response	Source	Degree of Freedom	Sum of Squares	Mean Square	R^2	F ratio	Prob > F
	Model	8	276.9525	34.6191			
	Error	6	28.0586	4.6764	0.91	7.4029	0.0126
DEG270	Total	14	305.0111				
	Model	8	6312.5184	789.0650			
	Error	6	580.6228	96.7700	0.92	8.1540	0.0098
EE/O	Total	14	6893.1412				

4.2.3.3 Model fitting and error estimation

Fitting of the model to the experimental data was examined with error analysis. As can be seen from Table 4.9, error values are from 0.33% to 2.31% and from 0.40% to 10.92% for DEG270 and EE/O, respectively, i.e. developed models fit well the experimental data.

In order to ensure the adequacy between experimental and calculated data, a good fit of the model should be given to avoid poor or ambiguous results. The fitted quality between experimental and predicted data for DEG270 and EE/O was reported in Figure 4.9 a and b. The blue line is the mean line; the red line is the fit line, while the red-scanned area is the confidence zone of 95%. It could be seen at a glance that the models fit very well, since all experimental points (except one) are within the 95% confidence zone.
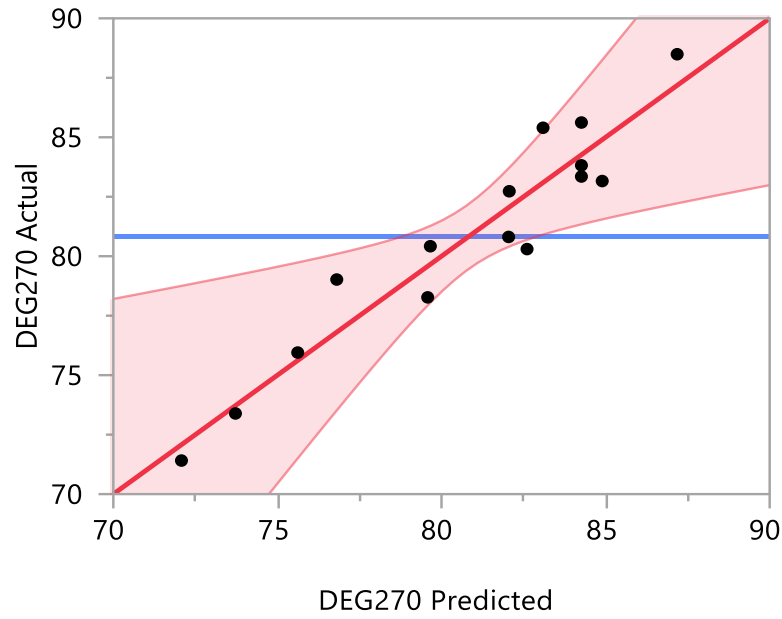
a/- Predicted versus experimental values for DEG
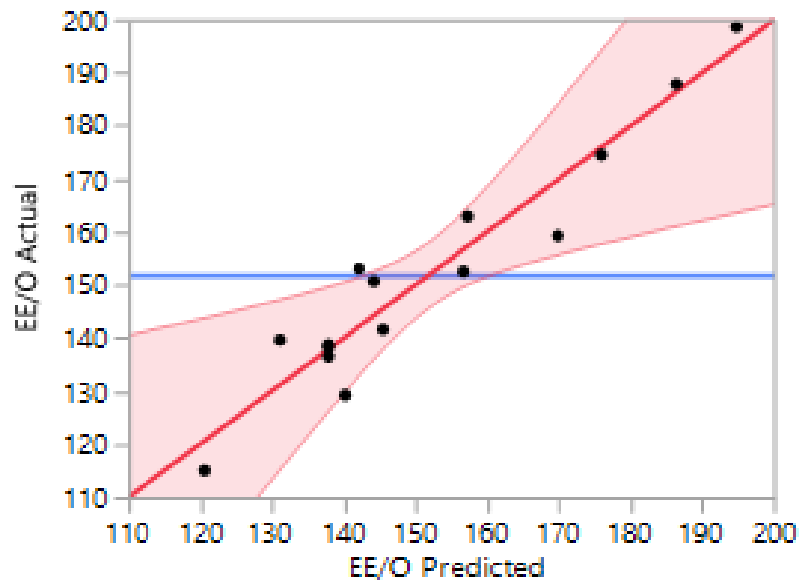
b/- Predicted versus experimental values for EE/O

Figure 4.9 Predicted versus experimental values for both DEG270 (a) and EE/O (b)

The correctness and goodness of the model were checked by the coefficient of determination (R^2). The values of R^2 is 0.91 and 0.92 for DEG270 and EE/O, respectively. This indicated relatively good predictability of the model for both DEG270 and EE/O. Therefore, it can be concluded that the two regression models developed in this study (Eq. (4.3) and (4.4)) were satisfactory for the prediction of DEG270 and EE/O respectively.

4.2.3.4 Effect of process parameters

Effects of process parameters on THX degradation efficiency and Electric Energy per Order was evaluated in terms of interaction plots, which were obtained from JMP® software (Figure 4.10 a and b). Interaction plots represent two factors simultaneously, by keeping other factors constant. Figure 4.10 evidenced that there is an interaction between pH and AF that is also the case between pH and PT for both DEG270 and EE/O. At pH 6, DEG270 is very high when AF is high, whereas degradation is low for the case of pH 9 even at higher air flow rate. A similar trend was observed between pH and PT, while the interaction between PT and AF is negligible. pH has a distinctive effect on the other parameters due to the fact that the surface charge of the photocatalyst, size of aggregates and generation of oxidizing species are determined by pH [133]. Highest THX degradation efficiency and lowest electric energy consumption can be obtained at low pH and high AF conditions [133]. The rate of degradation increased with decrease in pH. This is in accordance with the previous study performed on THX and other pesticides [133, 134].

The effect of pH on photocatalytic oxidation performance can be explained by the point of zero charge (pH_{pzc}) [11,31]. At pHpzc, the surface charge of TiO_2 is zero, and Degussa P25 used in this study have a pH_{pzc} at 6.9 [24, 133]. At pH < pH_{pzc}, the titanium oxide surface is positively charged and gradually exerted an electrostatic attraction force towards the negatively charged compounds. This intensifies the adsorption onto the photon activated TiO_2 surface for photocatalytic reactions [24, 135]. The positive holes are considered as the main oxidizing species at low pH. In that case, the surface charge of TiO_2 is affected according to Eq. (4.5):

$$TiOH + H^+ \leftrightarrow TiOH_2^+ \tag{4.5}$$

At pH > pH_{pzc} (TiO_2), the TiO_2 surface is negatively charged due to hydroxyl ions, thus, anionic compounds in water are repulsed. Eq. (4.6) shows the influence of the surface charge of the TiO_2 by pH:

$$TiOH + OH^- \leftrightarrow TiO^- + H_2O \tag{4.6}$$

In our study, a low concentration of THX and a high number of electron donor atoms like nitrogen (5), oxygen (3), sulphur (1) and chloride (1) which can be found in the THX ($C_8H_{10}ClN_5O_3S$) may increase adsorption at pH < pH_{pzc}. It is also clear from the figure that an excess amount of PST in the system is adverse for the reaction, bringing out a

66

negative influence on the photocatalytic efficiency and increase EE/O. This can be explained by blocking UV radiations by an excess of PST and their absorption by PST, and thus the low production of $\cdot$OH and $O_2\cdot$ radicals, which are responsible for the degradation reaction. However, an excess amount of air provides higher efficiency, except at elevated pH. Air flow brings oxygen to the system and dissolved oxygen help to assure sufficient electron scavengers present to trap the exited conduction-band electron from recombination [24]. AF is also useful for mixing the solution for a better THX adsorption and UV absorption before degradation.
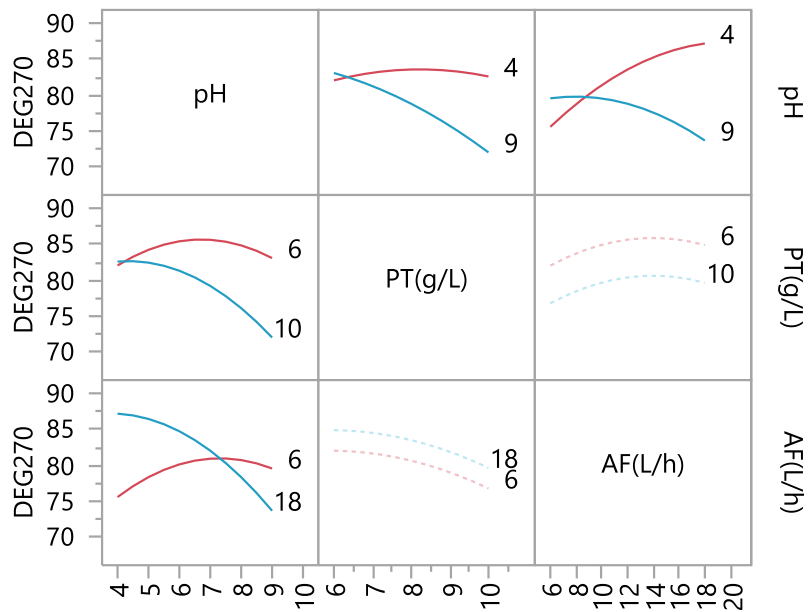
a/- Interaction plot between pH, PT and AF for DEG270
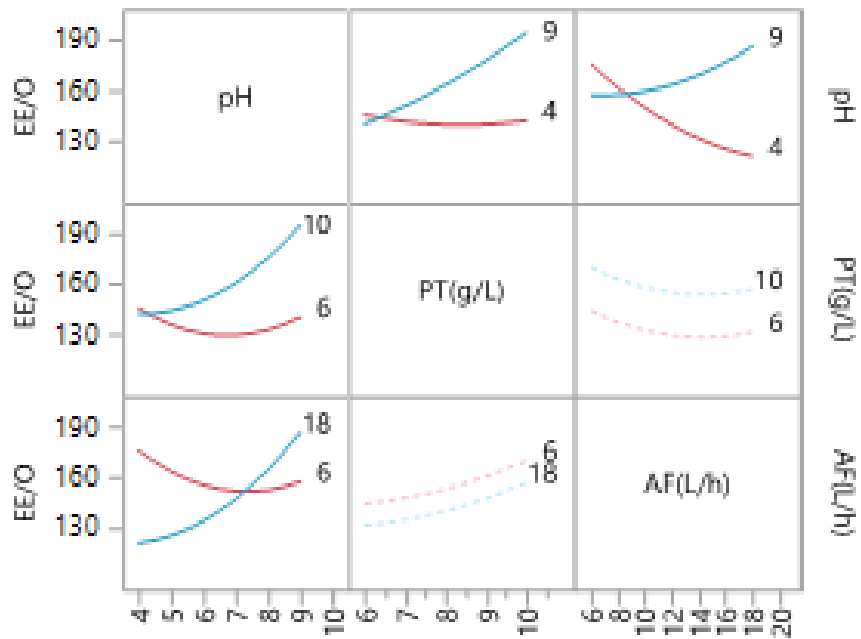
b/- Interaction plot between pH, PT and AF for EE/O

Figure 4.10 Interaction plot between pH, PT and AF for DEG270 and EE/O

4.2.3.5 Response surface plots

3D response surface plots were used to evaluate the effects of selected variables on DEG270 and EE/O. The examination of surface plots as a function of two factors is the best way to check the relations between the factors and the response. In these graphs, a factor was set at a constant level when the other two factors were changed within the experimental ranges. It is clear that DEG270 is high at pH 4 and 18 L/h air flow rate (Figure 4.11 a and b) and EE/O is low at the same values (Figure 4.11 c. and d.).
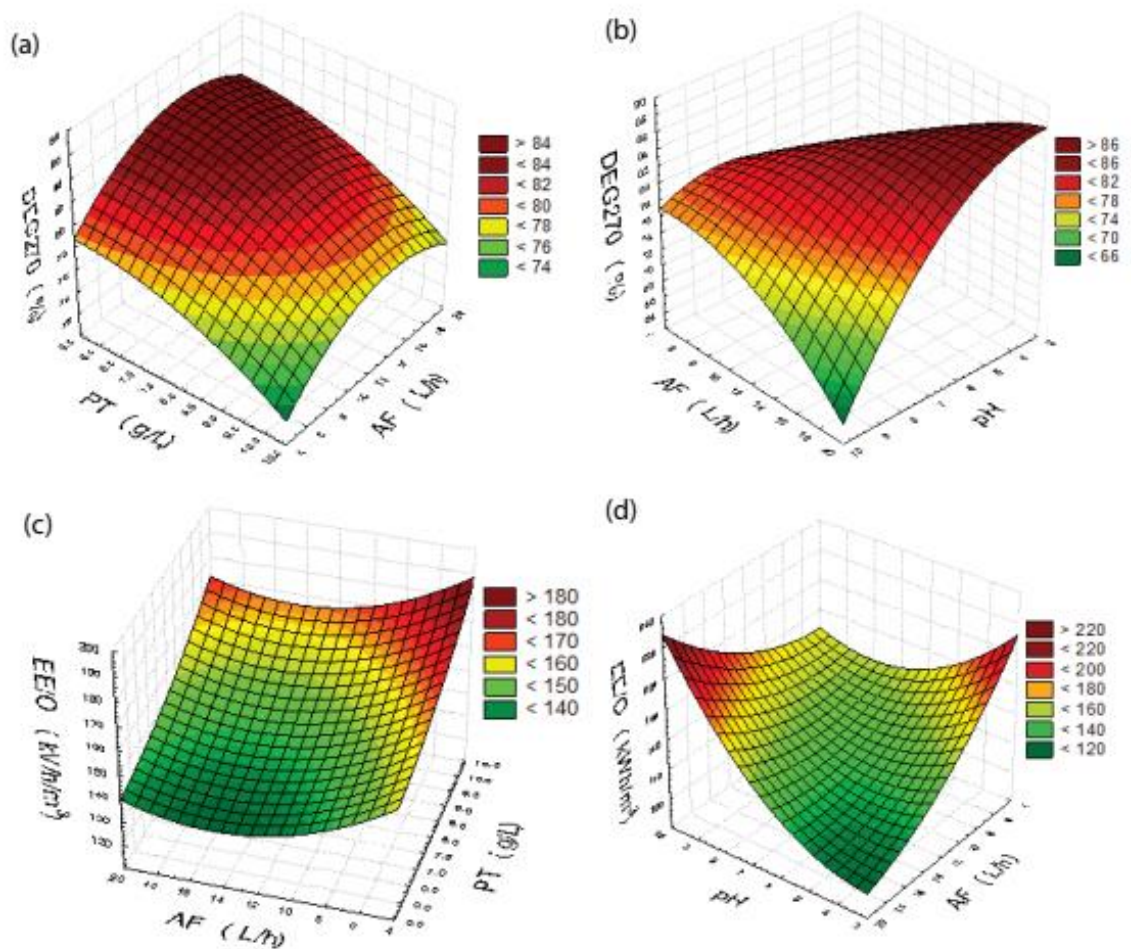
Figure 4.11 3D surface Plots a) DEG270 against AF and PT, b) DEG270 against pH and AF, c) EE/O against AF and PT, d) EE/O against pH and AF

When increasing PT in a range of air flow between 10 and 18 L/h, the degradation percentage slightly increased before reaching a critical value and then it decreased. In all cases, the degradation appeared to be greater for PT values less than or equal to approximately 8 g/L (Fig 4.11 a). In acidic initial pH, the increase of the air flow caused an increase of DEG270 beyond 82% (Figure 4.11 b.). With regard to EE/O, PT values between 5.5 and 8 g / L, high air flow rates would result in energy savings (Figure 4.29 c). The energy consumption was also minimal at a high air flow rate and acidic conditions (Fig 4.11 d).

Since there a was similarity between information given by response surface plots, only the 3D surface plot of DEG270 and EE/O against PT and AF, and against pH and AF were shown in Figure 4.11 a, b, c and d, respectively.

4.2.3.6 Optimization

Response goals (maximization of DEG270 and minimization of EE/O) were used by JMP® to construct a desirability function. The desirability function indicates that the target goal is the most desirable. It can be said that the optimal conditions (reported in Table 4.12) are the best combination of factor settings for achieving the expecting responses. The Prediction profiler obtained from JMP showed in Figure 4.12 indicated the optimum parameters. These results were found to be in good accordance with those obtained from the surface plots (Figure 4.11).

Table 4.12 Optimal conditions for THX photocatalytic degradation

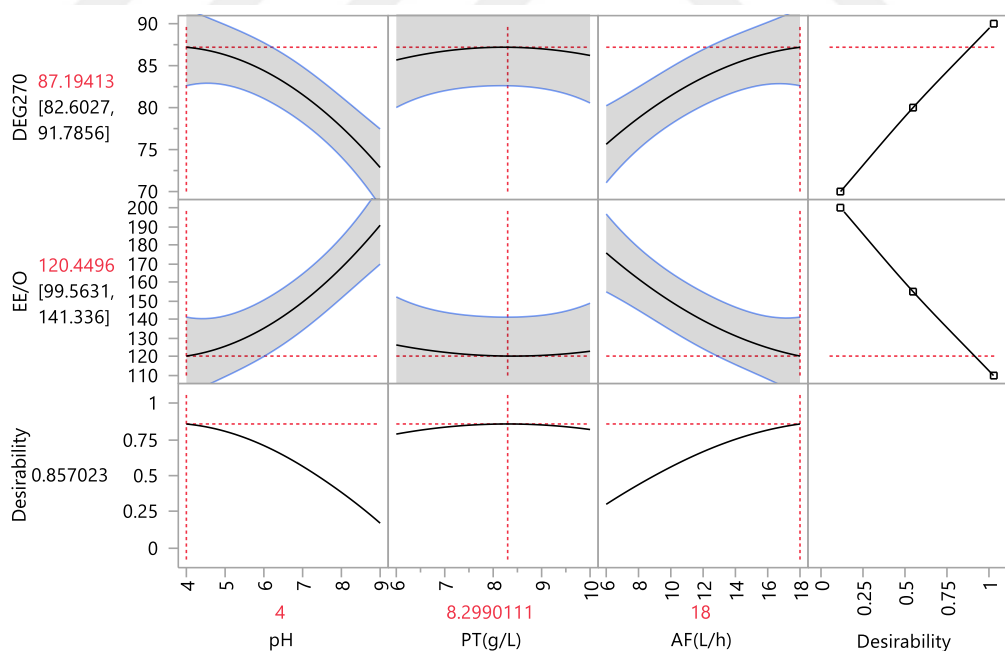| Factor	Factor values	DEG270 (%)		EE/O(KWh/m^3)		Desirability
pH	4	predicted	experimental	predicted	experimental	
PT (g/L)	8.30	87	87±5	120	120±21	0.86
AF (L/h)	18					

Figure 4.12 Prediction profiler obtained from JMP

Photocatalytic degradation was set at optimum conditions and verified experimentally. As can be seen from Table 4.12, predicted values were closer to the experimental values. This confirmed the suitability of the model for the prediction of process behaviour.

4.2.4   Stability and reusability of PST

Stability and reusability of PST were also studied by six photocatalytic degradation cycles. The photocatalyst was separated from the aqueous solution after each cycle, followed by washing with distilled water for 2 times and drying at room temperature for at least 12 h before the next usage. Then, the PST was used in the subsequent reaction under the same conditions. The activity of PST slightly decreased from 85% to 75% with the increasing repetition (Figure 4.13). This fall can be explained by the loss of some fragments due to the weak mechanical strength of expanded perlite. However, PST could be used repetitively more than six times without significant deactivation and also without specific regeneration. To our knowledge, it was the first time that supported TiO_2 was used without any regeneration process. In addition, for the recovery of photocatalysts, PST can be collected from the aqueous media by simple floatation process easily.
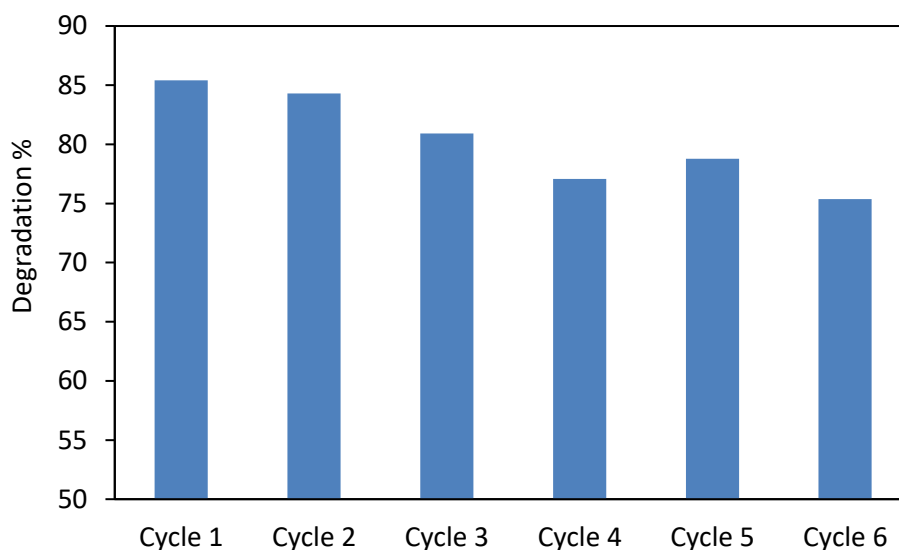

Figure 4.13 THX degradation throughout the cycles

4.2.5   Photocatalytic degradation of EFORIA 247 ZC

Photocatalytic degradation of THX commercial formulation, EFORIA 247 ZC, was also investigated at the optimum conditions obtained for THX degradation studies. Concentration variations of each pesticide molecules (thiamethoxam and lambda cyhalothrin) in the EFORIA formulation during photocatalytic degradation can be seen in Fig.4.14. 73% of THX and 78% of λ-CHT in EFORIA were degraded after 270 min of irradiation. Compared to pure THX degradation results, THX degradation percentage slightly decreased in the EFORIA formulation. About 85 % of THX degradation was achieved in its pure form while 73% of THX-E was degraded in commercial formulation.

71

It can be concluded that both THX and λ-CHT could be removed efficiently whether in pure or in commercial formulation by photocatalytic degradation with perlite supported TiO_2.
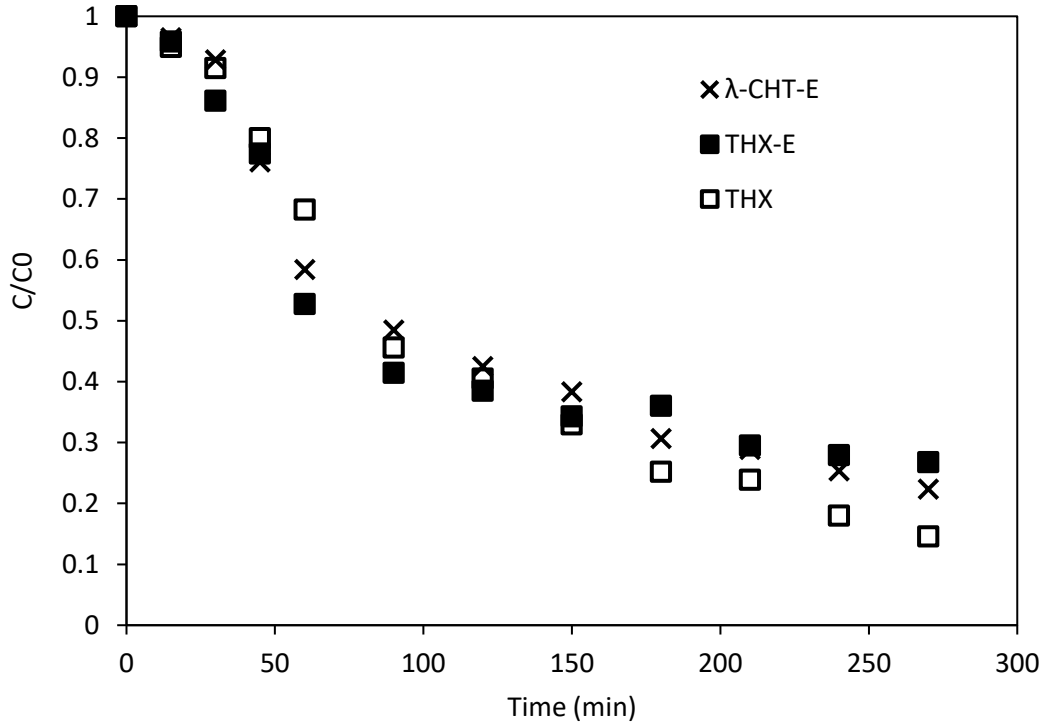

Figure 4.14 Relative concentrations of pesticides during photocatalytic degradation of EFORIA by PST at optimal conditions

4.2.6 Effect of photoreactor design

Electric energy per order (EE/O) values obtained at the same optimum conditions in different photoreactor design for pure TiO_2 and PST can be seen in Fig. 4.15. As can be seen, in case of using PST, the consumption of electric energy for the used photoreactor design (SY1) is less than that of the system, in which UV lamp (6W, 365nm, Analytic Jena) is located horizontally at the top of the reactor (SY2). This can be interpreted with the fact that floating perlite on the solution surface inhibited the light flow tohrought to the solution in System 2. Consequently, it can be concluded that photoreactor design of System 1 is more convenient for THX degradation in case of PST. Hovever, there is no considerable difference for pure TiO_2, hence, both photoreactor design can be used efficiently for pure TiO_2.
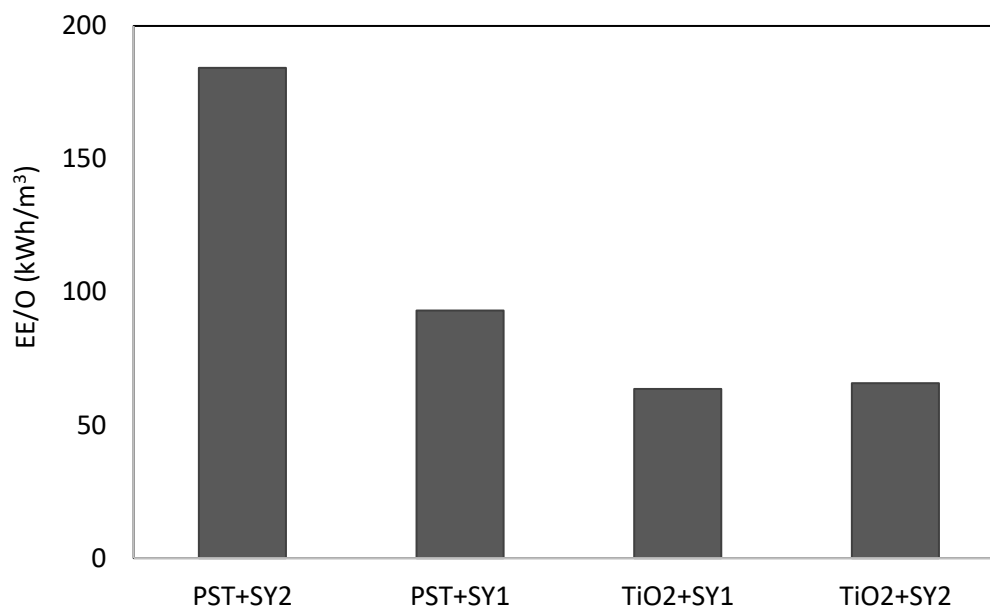
Figure 4.15 Effect of photoreactor design (SY1: UV lamp is located in the center of the reactor vertically, SY2: UV lamp is located at the top of the reactor horizontally)

4.2.7 Effect of UV wavelength on degradation efficiency

The UV wavelength effect on THX photodegradation efficiency of PST was investigated by comparing the experiments at the optimal conditions using a long wavelength (LW) (365 nm) and a short wavelength (SW) (254 nm) UV lamp, respectively (Fig. 4.16). As a result, 74% of THX was degraded using LW while 83% of THX was removed by using SW after 180 degradation minutes. As expected, using short wavelength resulted in slightly high degradation capacity compared to LW. On the other hand, short wavelength requires more attention to handle since it is very harmful and carcinogen for living organisms.
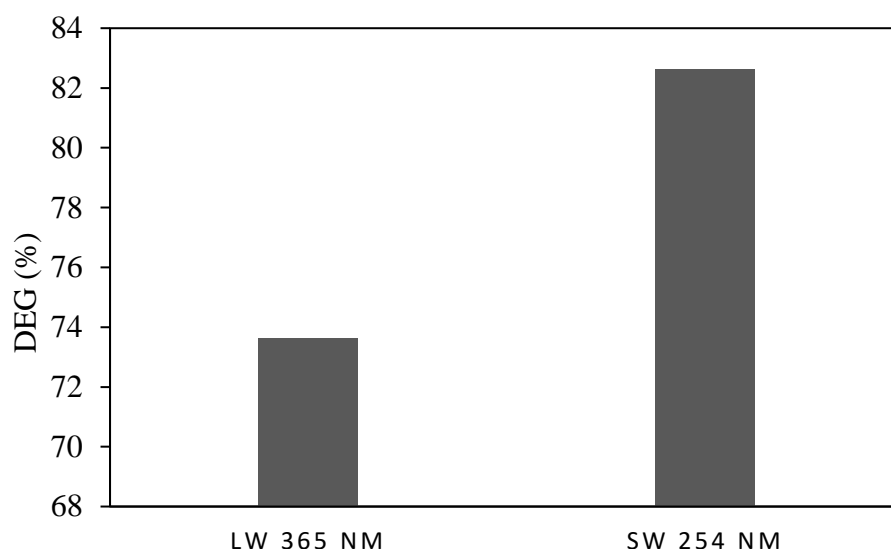
Figure 4.16 Degradation efficiency obtained by using different wavelength UV lamp

4.3 Investigation of degradation pathway

LC-MS, Total Organic carbon (TOC), chemical oxygen demand (COD) were performed in order to illuminate the photocatalytic degradation mechanism of THX.

4.3.1 Total organic carbon (TOC) analysis

The level of organic molecule or contaminants in water was measured by TOC analytical technique. It is one of the most commonly used methods for observing mineralization. TOC analysis is specific to organic compounds and theoretically measures all the covalently bonded carbon in water. As can be seen in Fig. 4.17, for THX, TOC decreased from 12.21 to 1.76 $mg.L^{-1}$ while it decreased from 16 to 3.6 $mg.L^{-1}$ for THX in commercial formulation (TOC-E) after 270 min degradation. Then, 85.58% (for THX) and 77.50% (for THX-E) of the organic carbons presented in the solution are supposed to be removed after 270 minutes of degradation. Having compared to THX degradation percentage (about 87%) we can conclude that almost all degraded THX was fully mineralized in the photoreactor.
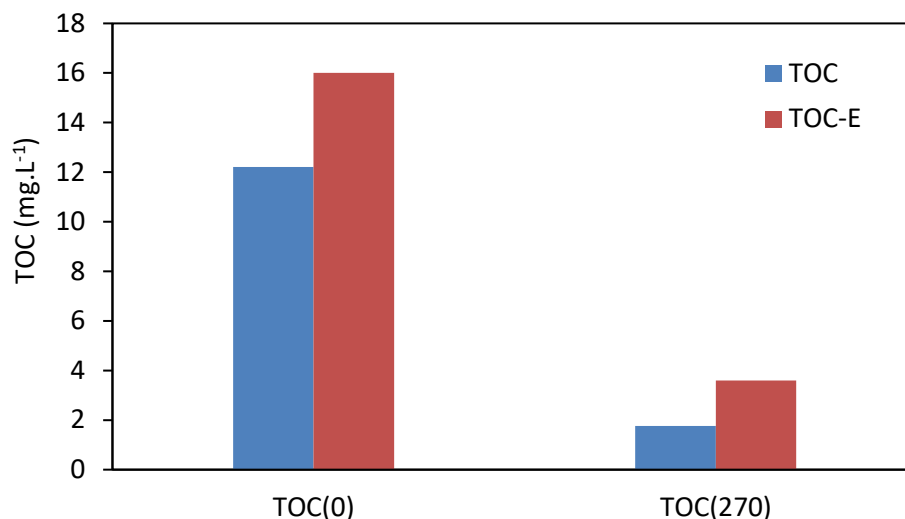
Figure 4.17 TOC analysis results for THX (TOC) and Eforia (TOC-E)

4.3.2 Chemical oxygen demand (COD) analysis

COD analysis was performed to determine the amount of oxygen required to oxidize the organic matter present in the solution under our specific condition. Figure 4.18 shows a gradually drop of COD for Eforia (COD-E) and THX solution (COD-THX) until 270 minutes. As can be seen in Fig. 4.18, for THX, COD decreased from about 10 to 3 mg.L^{-1} while it decreased from about 16 to 5 mg.L^{-1} for THX in commercial formulation (COD-E) after 270 min degradation period. In another words, the THX solution needs 3 mg.L^{-1} while that of Eforia will require 5 mg.L^{-1} of oxygen to oxidize all the organic matter still present in the solution after degradation. As a conclusion about 70% (for THX) and 69% (for THX-E) of the COD content decreased by irradiation.
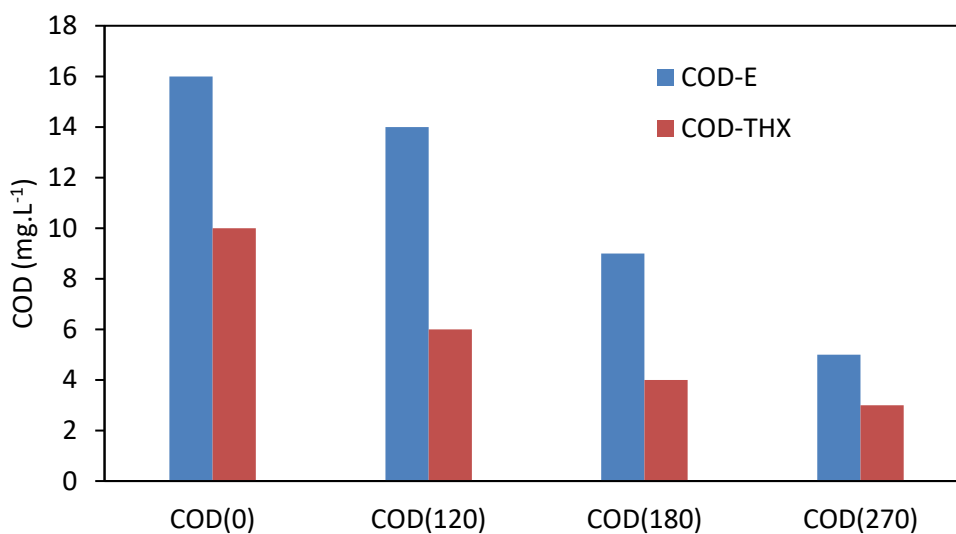

Figure 4.18 Variation **of** COD-E and COD-THX during the process

75

4.3.3   Intermediate products research

LC-MS-MS analyses were conducted in order to identify the intermediate products generated during photocatalytic degradation. The total mineralization of THX can be mainly done via photocatalytic oxidation according to the stoichiometry proposed in Eq. 4.7.

$$C_8H_{10}ClN_5O_3S + \frac{33}{2}O_2 \rightarrow 8CO_2 + 5NO_3^- + SO_4^{2-} + Cl^- + H_2O + 8H^+ \qquad (4.7)$$
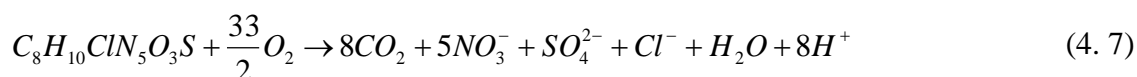
The first investigation for the intermediate compounds was carried out on three samples obtained before and after degradation experiment at optimal conditions (THX at time t = 0 minutes and two samples after 180 and 270 minutes of photocatalytic degradation.) Due to the availability of the device, a few days were passed before the analysis. Obtained LC-MS-MS chromatograms from this measurement were given Fig. 4.19. It can be seen that about 80% of the THX concentration decreased by 270 min of irradiation, but we do not notice the appearance of another peak than that of THX. Partial mineralization is the most likely hypothesis since it is consistent with the observations of other researchers reported in Table 4.13 [26, 20, 30]. In all these studies, intermediate products containing sulfur and nitrogen elements are mentioned. However, no intermediate product was detected in our working conditions (Fig. 4.19), which could be due to the low THX concentration in this study. However, no intermediate products were observed even at higher initial THX concentrations (5 and 100 ppm) (Table 4.13). Due to the different conditions like applied wavelengths and UV sources (Table 4.13), it is not easy to compare the literature studies with ours. It is important to note that with a short wavelength (265nm) and a power of 125 W, 12 intermediate products have been identified [30], a long wavelength (355 nm) and an almost similar power (120 W) has leads to 5 intermediate products. In this study we used 365 nm with only 12 W, and there was no intermediate product detected. It was concluded that the intermediate compounds could be unstable and decompose during the waiting time of the availability of the device (about a few days). An analysis available immediately after the sampling allowed us to better understand what would happen in the photoreactor as it can be seen in the next paragraph.

Table 4.13 Literature review of intermediate products of THX after photocatalytic degradation

[THX]$_0$ (ppm)	Method of detection	UV, wave length and Power	Number of intermediate products	Photocatalyst	Irradiation period (min)	Reference
26.3	GC-MS	265nm 125W	12[a]	TiO$_2$ P25 (1g.L^{-1})	360	[30]
100	LC-ESI-MS/MS	355nm 6X20W	5[b]	TiO$_2$ 60 mg / 6 Glass Slides in 250 mL volume	120	[26]
1.46	LC-ESI-MS/MS	365nm 2X6W	< LOD	TiO$_2$/perlite (8g.L^{-1})	180 and 270	This work
10	LC-ESI-MS/MS	365nm 2X6W	unstable	TiO$_2$/perlite (8g.L^{-1})	180 and 270	This work

[a] C$_8$H$_{10}$ClN$_5$O$_3$S, C$_7$H$_{12}$ClN$_5$O$_2$S, C$_9$H$_{12}$ClN$_3$OS, C$_8$H$_8$ClN$_5$OS, C$_5$H$_4$ClN$_3$S, C$_7$H$_9$ClN$_4$OS, C$_6$H$_9$N$_3$O$_3$S, C$_8$H$_{11}$N$_5$O$_2$S, C$_5$H$_{10}$N$_4$O, C$_3$H$_3$NO.

[b] C$_8$H$_{11}$ClN$_5$O$_3$S (m/z:292), C$_6$H$_8$ClN$_5$O$_2$S (m/z:250), C$_5$H$_4$ClN$_3$O$_2$S (m/z:292, 294), C$_6$H$_8$ClN$_3$OS (m/z:206, 208, 175, 205, 177), C$_8$H$_{10}$ClN$_3$O$_2$S (m/z:248, 250).
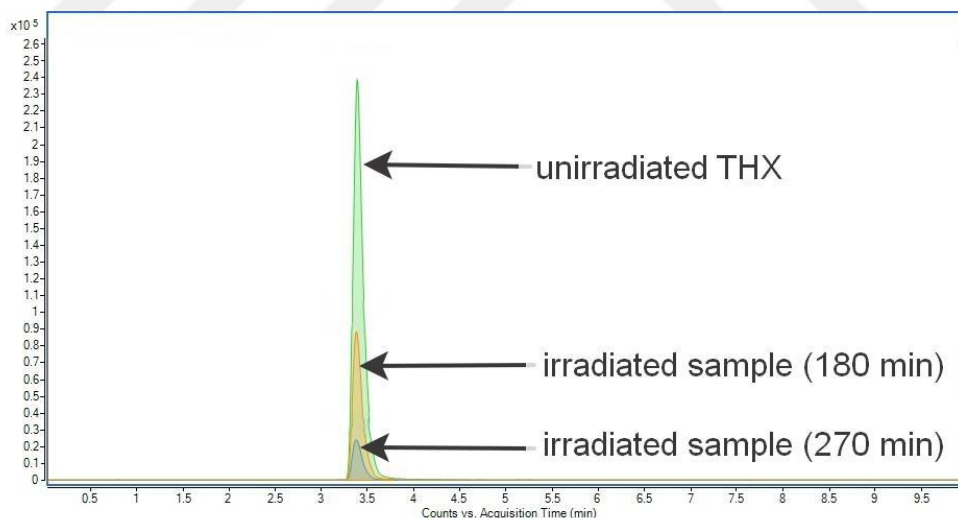

Figure 4.19 Chromatogram of unirradiated THX and irradiated samples within 180 min and 270 min at optimal conditions.

The second investigation for intermediate compounds took place on samples taken in the same way as in the first study. With the only difference that the analyses were carried out immediately after the sampling and the initial THX concentration was 10 ppm. Figure 4.20 described the intermediate degradation products separated by using HPLC.
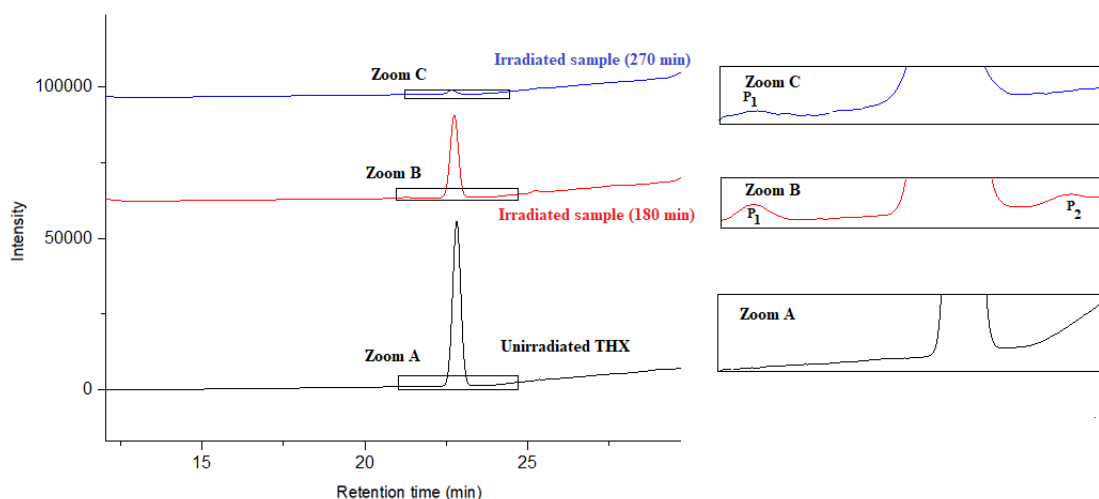
Figure 4.20 Chromatogram of unirradiated THX and irradiated samples obtained just after degradation process

As can be seen, two different peaks, P_1 (Fig.4.21) and P_2 (Fig 4.22), was detected in the sample obtained just after 180 min degradation, then only P_1 was observed in the sample obtained just after 270 min (Fig. 4.20). However, there were neither P_1 nor P_2 observed in the sample (in the same analysis condition), which kept in the fridge for a few days after irradiation. These results were in accordance with those obtained during the first investigation. This chromatogram (Fig. 4.20) and the previous one (Fig. 4.19) showed that the intermediate products obtained in our photocatalytic degradation process are unstable.

The retention time of P_1 was shorter than that of THX, indicating their increased polarity. However, the retention time of P_2 was higher compared to THX that can be explain by the weigh and the decreasing polarity of P_2. The odd mass of P_1 made it possible to envisage the presence of an odd number of nitrogen atoms in accordance with the rule of nitrogen for mass spectroscopy. This number was probably five as in the THX molecule. The isotopic peak profile revealed the presence of Cl in P_1. In addition, the mass of P_1 [M + 2x17] allowed to envisage the addition of two OH groups onto the THX. According to the study from Yang et al. (2014), the carbon linked to chlorine and sulfur followed by the other two carbon in thiophene ring, were respectively the most likely to be attacked by the OH radical initially. The structure of P_1 shown in Figure 4.21 was similar to one of the intermediate products obtained by Yang et al. (2014) [34].
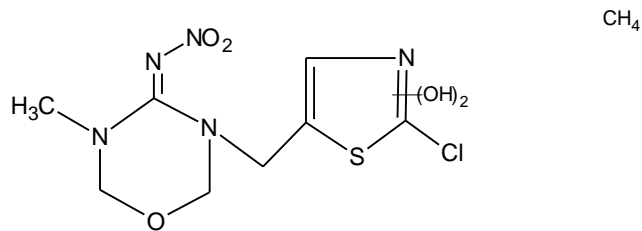
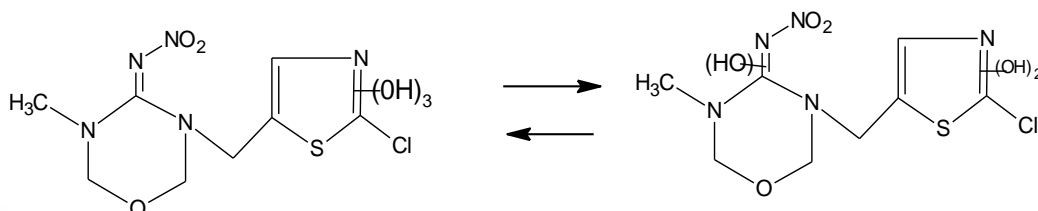Figure 4.21 Purposed molecular formula of P_1 (m/z 325)

Figure 4.222 Purposed molecular formula of P_2 (m/z 339)

The P_2 structure was proposed by doing an analysis similar to the previous one. The three OH radicals may be in equilibrium as shown in Figure 4.22. Then, it was concluded that we just captured a phase of degradation namely the attack of THX by the ˙OH radical. P_1 and P_2 were therefore highly unstable compounds. The fragmentation during the MS analysis resulted in the appearance of several fragments as shown in Table 4.14 and Table 4.15. Finally, it was proposed a reaction route for the photodegradation of THX in an aqueous medium and the fragmentation pathway of P_1 and P_2 (Fig. 4.23).

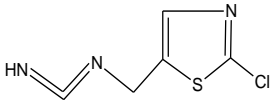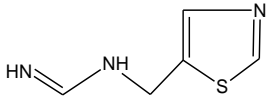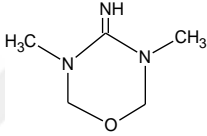Table 4.14 Retention time, mass fragmentation pattern and formula for P_1
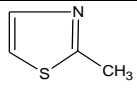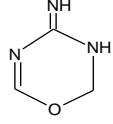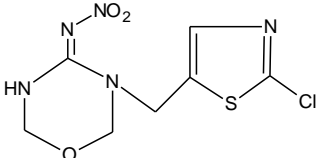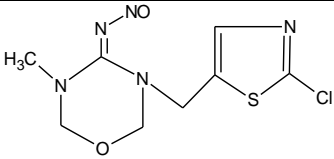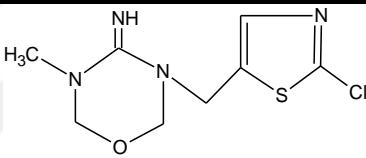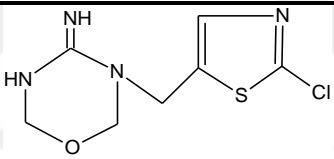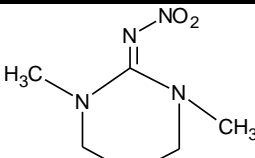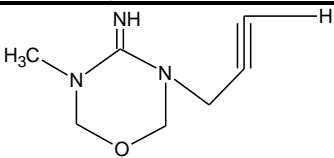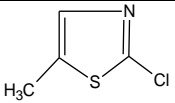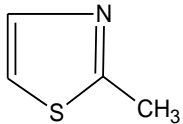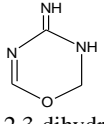
Molecular peak (m/z)	RT (min)	Mass fragmentation pattern (m/z)	Mass fragmentation formula
P_1 (325)	21.27	170/172/174	N-[(2-chloro-1,3-thiazol-5-yl)methyl]carbodiimide
		141	N-(1,3-thiazol-5-ylmethyl)imidoformamide
		129/131,	3,5-dimethyl-1,3,5-oxadiazinan-4-imine
		115	3-methyl-1,3,5-oxadiazinan-4-imine
		99	2-methyl-1,3-thiazole
			2,3-dihydro-4H-1,3,5-oxadiazin-4-imine

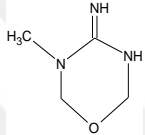Table 4.15 Retention time, mass fragmentation pattern and formula for P₂

Molecular peak (m/z)	RT (min)	Mass fragmentation pattern (m/z)	Mass fragmentation formula
P₂(339)	23.69	279	(4Z)-3-[(2-chloro-1,3-thiazol-5-yl)methyl]-N-nitro-1,3,5-oxadiazinan-4-imine
		262/264	(4Z)-3-[(2-chloro-1,3-thiazol-5-yl)methyl]-5-methyl-N-nitroso-1,3,5-oxadiazinan-4-imine
		246/248	3-[(2-chloro-1,3-thiazol-5-yl)methyl]-5-methyl-1,3,5-oxadiazinan-4-imine
		232/234	3-[(2-chloro-1,3-thiazol-5-yl)methyl]-1,3,5-oxadiazinan-4-imine
		171	3,5-dimethyl-N-nitro-1,3,5-oxadiazinan-4-imine
		153/ 155	3-methyl-5-(prop-2-yn-1-yl)-1,3,5-oxadiazinan-4-imine
		127	2-chloro-5-methyl-1,3-thiazole
		99	2-methyl-1,3-thiazole 2,3-dihydro-4H-1,3,5-oxadiazin-4-imine

81
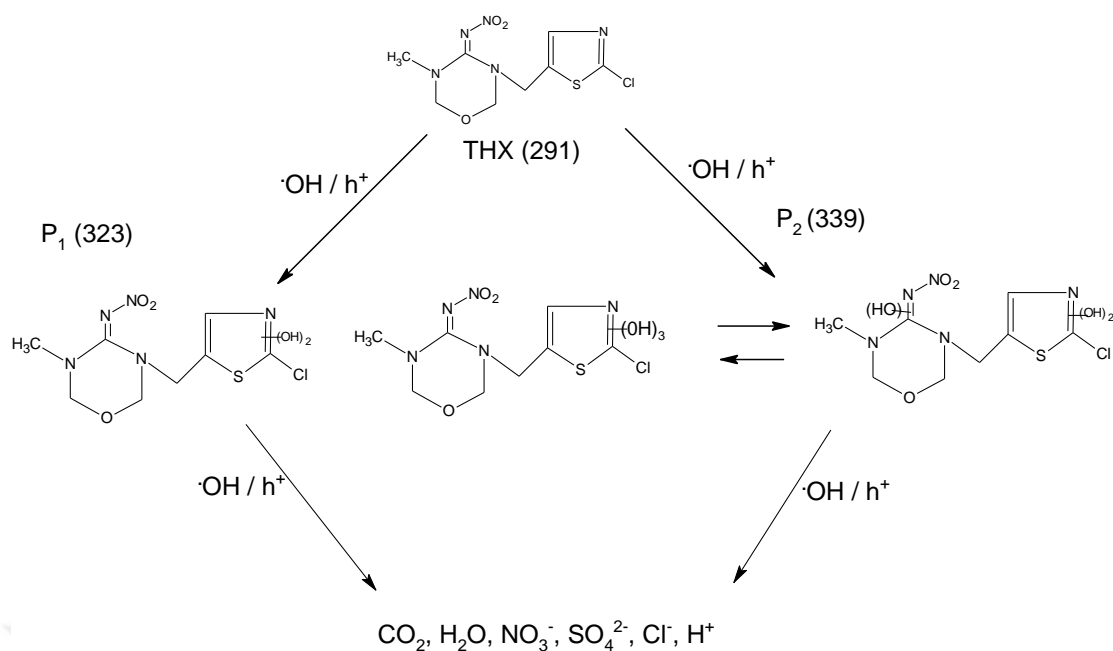
Figure 4.23 Purposed photocatalytic degradation pathway of Thiamethoxam

4.4 Conclusion

In this study, our first scientific objective was to evaluate the leaching potential of THX and THX-E in the soils taken from different regions of Tekirdağ. In order to reach this objective, we conducted batch adsorption experiments to access the main parameters governing the retention and transfer of the molecules in soil. The different analyses carried out showed great similarity in terms of soil composition. Once the soils were characterized, their affinity to thiamethoxam was then studied by means of the sorption experiments (kinetics and equilibrium). THX and THX-E exhibited relatively low affinity towards studied soils. K_{oc} was very variable; this showed that the just organic matter cannot be responsible for the adsorption of THX on the soils. Moreover, very low adsorption of THX and THX-E and high desorption characteristics of these compounds for the three studied soils, showed that migration to the groundwater could be higher for each system, involving a significant risk for the environment. This was also confirmed by the GUS and GLI index, which has led to the estimation of intermediate and high leaching potential depending on the soils.

This conclusion can justify the second part of our study that evidenced the potential of perlite supported TiO_2 as photocatalyst for degradation of THX in aqueous solution. Perlite presented a porous structure and was suitable as support material of TiO_2 for the elimination of pollutants from polluted water. Box Benkhen Experimental Design was an

efficient method for checking the effect of operating conditions on the photocatalytic degradation of THX in the presence of perlite supported TiO_2. The quadratic model was developed and the statistical analysis showed a good fit for DEG270 (degradation percentage after 270 min) (with R^2 value of 0.91 and P-value of 0.0126) and for EE/O (required electrical energy per order) (with R^2 value of 0.92 and P-value of 0.0098). We observed that the effect of initial pH and its interactions with PT (load of perlite supported TiO_2) and AF (air flow rate) seemed to be significant. PT has an optimum value around 8.30 g/L. Effect of AF is also significant, increasing that parameter positively impacted the process until 18 L/h. Thus, the optimal conditions were found to be pH 4, PT 8.30 g/L and AF 18 L/h at the studied conditions. DEG270 was around 87 % and, EE/O value was around 120 kWh / m^3 at the optimal conditions. The experimental results were in good agreement with those predicted by the model. The reusability of PST was also successfully tested without regeneration. THX mineralization was observed by COD and TOC measurements and also the fact that only unstable intermediate products were detected by both LC-MS-MS studies. After usage, separation of PST was easily achieved by flotation from the water surface. As a conclusion, pure THX and also in commercial formulation (THX-E) has high environmental risk, and perlite supported TiO_2 presented suitable properties to be used as photocatalyst for degradation of thiamethoxam and also its commercial formulation.

REFERENCES

[1]   Aktar, W. Sengupta, D. and Chowdhury, A. (2009). "Impact of pesticides use in agriculture: their benefits and hazards" Interdisciplinary Toxicology, 2(1):1-12.

[2]   Klarich, K. L., Pflug, N. C., Dewald, E. M., Hladik, M. L., Kolpin, D. W., Cwiertny, D. W. and Lefevre, G. H. (2017). "Occurrence of Neonicotinoid Insecticides in Finished Drinking Water and fate during Drinking Water Treatment" Environmental Science & Technology. Lett. 4, 168-178.

[3]   Landry, D., Dousset, D. and Andreux, F. (2004). ''Laboratory leaching studies of oryzalin and diuron through three undisturbed vineyard soil columns'' Chemosphere, 54: 735–742.

[4]   United Nations, Department of Economic and Social Affairs, Population Division (2017). World Population Prospects: The 2017 Revision, Key Findings and Advance Tables. Working Paper No. ESA/P/WP/248.

[5]   Kurwadkar, S., Wheat, R., McGahan, D. G. and Mitchell, F. (2014). ''Evaluation of leaching potential of three systemic neonicotinoid insecticides in vineyard soil Journal of Contaminant'' Hydrology, 170:86–94.

[6]   Traisup, K.,(2012). Fate of two currently used pesticides in water sediment systems, PhD. Thesis, University of York.

[7]   Senn, R., Hofer, D., Hoppe, T., Angst, M., Wyss, P., Brandl, F., Maienfisch, P., Zang, L. and White, S. (1998). CGA 293'343: a novel broad-spectrum insecticide supporting sustainable agriculture worldwide. The 1998 Brighton Conference – Pests and Diseases, 27–36.

[8]   Bonmatin, J.-M., Giorio, C., Girolami, V., Goulson, D., Kreutzweiser, D. P., Krupke, C. Liess, M., Long, E., Marzaro, M., Mitchell, E. A. D., Noome, D. A., Simon-Delso, N. and Tapparo, A. (2015). ''Environmental fate and exposure; neonicotinoids and fipronil,» Environmental Science and Pollution Research International'' 22:35–67.

[9]   Calvet, R., Barriuso, E., Bedos, C., Benoit, P., Charly, M. and Coquet, Y. (2005). Les pesticides dans le sol, Edition France Agricole.

[10]   Banerjee, K., Sangram, H. P., Dasgupta, S., Oulkar, D. P. and Adsule, P. G. (2008). ''Sorption of thiamethoxam in three Indian soils'', Journal of Environmental Science and Health Part B, 43:151–156.

[11] Campbell, S., Chen, L., Yu, J. and Li, Q. X. (2005). ''Adsorption and Analysis of the Insecticides Thiamethoxam and Indoxacarb in Hawaiian Soils'', Journal of Agricultural and Food Chemistry, 53(13):5373-6.

[12] Carbo, L., Martins, E. L., Dores, E. F. G. C. and Spadotto, C. A. (2007). ''Acetamiprid, carbendazim, diuron and thiamethoxam sorption in two Brazilian tropical soils'' Journal of Environmental Science and Health, Part B, 42(5):499-507.

[13] Papa, E. Castiglioni, S. Gramatica, P., Nikolayenko, V., Kayumov, O. and Calamari, D. (2004). ''Screening the leaching tendency of pesticides applied in the Amu Darya Basin (Uzbekistan)'', Water Reseach, 38:3485–3494.

[14] Gün, S. and Kan, M. (2009). ''Pesticide Use in Turkish Greenhouses: Health and Environmental Consciousness'' Polish Journal of Environmental Studies, 18(4):607–615.

[15] Akay, A. E. (2016). Ranking of pesticides according to leaching potentials to groundwater for the selected river basins in turkey – index-based approach, ankara. Master Thesis, Middle East Technical University, Environmental Engineering Department.

[16] Malato, S. (2002). ''Photocatalytic Treatment of Water-Soluble Pesticides by Photo-Fenton and TiO_2 using Solar Energy'', Catalysis Today, 76(2-4):209-220.

[17] Mandal, S. (2018). ''Reaction Rate Constants of Hydroxyl Radicals with Micropollutants and Their Significance in Advanced Oxidation Processes'', Journal of Advanced Oxidation Technologies, 21(1).

[18] Cao, H., Lin, X., Zhan, H., Zhang, H. and Lin, J. (2013). ''Photocatalytic degradation kinetics and mechanism of Phenobarbital in TiO_2 aqueous solution'', Chemosphere, 90:1514-1519.

[19] Leshuk, T., Livera, D. D. O., Peru, K. M., Headley, J. V., Vijayaraghavan, S., Wong, T. and Gu, F. (2016). ''Photocatalytic degradation kinetics of naphthenic acids in oil sands process-affected water: Multifactorial determination of significant factors'', Chemosphere, 165:10-17.

[20] Zhao, Q., Ge, Y., Zuo, P., Shi, D. and Jia, S. (2016). ''Degradation of Thiamethoxam in aqueous solution by ozonation: Influencing factors, intermediates, degradation mechanism and toxicity assessment'', Chemosphere, 146:105-112.

[21] Shan, A. Y., Ghazi, T. I. M. and Rashid, S. A. (2010). ''Immobilisation of titanium dioxide onto supporting materials in heterogeneous photocatalysis: a review'', Applied Catalysis A: General, 389(1-2):1-8.

[22] Duranoğlu, D. and Ngaha, E. (2018). ''An investigation on Thermal and UV Regeneration of TiO_2/Perlite Composites'', Journal of Advanced Oxidation Technologies, 21(1).

[23] Vishnuganth, M., Remya, N., Kumar, M. and Selvaraju, N. (2016). ''Photocatalytic degradation of carbofuran by TiO_2-coated activated carbon: Model for kinetic, electrical energy per order and economic analysis'', Journal of Environmental Management, 181:201-207.

[24] Chong, M. N., Jin, B., Chow, C. W. K., and Saint, C. (2010). ''Recent developments in photocatalytic water treatment technology: A review'', Water Research, 44:2997-3027.

[25] Hosseini, S. N., Borghei, S. M., Vossoughi, M. and Taghavinia, N. (2007). ''Immobilization of TiO_2 on Perlite Granules for Photocatalytic Degradation of Phenol'', Applied Catalysis B: Environmental, 74(1-2):53-62.

[26] Zabar, R., Komel, T., Fabjan, J., Kralj M. B. and Trebše, P. (2012). ''Photocatalytic degradation with immobilised TiO_2 of three selected neonicotinoid insecticides: Imidacloprid, thiamethoxam and clothianidin'', Chemosphere, 89:293–301.

[27] Duranoğlu, D. (2016). ''Preparation of TiO_2/Perlite Composites by Using 2^{3-1} Fractional Factorial Design'', JOTCSA, 3(3):299-312.

[28] Giannouri, M., Kalampaliki, T., Todorova, N. Giannakopoulou, T. Boukos, N., Petrakis, D. V. T. and Trapalis, C. (2013). ''One-Step Synthesis of TiO_2/Perlite Composites by Flame Spray Pyrolysis and Their Photocatalytic Behavior'', International Journal of Photoenergy.

[29] Borghei, S. N., Vossoughi, M. and Taghavinia, M. N. (2008). ''Photocatalytic degradation of phenol in aqueous phase with TiO_2 immobilized on three different supports with a simple method'', International Conference on Energy & Environment.

[30] Mir, N. A., Khan, A. Muneer, M. and Vijayalakhsmi, S. (2013). ''Photocatalytic degradation of a widely used insecticide Thiamethoxam in aqueous suspension of TiO_2: Adsorption, kinetics, product analysis and toxicity assessment'', Science of the Total Environment, 458–460, 388–398

[31] Chen, X. and Mao, S. S. (2007). ''Titanium Dioxide Nanomaterials: Synthesis, Properties, Modifications, and Applications'', Chemical Reviews 107:2891-2959.

[32] De Urzedo, A. P., Diniz, M. E. Nascentes, C. C., Catharino, R. R., Eberlin, M. N. and Augusti, R. (2007). ''Photolytic degradation of the insecticide thiamethoxam in aqueous medium monitored by direct electrospray ionization mass spectrometry'', Journal of Mass Spectrometry, 42(1).

[33] Peña, A., Rodríguez-Liébana, J. A. and Mingorance, M. D. (2011). ''Persistence of two neonicotinoid insecticides in wastewater and in aqueous solutions of surfactants and dissolved organic matter'', Chemosphere, 84:464-470.

[34] Yang, H., Liu, H., Hu, Z., Liang, J., Pang, H. and Yi, H. (2014). ''Consideration on degradation kinetics and mechanism of thiamethoxam by reactive oxidative species (ROSs) during photocatalytic process'', Chemical Engineering Journal 245:24–33.

[35] Saquib, M. and Muneer M. (2003). ''TiO_2-mediated photocatalytic degradation of a triphenylmethane dye (gentian violet), in aqueous suspensions'', Dyes Pigments, 56:37- 49.

[36] Reza, K. M., Kurny, A. and Gulshan, F. (2017). ''Parameters affecting the photocatalytic degradation of dyes using TiO_2: a review'', Applied Water Science, 7:1569-1578.

[37] Giwa, A., Nkeonye, P. O., Bello, K. A. and Kolawole, E. G. (2012). ''Solar photocatalytic degradation of reactive yellow 81 and reactive violet 1 in aqueous

solution containing semiconductor oxides'', International Journal Applied Science Technology, 2:90–105.

[38]   Sakkas, V. A., Islam, M. A., Stalikas, C. and Albanis, T. A. (2010) ''Photocatalytic degradation using design of experiments: A review and example of the Congo red degradation'', Journal of Hazardous Materials, 175(1-3):33-44.

[39]   D. 98/8/EC. (2012). ''Directive 98/8/EC concerning the placing biocidal products on the market Inclusion of active substances in Annex I or IA to Directive 98/8/EC Assessment Report Thiamethoxam Product-type 18 (Insecticides, acaricides and products to control other arthropods'', Directive 98/8/EC Assessment Report Thiamethoxam Product-type 18 (Insecticides, acaricides and products to control other arthropods.

[40]   United States Code (2012). Title 7 – Agriculture, chapter 6 - Insecticides and environmental pesticide control sec. 136 – definitions'', u.s. government publishing office.

[41]   Syngenta United State, http://www.syngentacropprotection.com, 15th December 2017.

[42]   Ortiz-Hernández, M. L., Sanchez-Salinas, E., Dantan-Gonzalez, E., and Castrejon-Godinez, M. L. (2013). ''Pesticide Biodegradation: Mechanisms, Genetics and Strategie to Enhance the Process'', IntechOpen, 33(6):309-368.

[43]   Maienfisch, P., Huerlimann, H., Rindlisbacher, A., Gsell, L., Dettwiler, H., Haettenschwiler, J., Sieger, E. and Walti, M. (2001). ''The discovery of thiamethoxam: a second-generation neonicotinoid,'' Pest Management Science, 57(2):165-76.

[44]   Shobana, N. and Farid, P. (2008). Six-membered Rings with Three or more Heteroatoms and their Fused Carbocyclic Derivatives: Comprehensive Heterocyclic Chemistry III, Thiamethoxam.

[45]   Sparling, D. W. (2016). ''Environmental Contaminants and Their Biological Effects on Animals and Plants'', Ecotoxicology Essentials.

[46]   Stoye, E. (2018), ''Europe to impose near-total ban on neonicotinoids'', Chemistry World, 30 April 2018.

[47]   He, L. M., Troiano, J., Wang, A. and Goh, K. (2008). ''Environmental chemistry, ecotoxicity, and fate of lambda-cyhalothrin'', Reviews of Environmental Contamination and Toxicology, 195:71-91.

[48]   Arslan, S. (2016). ''Pesticide Usage and Environmental Impacts in Turkey'' Süleyman Demirel University, Faculty of Agriculture, Department of Agricultural Economics, National Agricultural Economics Congress, 2215-2224.

[49]   Tiryaki, O. and Temur, C. (2010). ''The Fate of Pesticide in the Environment'', Journal of Biological and Environmental Sciences, 4(10):29-38.

[50]   Amalric, L., Baran, N., Jeannot, R., Martin, J. C. and Mouvet C. (2003). Mechanisms for transfer of phytosanitary products from soil to groundwater and methods of analysis of phytosanitary products in waters, BRGM/RP-51590-FR, 116, P31.

[51]   Yeo, H.-G., Choi, M., Sunwoo, Y. (2004). Seasonal variations in atmospheric concentrations of organochlorine pesticides in urban and rural areas of Korea, Atmospheric Environment, 38(28):4779-4788.

[52]   Directive 98/8/EC (2012). Concerning the placing biocidal products on the market Inclusion of active substances in Annex I or IA to Directive 98/8/EC Assessment Report Thiamethoxam Product-type 18 (Insecticides, acaricides and products to control other arthropods.

[53]   Katja, K. (2016). ''Pesticides in surface waters: a comparison with regulatory acceptable concentrations (RACs) determined in the authorization process and consideration for regulation'', Environmental Sciences Europe 28:1.

[54]   ''Le monde'' Newspaper website https:www.lemonde.fr/societe/article/ 2018/08/20/micmac-aquatique-en-bourgogne_5344075_3224.html? 20th August 2018.

[55]   UFC Que Choisir Association Service (2014). ''The quality of drinking water in France'', A report.

[56]   Thakur, I. S. (2006) ''Industrial Biotechnology problems and remedies'', I K International Publishing House Pvt. Ltd.

[57]   Renaud, F. G., Brown, C. D., Fryer, C. J. and Walker, A. (2004). ''A lysimeter experiment to investigate temporal changes in the availability of pesticide residues for leaching'', Environmental Pollution, 131(1):81-91.

[58]   Beulke, S., Brown, C. D., Fryer, C. J. and van Beinum, W. (2004). ''Influence of kinetic sorption and diffusion on pesticide movement through aggregated soils'', Chemosphere., 57(6): 481-90.

[59]   Katagi, T. (2010). ''Bioconcentration, bioaccumulation, and metabolism of pesticides in aquatic organisms'', Reviews of Environmental Contamination and Toxicology, 204:1-132:4419-1440.

[60]   Jinde, C. D. (1994). ''Physico-Chemical Properties and Environmental Fate of Pesticides'' Environmental hazards assessment program, State of California, Environmental Protection Agency Department of Pesticide Regulation, Environmental Monitoring and Pest Management.

[61]   Huang, P. M. and Iskandar, I. K. (1999). ''Soils and groundwater pollution and remediation Asia, Africa and Oceania'', CRC Press LLC.

[62]   Calvet, R. (2013). Le Sol FA Env Agricole, Edition 2, France Agricole.

[63]   EPA. (1999). ''United States Office of Air and Radiation EPA 402-R-99-004A Environmental Protection August 1999 Agency understanding variation in partition coefficient, Kd, values Volume I: The Kd Model, Methods of Measurement and Application of Chemical Reaction Codes''.

[64]   EPA. (2009). Drinking water: perchlorate supplemental request for comments. 74(159):41883.https://federalregister.gov/aE9-19507 24 june 2017.

[65]   Vanloon, G. W. and Duffy, S. J. Environmental chemistry: A global perspective, Oxford University Press Fourth Edition, 16 November 2017.

[66]   Singera, M. J. and Warkentin, B. P. (1996). ''Soils in an environmental context: an American perspective'', Catena, 27 (3-4):179-189.

[67] Montoya, J. M., Pimm, S. L. and Solé, R. V. (2006). ''Ecological networks and their fragility'', Nature, 20:442(7100):259-64.

[68] Nath, K., Panchani, S., Bhakhar, M. S. and Chatrola, S. (2013). ''Preparation of activated carbon from dried pods of Prosopis cineraria with zinc chloride activation for the removal of phenol'', Environmental Sciences and Pollution Research 20:4030-4045.

[69] Nethaji, S., Sivasamy, A., Kamar, R. V. and Mandal, A. B. (2012). ''Preparation of char from lotus seed biomass and the exploration of its dye removal capacity through batch and column adsorption studies'', Environmental Science and Pollution Research international, 20(6):3670-8.

[70] Graouer-Bacart, M., Sayen, S. and Guillon, E. (2015). ''Adsorption of enrofloxacin in presence of Zn(II) on a calcareous soil Saf'', Ecotoxicology and Environmental Safety 122:470–476.

[71] Langmuir, I. (1918). ''The adsorption of gases on plane surfaces of glass, mica and platinum'', Journal of the American Chemical Society, 40:1361-1403.

[72] Freundlich, H. M. F. (1906). ''Over the adsorption in solution'', Journal of Physical Chemistry A 57:385–470.

[73] Katagi, T. (2018). ''Direct photolysis mechanism of pesticides in water'', Journal of Pesticide Science: a review, 43(2):57-72.

[74] Katagi, T. (2002). ''Abiotic hydrolysis of pesticides in the aquatic environment'', Reviews of Environmental Contamination and Toxicology, 175:79-261.

[75] Chapman, R. A. and Cole, C. M. J. (1982). ''Observations on the influence of water and soil pH on the persistence of insecticides'', Journal of Environmental Science and Health, Part B: 17(5):487-504.

[76] Huil, T. J., Ariffin, M. M. and Tahir (2010). ''Hydrolysis of chlorpyrifos in aqueous solutions at different temperatures and pH'', The Malaysian Journal of Analytical Sciences, 14(2):50 – 55.

[77] Singh, D. K. (2008). ''Biodegradation and bioremediation of pesticide in soil: concept, method and recent developments'', Indian Journal of Medical Microbiology 48:35–40.

[78] Sihag, S. Pathak, H. Jaroli, D. P. (2014). ''Factors Affecting the Rate of Biodegradation of Polyaromatic Hydrocarbons'', International journal of pure and applied bioscience, 2(3):185-202.

[79] Ribeiro, A. R., Nunes, O. C., Pereira, M. F. and Silva, A. M. (2015). ''An overview on the advanced oxidation processes applied for the treatment of water pollutants defined in the recently launched Directive 2013/39/EU'', Environment International, 75:33-51.

[80] Glaze, W. H., Kang, J. W. and Chapin, D. H. (1987). ''The chemistry of water treatment processes involving ozone, hydrogen peroxide and UV radiation'', Ozone Science and Engineering 9:335–352.

[81] Tchobanoglous, G., Burton, F. T. and Stensel, H. D. (2002). Wastewater Engineering Treatment and Reuse, Metcalf & Eddy, Inc. 4th.

[82] Comninellis, C., Kapalka, A., Malato, S., Parsons, S. A., Poulios, I. and Mantzavinos, D. (2008). ''Perspective Advanced oxidation processes for water treatment: advances and trends for R&D Christos'', Journal of Chemical Technology & Biotechnology 83:769–776.

[83] Chen, X. and Mao, S. S. (2007). ''Titanium Dioxide Nanomaterials: Synthesis, Properties, Modifications, and Applications'', Chemical Reviews, 107:2891-2959.

[84] Rauf, M. A. and Ashraf, S. S. (2009). ''Fundamental principles and application of heterogeneous photocatalytic degradation of dyes in solution'', Chemical Engineering Journal, 151:10-18.

[85] Verma, A. Dixit, P. D., (2012). ''Photocatalytic degradability of insecticide Chlorpyrifos over UV irradiated Titanium dioxide in aqueous phase'', International journal of environmental sciences, 3:2.

[86] Ahmed, S., Rasul, M. G., Martens, W., Brown, R. and Hashib, M. A. (2011). ''Influence of Parameters on the Heterogeneous Photocatalytic Degradation of Pesticides and Phenolic Contaminants in Wastewater: A Short Review'' Journal of Environmental Management, 92(3):311-330.

[87] E. W. Contributors. Basic principles of statistical analysis Available: http://edutechwiki.unige.ch/fmediawiki/index.php?title=Principes_de_base_d%27 analyse_statistique&oldid=92715, 20 November 2017.

[88] Antony, J. (2003). Design of Experiments for Engineers and Scientists, Fundamentals of Design of Experiments, 6–16.

[89] John, P. W. M. (1971). Statistical design and analysis of experiments, Philadelphia, PA: SIAM Classics in Applied Mathematics.

[90] Ferreira, S. C., Bruns, R., Ferreira, H., Matos, G., David, J., Brandao, G., Silva, E. P. L., Portugal, L., Dos Reis, P. and Souza, A. (2007). ''Box-Behnken design: An alternative for the optimization of analytical methods'', Analytica chimica acta , 597(2):179-18.

[91] Açıkalın, K. (2010). Pyrolysis of various biomass waste materials and analysis of obtained products, Ph.D Thesis, Istanbul, Yıldız Technical University, Institute Of Natural And Applied Sciences.

[92] Box, G. E. P. and Behnken, D. W. (1960). Some new three level designs for the study of quantitative variables, Technometrics, 2:455-75.

[93] Barrak, N., Mannai, R., Zaidi, M., Kechida, M. and Helal, A. N. (2016). ''Experimental Design Approach with Response Surface Methodology for Removal of Indigo Dye by Electrocoagulation'', Journal of Geoscience and Environment Protection, 4:50-61.

[94] Marget, W. M. (2015). Experimental designs for multiple responses with different models, Theses and Dissertations Graduate College, Doctorat Thesis, Iowa State University, United State of America.

[95] Lundstedt, T., Seifert, E., Abramo, L., Thelin, B., Nyström, A., Pettersen, J. and Bergman, R. (1988). ''Experimental design and optimization'', Chemometrics and intelligent laboratory systems, 42(1):3-40.

[96] Goupy, J. and Creighton, L. (2006). Introduction to Design of Experiments, 3. Edition Dunod.

[97] Lee, K. M. and Hamid, S. B. A. (2015). ''Simple Response Surface Methodology: Investigation on Advance Photocatalytic Oxidation of 4-Chlorophenoxyacetic Acid Using UV-Active ZnO Photocatalyst'', Materials, 8: 339-354.

[98] Vivier, S. (2002). Optimisation strategies using the Experimental Design Method and Application to electrotechnical devices modelled by finite elements, Lille: Ph.D in Electrical Engineering Ecole Centrale de Lille / University of Science and Technology.

[99] S. Karam, Experimental designs and data analyses for the optimization of deposition processes, Limoges: Doctorat thesis University of Limoges Doctoral School Science - Technology - Health Faculty of Science and Technology, 2004.

[100] Bernate, L. A., Entzmann, F., Dugardin, F., Yalaoui, F. and Amodeo, L. (2012). ''Optimization of Chemical Production: A Case Study'', 14th IFAC Symposium on Information Control Problems in Manufacturing, Bucharest, Romania, May 23-25, 2012.

[101] Tekirdag, «Environmental situation report,» Tekirdag, 2015.

[102] T. C. Tekirdağ Metropolitan Municipality, General Directorate of Water and Sewerage Administration, https://www.teski.gov.tr/ 23 Mars 2018

[103] Boudesocque, S., Guillon, E., Aplincourt, M. Marceau, E. and Stievano, L. (2006). ''Sorption of Cu (II) onto vineyard soils: Macroscopic and spectroscopic investigations'', Journal of Colloid and Interface Science, 307:40-49.

[104] AFNOR. 2003. Soil quality - Determination of the particle size distribution of soil particles - Pipette method, NF X31-107.

[105] AFNOR. 2005. Soil quality - Determination of pH, NF ISO 10390.

[106] AFNOR. 1998. Soil quality - Determination of organic carbon by sulfochromic oxidation,NF ISO 14235.

[107] AFNOR. 1999. Soil quality - Chemical methods - Determination of Cation Exchange Capacity (CEC) and extractable cations, NF X31-130.

[108] AFNOR. 1995. Soil quality - Determination of carbonate content – Volumetric Method, NF ISO 10693.

[109] Achouak, E. A. A. (2010). Study of the adsorption and desorption processes of phytosanitary products in calcareous soils, Reims: Doctoral thesis University of Reims Champagne Ardenne, France.

[110] OECD, 2000. ''Adsorption Desorption using a Batch equilibrium Method''.

[111] FAO, «Food and Agriculture Organisation of United Nations,» Available:http://www.fao.org/fileadmin/templates/agphome/documents/Pests_Pes ticides/JMPR/Evaluation10/Thiamethoxam.pdf. 24 may 2019.

[112] Sigma Aldrich https://www.sigmaaldrich.com/catalog/product/sial/31058?lang= en&region=TR, 13 may 2019.

[113] Syngenta, EFORIA 247 ZC Safety data sheet made according to Regulation (EC) No. 1907/2006, 2015.

[114] EPA. Air Quality Criteria for Carbon Monoxide (1991). U.S. Environmental Protection Agency, Washington, DC, EPA/600/8-90/045F.

[115] Suttiponparnit, K., Manoranjan, J. J., Suvachittanont, S., Charinpanitkul, T., Biswas, P. (2011). ''Role of Surface Area, Primary Particle Size, and Crystal Phase on Titanium Dioxide Nanoparticle Dispersion Properties'', Nanoscale Research Letters 6:27.

[116] Lan, Y., Lu, Y. and Ren, Z. (2013). ''Mini review on photocatalysis of titaniumdioxide nanoparticles and their solarapplications'', Nano Energy, 2: 1031–1045.

[117] Wheelwright, W., Cooney, R. P., Ray, S., Zujovic, Z. and Silva, K. (2017). ''Ultra-high surface area nano-porous silica from expanded perlite: Formation and characterization'', Ceramics International, 48(14):11495-11504.

[118] Hatami, M., Cuijpers, M. C. M. and Boot, M. D. (2015). ''Experimental optimization of the vanes geometry for a variable geometry turbocharger (VGT) using a Design of Experiment (DOE) approach'', Energy Conversion Management, 106:1057–1070.

[119] Montgomery, D. C. (2013). Design and analysis of experiments, 2013.

[120] Behnajady, M., Vahid, B., Modirshahla, N. and Shokri, M. (2009). ''Evaluation of electrical energy per order (EEO) with kinetic modeling on the removal of Malachite Green by US/UV/H_2O_2 process'', Desalination, 249:99-103.

[121] Bolton, J. R., Bircher, K. G., Tumas, W. and Tolman, C. A. (1995). ''Figures-of-Merit for the Technical Development and Application of Advanced Oxidation Processes'', Journal of Advanced Oxidation Technology,1(1):13-17.

[122] Bolton, J. R., Bircher, K. G., Tumas, W. and Tolman, C. A. (2001). ''Figures-of-Merit for the Technical Development and Application of Advanced Oxidation Technologies for both electric-and solar- driven systems'', Pure and Applied Chemistry, 73(4):627–637.

[123] Wang, Q., Li, Y. and Klassen, W. (2004). ''Determination of Cation Exchange Capacity on Low to Highly Calcareous Soils'', Communications in Soil Science and Plant Analysis, 36(11-12):1479-1498.

[124] Guckel, W., Rittig, F. R. and Synnats, G. (1974). ''Method for determining volatility of active ingredients used in plant protection. 2. Applications to formulated products'', Pesticide Science, 5:393-400.

[125] Gustafson, D. I. (1989). ''Ground Water Ubiquity Score: A Simple Method for Assessing Pesticide Leachability'', Environmental Toxicology and Chemistry, 8:339-357.

[126] Hilton, M. J., Emburey, S. N., Edwards, P. A., Dougan, C. and Ricketts, D. C. (2019) ''The route and rate of thiamethoxam soil degradation in laboratory and outdoor incubated tests, and field studies following seed treatments or spray application'', Pest Management Science, 75(1):63-78.

[127] Kumar, N. Srivastava, A. Chauhan, S. S. and Srivastava, P. C. (2014). ''Studies on dissipation of thiamethoxam insecticide in two different soils and its residue in potato crop'', Plant Soil and Environment, 60(7):332–335.

[128] Hilton, M. J., Jarvis, T. D. and Ricketts, D. C. (2015). ''The degradation rate of thiamethoxam in European field studies'', Pest Management Science, 72:388–397.

[129] Agrawal, A. Pandey, R. S, Sharma, B. (2010). ''Water Pollution with Special Reference to Pesticide Contamination in India'', Journal of Water Resource and Protection, 2:432-448.

[130] Hinojosa-Reyes, M., Arriaga, S., Diaz-Torres, S. V. and Rodríguez-González (2013). ''Gas-phase photocatalytic decomposition of ethylbenzene over perlite granules coated with indium doped TiO_2'', Chemical Engineering Journal, 224:106-113.

[131] Gomez, S., Marchena, C. L., Renzini, M. S., Pizzio, L. and Pierella, L. (2015). '' In situ generated TiO_2 over zeolitic supports as reusable photocatalysts for the degradation of dichlorvos'', Applied Catalysis B: Environmental, 162:167-173.

[132] Antony, K. J. and Vismanathan, R. B. (2009). ''Effect of surface area, pore volume and particle size of P25 titania on the phase transformation of anatase to rutile'', Indian Journal of chemistry. Sec A, 48:1378-1382.

[133] Xiao, J., Xie, Y. and Cao, H. (2015). ''Organic pollutants removal in wastewater by heterogeneous photocatalytic ozonation: Review'', Chemosphere, 121:1–17.

[134] Sivagami, K., Krishna, R. R. and Swaminathan, T. (2016). ''Optimization studies on degradation of monocrotophos in an immobilized bead photo reactor using design of experiment'', Desalination and Water Treatment, 57:28822–28830.

[135] Xu, Y. and Langford, C. H. (2000). ''Variation of Langmuir adsorption constant determined for TiO_2-photocatalyzed degradation if acetophenone under different light intensity'', Journal of Photochemistry and Photobiology A, 133:67-71.

CURRICULUM VITAE

PERSONAL INFORMATION

Name Surname   : Emmanuel NGAHA

Date of birth and place   : 01/01/1977 / Bokito - Cameroon

Foreign Languages   : French, English, Turkish

E-mail   : emmangaha@gmail.com

EDUCATION

Degree	Department	University	Date of Graduation
Master	Master: Inorganic and Environmental Chemistry	Dschang	2010
	Master in Chemistry Education	Ecole Normale Superieure (Yaoundé)	2006
	Maitrise: General Chemistry	Yaoundé I	2005
Undergraduate	Bachelor: Chemistry	Yaoundé I	2003
High School	Baccalaureat D	GHS Bokito	1997

WORK EXPERIENCE

Year	Corporation/Institute	Enrollment
2012	Ministry of Education (Cameroon)	2007

94

PUBLISHMENTS

Papers

1. Ngaha, E., Sayen, S., Guillon, E., Duranoğlu, D. 2019 Process Optimization with Box-Behnken Experimental Design For Photocatalytic Degradation Of Thiamethoxam Using Perlite Supported TiO_2 Desalination and water treatment (doi: 10.5004/dwt.2019.24402).

2. Duranoğlu, D., Ngaha, E. 2018 An investigation on Thermal and UV Regeneration of TiO2/Perlite Composites. Journal of Advanced Oxidation Technologies; 21(1).

3. Ngaha, E., Duranoğlu, D., Benea, B. 2016 New challenges of water pollution in Europe and their socioeconomical impact. Annals faculty of Economic, Economic Sciences Series, 2016, Vol. 15, 67-74.

Conference Papers

1. Ngaha, E, Sayen, S., Guillon, E., Duranoğlu, D. 2018 Prediction of the electrical energy per order used during photocatalytic degradation of thiamethoxam by using Box Behnken Design. 48th Congress of the French Group of pesticides 2018.

2. Emmanuel, N., Stéphanie, S., Emmanuel, G., Duranoğlu, D., "Photocatalytic Degradation of Thiamethoxam in Aqueous Solution by Using Perlite Supported TiO2" International Conference on Energy and Thermal Engineering. Istanbul, Turkey, 25-28 April, 2017.

3. Ngaha, E, Sayen, S., Guillon, E., Duranoğlu, D. 2016 Adsorption et désorption du thiamethoxam et de la lambda-cyhalothrine sur trois sols de grande culture. 46th Congress of the French Group of pesticides 2016.

4. Ngaha, E., Duranoğlu, D. 2015 Environmental risk assessment for 3 Pharmaceutical products of different classes in Turkey: paracetamol, diclofenac and metoprolol." Eighth edition days of Analytical Chemistry (J.C.A. 2015) University of Douala, I.U.T., Douala, Cameroon, September 30, 1-2 October 2015.

Projects

1. Ngaha, E., Duranoğlu, D. ''Project number: 2015-07-01-DOP02''. Yildiz Technical University Scientific Research Projects Coordinating Department. (2015-2019).

2. Ngaha, E "Detection of Lead (II) ions by differential pulse voltammetry at a carbon paste electrode modified by a thiolated clay" Master thesis in chemistry and electrochemistry of water treatment materials. University of Dschang, Cameroon, 2010.

3. Ngaha, E "Synthesis and characterization of some toxic metals complexs: Cu, Al, Zn and Cd with amino acid ligands and their interaction with oxalate" Thesis for Ecole Normale Supérieur graduation in laboratory of chemistry of coordination compounds; University of Yaoundé I, Cameroon, 2006.

4. The initiator of the project "ETIC ENVIRONMENT" which consists in designing a viable system of faecal sludge management for Africans town including mobile Application, training (online and on field), solar energy, natural coagulant and without chemicals. The project is carried by ENG Consulting from Cameroon. Cameroon, 2018.